

NORTHWESTERN UNIVERSITY

Functional Organization of Promyelocytic Leukemia Bodies During Proteotoxic Stress

A DISSERTATION

SUBMITTED TO THE GRADUATE SCHOOL
IN PARTIAL FULFILLMENT OF THE REQUIREMENTS

for the degree

DOCTOR OF PHILOSOPHY

Field of Driskill Graduate Training Program in Life Sciences

By

Danielle Fanslow

EVANSTON, ILLINOIS

December 2018

Abstract

Promyelocytic leukemia (PML) nuclear bodies act as quality control centers in the nucleus, participating in a plethora of nuclear functions. As such, PML bodies are a signature model for functional nuclear organization. PML bodies have a dynamic protein composition that responds to changing conditions of the cell. Many of the protein binding-partners of PML have been functionally characterized into a SUMO-dependent post-translational modification pathway for proteins. However, others such as nascent mRNA and translation machinery, suggest an additional uncharacterized function of PML-localized translation. Growing evidence supports the presence of translation in the eukaryotic nucleus, yet a clear demonstration of its functional relevance remains to be established.

Here we demonstrate that nuclear polypeptides synthesized localizes to PML bodies during cell stress. Analysis of proteotoxic stress associated with the expression of mutant Ataxin-1 (ATXN1), a gene that causes the neurodegenerative disorder spinocerebellar ataxia type 1 (SCA1), reveals that PML bodies couple polypeptide synthesis with mRNA surveillance and protein quality control. Specifically, we find repeat-expanded *ATXN1* mRNA foci and protein aggregates localized at PML bodies where they are subject to regulation by the no-go decay (NGD) pathway and protein degradation. To expand upon our mechanistic study, we identify protein binding-partners of PML during different cell stressors using an unbiased proteomics approach. Our study suggests a novel PML-localized regulatory system underlying nuclear translation that plays a critical role in the cell stress response.

Acknowledgments

I would first like to thank my mentor, Dr. Steven Kosak. He encouraged my fellow labmates and I to focus on big biological questions and challenged us to think in innovative ways. From the beginning, he was confident in my technical expertise and was always open to exploring new experimental avenues with me. He also fully supported the valuable time and energy I spent on career development outside of the lab. Without his support in this area, I would not have discovered my enthusiasm for public outreach and science writing.

I would like to thank all of the members of the Kosak lab I've worked over the years. The lab has truly seen some exceptionally talented people who also had the biggest hearts. Firstly, I felt lucky to have Dr. Erica Smith as a co-mentor. She was always willing to take a deep dive into my proposals, experiments and presentations, giving me valuable critique that helped me grow as a scientist. Without her guidance and her generosity, I don't think I would have made it. Dr. Alexis Cogswell was my teammate, my project partner, and my friend. It was a pleasure to work closely with her for several years. She helped me grow immensely as a writer through her thorough review on my proposals and assignments. Her encouragement and bright personality was really a source of inspiration for me. Chelsee Strojny-Okyere was a lifesaver for the project and for the lab, joining at a time I needed her the most. She was the hardest worker I've ever met and was never willing to give up on an experiment. Also, her outgoing nature and kindness bonded our lab together. Dr. Arturo Garza-Gongora was a buddy since the day I walked into the lab. I admired the way he thought about biological concepts and his ever laid-back nature. Dr. Agnes Laskowski and Dr. Ashley Wood were both so talented and so kind. They were also so full of valuable advice even after their departure. Elizabeth Daley was an endless source of

enthusiasm and collaboration that connected everyone together. I will really miss our lunches at our favorite burrito chain. My mentee Alessandra Garcia, fellow graduate students Dr. Kyle Laster, Dr. Daniel Neems, medical fellow Dr. Kyle MacQuarrie, as well as technicians Brian Poll, Ellen Rice, and Michael Gutbrod were always sources of intellectual inspiration and companionship.

I'd like to thank my committee members Dr. Vladimir Gelfand, Dr. Sui Huang, and Dr. Evangelos Kiskinis. They provided their expertise and advice whenever I needed it. They challenged me during the committee meetings to think critically about every experiment I did, often improving my perspective on my project. Thank you to Sui for letting me get her perspective on women in science for an AWIS profile.

I'd like to thank the network of support from my department and core facilities at Northwestern. Thank you to Dr. Josh Rappoport and Dr. Constadina Arvanitis at the Nikon Imaging Core. My project wouldn't have gone anywhere without excellent microscopy. Thank you to Paul Thomas and Young Ah Goo at the Proteomics Core for the excellent collaboration I needed for my BioID experiments. Thank you also to Dr. Puneet Opal and Dr. Steve Adam, who provided valuable insight into my manuscript for several years.

I'd like to thank those who have helped me along my path of professional development. I'd like to give many thanks to Sara Grady at the Science and Society Center, who turned my weird fascinations into meaningful stories. She totally changed my perspectives as a writer and supported my ambition for science writing. Thanks also to Dr. Patti Wolter and Dr. Donna Leff who, along with Sara, gave me the inspiration to tell stories about science. Thank you to the members of the Chicago Graduate Student Association who gave me the opportunity to develop

my leadership and event planning skills. Thank you to Michelle Paulsen, Byron Stewart, and Beth Bennet from the Ready, Set, Go Research Communications Workshop, who helped me step out of my comfort zone and into the literal spotlight. Thank you to Dr. Suji Jeong who helped cultivate my social media marketing skills. Thank you to Dr. Victoria Can who joyously served the City of Chicago and taught me how to teach a classroom full of kids.

Thank you to the Driskill Graduate Program and its administrators, who cultivated a sense of community on our campus and supported me through everything. Thanks especially to Dr. Pamela Carpentier for the guidance and the opportunity to write for the program's website.

Lastly, I'd like to thank my friends and family. These people mean the world to me and I dedicate this dissertation to them. First, thank you to my friends old and new, who journeyed through graduate school with me. Thank you to Dr. Lindsay Stolzenburg and Dr. Laura Johnston for moral support and several fun "girls nights" with sushi and movies. Thank you to Dr. Kyle Smith for being a great buddy, especially during the last few months of graduate school filled with writing and coffee. Thank you to Dr. Megan Wood and her husband Dan, two people who's friendship and loyalty know no bounds. They've been there for emotional support in so many ways. My mom, Patty, and my dad, Gerry have always embraced and encouraged the pursuit of my passions and curiosities throughout my life, from ballet to cell biology. I'm eternally grateful for their unconditional love and support. To my sister Devin and my brother Blair, they have been and will always be my companions. Finally, thank you to my partner Dr. Justin Luebke, who has gone through this journey with me since I was a technician. His love, friendship, encouragement, and first-hand knowledge of the challenges of graduate school have helped me reach my goals.

Funding Acknowledgments

My studies and activities were made possible by: the Driskill Graduate Program Fellowship, the Northwestern Cell and Molecular Basis of Disease Training Program (NIH grant T32 GM008061), the Lurie Cancer Center H Foundation Pilot Project Award, The Graduate School John N Nicholson Fellowship and The American Society for Cell Biology COMPASS Outreach Grant. Additional funding sources for the Kosak lab and my thesis project include: The National Institutes of Health New Innovator Award (DP2 OD008717), the Liz and Eric Lefkofsky Innovation Research Award, and a Chicago Biomedical Consortium grant (PDR-003).

List of Abbreviations

ALS	Amyotrophic Lateral Sclerosis
APL	Acute Promyelocytic Leukemia
ATXN1	Ataxin-1
BioID	proximity-dependent biotinylation
BirA	Biotin Ligase A
DSB	Double Strand Break
Dom34	Duplication of Multilocus Region 34
FISH	Fluorescence <i>in situ</i> hybridization
HBS1	Hsp70 subfamily B Suppressor
HBS1L	HBS1-like protein
HD	Huntington's Disease
HPG	homopropargylglycine
HTT	Huntington
IFN	Interferon
MHC	Major Histocompatibility Complex
NB	Nuclear Body
ND10	Nuclear Domain 10
NGD	No-Go Decay
NMD	Nonsense Mediated Decay
NSD	Non-Stop Decay

PELO	Human Pelota
PFA	paraformaldehyde
PML	Promyelocytic Leukemia
PMY	puromycin
PolyQ	Poly-glutamine
PQC	Protein Quality Control
PTC	Pre-mature Stop Codon
RAN	Repeat-associated non-AUG
RARA	Retinoic acid receptor alpha
ROS	Reactive oxygen species
RP	Ribosomal Protein
RPM	Ribopuromylation
RT	Room Temperature
SCA1	Spinocerebellar Ataxia Type-1
snRNP	Small nuclear ribonucleoproteins
snoRNP	Small nucleolar ribonucleoproteins
SUMO	Small Ubiquitin-like Modifier
TRIM	Tripartite Motif
UV	Ultraviolet

Table of Contents

Abstract.....	3
Acknowledgments.....	4
List of Abbreviations	8
Table of Contents	10
List of Figures.....	13
Chapter 1: Introduction.....	15
1.1 The multiplicity of functions of nuclear bodies.....	15
1.1.1 Nucleoli	17
1.1.2 Cajal bodies	18
1.1.3 Nuclear Speckles.....	18
1.2 Form and function of Promyelocytic Leukemia (PML) bodies.....	21
1.2.1 Formation of PML bodies.....	21
1.2.2 Disparate Functions of PML bodies.....	22
1.2.3 PML bodies in protein quality control.....	24
1.3 SCA1: a model system for RNA and proteotoxic stress	28
1.3.1 SCA1 RNA toxicity	29
1.3.2 SCA1 proteotoxicity.....	30
1.4 mRNA surveillance mechanisms	33
1.5 Evidence for peptide synthesis in the nuclear compartment.....	36
1.6 Significance	40

Chapter 2: Materials and Methods	43
2.1 Cell propagation and manipulation	43
2.1.1 Plasmids and oligonucleotides	43
2.1.2 Cell culture.....	43
2.1.3 Transfection of cells	44
2.1.4 Generation of stable cell lines	45
2.1.5 Extrinsic stress and drug treatment.....	46
2.2 Cell and molecular biology experiments	46
2.2.1 Antibodies.....	46
2.2.2 Immunofluorescence	47
2.2.3 Nuclear Ribopuromylation (RPM).....	48
2.2.4 Immuno-RNA fluorescence in situ hybridization (FISH)	49
2.2.5 RPM-RNA FISH	50
2.2.6 L-homopropargylglycine Protein Synthesis Assay	51
2.2.7 3D DNA immunoFISH	51
2.2.8 Fluorescence microscopy and image analysis	52
2.2.9 Super Resolution Microscopy	54
2.2.10 RNA isolation, cDNA preparation, and qPCR	55
2.2.11 Cell lysis and nuclear-cytoplasmic isolation	56
2.2.12 Western Blot	57
2.3 BioID Proteomics Analysis	58
2.3.1 Immunoprecipitation and preparation for mass spectrometry.....	58
2.3.2 Proteomics analysis.....	59
Chapter 3: Results	61

	12
3.1 Regulatory peptide synthesis at PML bodies during cellular stress	61
3.1.1 Background	61
3.1.2 Results	62
3.2 Identification of proteins conditionally associated with PML bodies	93
3.2.1 Background	93
3.2.2 Results	94
Chapter 4: Discussion and Future Studies	114
4.1 Discussion	114
4.1.1 A model for protein synthesis as a function of PML localized quality control.....	114
4.1.2 Overcoming the enigma of nuclear translation.....	120
4.2 Future Studies.....	127
4.2.1 Identify the PML isoform-specific interactome.....	127
4.2.2 Quantitative proteomics analysis of PMLIV during cell stress conditions	128
4.2.3 Characterization of transcripts translated at PML bodies during cell stress	131
References	134

List of Figures

Figure 1.1 Illustrative interpretation of NB assembly.

Figure 1.2 PML bodies are sites of protein quality control.

Figure 1.3 Expanded-mutant Atxn1 causes both mRNA foci and aggregated protein products.

Figure 1.4 A collection of recent reports support the possibility of peptide synthesis in the nucleus.

Figure 3.1 84Q-ATXN1 mRNA is retained in the nucleus.

Figure 3.2 84Q-ATXN1 mRNA associates with PML bodies.

Figure 3.3 Nuclear speckle interaction with CAG repeat RNA remains constant in SCA1.

Figure 3.4 Knock-down of PML does not significantly alter *ATXN1* foci.

Figure 3.5 CAG-Repeat mRNA significantly associated with PML bodies in SCA1 patient cells.

Figure 3.6 Endogenous repeat expanded ATXN1 mRNA is absent from nucleoli.

Figure 3.7 PML bodies interact with expanded repeat HTT mRNA foci.

Figure 3.8 RPM technique is verified to detect nuclear translation in IMR-90 fibroblasts.

Figure 3.9 Translation signal relocalizes to PML bodies during 84Q-Atxn1 expression.

Figure 3.10 Active translation signal via HPG localizes with 84Q-Atxn1 inclusions.

Figure 3.11 Ribosomal Stalk Proteins associate with PML bodies.

Figure 3.12 RPLP0 associates with PML bodies during cell stress.

Figure 3.13 Active translation signal associates with PML bodies and 84Q-Atxn1 inclusions.

Figure 3.14 Active translation signal significantly increases in association with 84Q-ATXN1 mRNA.

Figure 3.15 Modulation of PML expression disrupts peptide synthesis and mutant Atxn1 aggregates.

Figure 3.16 Ifn β treatment disrupts nuclear translation localization and 84Q-Atxn1 expression.

Figure 3.17 Polypeptide synthesis localizes to nucleoli and PML bodies in human IMR90 fibroblasts.

Figure 3.18 Signature No-Go decay proteins associate with 84Q-ATXN1 mRNA foci.

Figure 3.19 Proteotoxic stress alters the nucleo-cytoplasmic distribution of No-Go decay proteins.

Figure 3.20 Diminished expression of Hbs1L and PELO increases mutant Atxn1 expression.

Figure 3.21 Ectopic expression of Hbs1 and PELO decreases expression of 84Q-Atxn1 and alters nuclear morphology.

Figure 3.22 In vivo crosslinking of cellular proteins do not yield PML binding partners.

Figure 3.23 Validation of BirA* fusion proteins in HeLa cells.

Figure 3.24 Timecourse of biotin incubation reveals proper incubation time for proteomics analysis.

Figure 3.25 Validation of BirA* fusion proteins in HEK293 cells.

Figure 3.26 Validation of mycBirA* fusion proteins stably expressed in HEK293 cells.

Figure 3.27 PML binding partners are enriched in BioID analysis of PMLIV.

Figure 3.28 Known binding partners of PML identified as a subset of interacting proteins.

Figure 3.29 PML interacting partners are predominantly nuclei acid binding proteins.

Figure 3.30 Identified proteins largely overlap between cell stress conditions.

Figure 3.31 RNA binding proteins are enriched at PML bodies during proteotoxic stress.

Figure 3.32 Cytoskeletal and RNA-binding proteins are enriched at PML bodies during UV irradiation stress.

Figure 3.33 Initial quantitative analysis of PML binding proteins during cell stress did not reveal enriched proteins.

Figure 4.1 Model of regulatory translation at PML bodies in response to proteotoxic stressed induced by 84Q-ATXN1.

Chapter 1: Introduction

1.1 The multiplicity of functions of nuclear bodies

The nucleus consists of an interconnected network of chromatin and nuclear bodies that dynamically assemble into defined spaces to carry out diverse functions. These spaces are non-random and represent distinct domains of the larger organelle (1). Nuclear bodies are sub-organelles that serve as distinct locations for condensed nuclear enzymatic or otherwise functional processes. Unlike the compartmentalization of cytoplasmic functions into membrane-bound organelles, nuclear bodies are non-membrane bound domains. Nuclear bodies consist of their signature proteins as well as associated proteins and nucleic acids. These domains classically represent distinct protein rich entities separate from the genome (2).

Nuclear bodies are largely multifunctional and their components can be dynamically exchanged with the nucleoplasm and assembled based on functional specificity. Nuclear bodies, including promyelocytic leukemia (PML) bodies, nucleoli, Cajal bodies, nuclear speckles, and polycomb group (PcG) bodies, are largely defined by their signature protein or nucleic acid counterparts in both composition and function. However, nuclear bodies are highly complex entities in both composition and function with several protein and nucleic acid components dynamically interacting with each nuclear body depending on cellular conditions (3). In fact, it is sometimes difficult to identify a key underlying function of a type of nuclear body due to its compositional diversity even within a single nucleus. Additionally, several components of a given nuclear body are shared with other types of nuclear bodies. Also, any component of a given nuclear body can initiate the assembly of the nuclear body, demonstrating that the

signature proteins of nuclear bodies are not the only assembly initiation factor. Lastly, some nuclear bodies only form in certain cell types or only during certain cellular conditions. The lack of membranes in nuclear bodies serve to promote this dynamic assembly and disassembly of functional proteins (2).

Nuclear bodies exemplify the phenomenon of self-organization. In the cell, components of a non-membrane bound organelle self-assemble into functional entities (4). In the nucleus, this assembly has been shown to not be hierarchical or step-wise. Rather, nucleation of a nuclear body can be initiated by diverse components and condensed by stochastic interactions (5). Our laboratory uses the analogy of crowdsourcing common to the Web 2.0. This analogy involves any entity that seeks an answer to a problem on the internet. The seeker requests an answer to their problem on a crowdsourcing forum, with a myriad of diverse entities that can potentially solve the problem. These entities assemble according to availability, expertise, or communicating network and offer information until an answer is generated (6). This analogy can be applied to nuclear body assembly where a given cellular function is signaled to be carried out, then depending on proximity and functional capacity, proteins and nucleic acids self-assemble to carry out the function until it is complete (Fig. 1.1). This dynamic assembly is advantageous to the cell because it allows for quick condensation of enzymatic functions.

Another recent analogy that describes the condensation of nuclear bodies as well as other membrane-less functional components of a cell that require fast enzymatic response is the liquid droplet model. This model postulates that proteins and nucleic acids condense according to hydrophobicity, proximity, binding affinity, and charge and result in liquid-liquid phase separation. These interactions are individually weak, allowing for the easy exchange of nuclear

body components with the nucleoplasm. This biophysical model can explain both physiologically functional entities of a cell that contain protein and RNA, as well as pathological formations in diseases that arise from aggregated proteins (7). Both the crowdsourcing model and the liquid droplet model are helpful visual representations of nuclear body composition and assembly.

There is a vast body of evidence for the multifunctionality and cooperation of nuclear bodies and the number of functions assigned to a given nuclear body is increasing. Below are brief examples of the multifunctionality of nucleoli, Cajal bodies, and nuclear speckles. PML bodies will be discussed in depth in section 1.2.

1.1.1 Nucleoli

Nucleoli are the most prominent and well-studied nuclear bodies. The most distinguishing characteristic of this complex and large nuclear body is the capacity for ribosome biogenesis. Unlike most nuclear bodies, that organize around a signature protein, nucleoli are organized around a core of rDNA repeat arrays. This self-organization of specific genomic loci makes nucleoli hubs for rRNA transcription and processing, in addition ribosomal subunit assembly (8, 9). Nucleoli have long been used as morphological markers for cancerous cells due to their prominence in the nucleus and the ease of detecting their disruption. Beyond well-known functions and morphology, nucleoli are highly multifunctional with important regulatory roles in cell-cycle progression, stress response, and p53 mediated senescence (10, 11). One focus of study shows that nucleoli act as stress sensors and when their formation is disrupted by UV irradiation or other cell stresses, levels of p53 increase and the tumor suppressor gene is stabilized. This response is dependent on nucleolar disruption because DNA damage alone

without rDNA disruption does not trigger p53 stabilization (11). The ability of nucleoli to detect cell stress make the nuclear body an important diagnostic tool.

1.1.2 Cajal bodies

Cajal bodies are classically defined as distinct NBs that serve as sites of initial processing and maturation of small nuclear ribonucleic particles (snRNPs) and small nucleolar ribonucleic particles (snoRNPs) (12). Cajal bodies are present in most eukaryotic cells and are visualized via immunofluorescence of the signature protein coilin. There is increasing interest in Cajal body function in telomere maintenance, as a subset of Cajal bodies interact with telomeres during S phase (13). Additionally, a body of research addresses Cajal bodies' role in supporting telomerase function in both stem cells and cancer cells (14). One study indicates that telomerase Cajal body protein 1 (TCAB1) and coilin-dependent Cajal body formation act independently to recruit telomerase to telomeres. Depletion of TCAB1 or coilin separately causes a reduction of telomerase recruitment, proving the requirement of Cajal bodies in telomerase function. This requirement seems to be based on the ability of the NB to concentrate telomerase at telomeres since overexpression of telomerase in the absence of coilin rescues telomerase localization (15). This study illustrates the importance of nuclear NBs in concentrating components to efficiently carry out nuclear processes.

1.1.3 Nuclear Speckles

Nuclear Speckles, also known as interchromatin granules or SC-35 domains, are classically defined as sites of storage and post-translational modification of mRNA splicing factors. There are 10-50 speckles in most mammalian cell lines with a jumbled beads-on-a-string morphology. Nuclear speckles are composed of SC-35 protein, snRNPs and serine-

arginine proteins, as well as several kinases and phosphatases for the processing of post-transcriptional machinery (16). Interestingly, several studies show that nuclear speckles tend to localize with several specific actively transcribing genes and on the edges of gene rich chromosome territories (17, 18). Based on their euchromatic localization, it is hypothesized that nuclear speckles support the structure and function of transcription factories. Actively transcribing genes loop away from their respective chromosome territories and localize to transcription factories. Looping of actively transcribed genes was confirmed by 3C analysis, RNA-TRAP and RNA-FISH (19). This looping and coalescing into transcription factories can occur between separate chromosomes from large distances. Studies on nuclear speckles exemplify the coordination between nuclear bodies and their functional components (20).

Several other nuclear bodies not discussed here have distinct and dynamic functions depending on their protein and nucleic acid composition. A central question in studying the cell biology of the nucleus is how numerous functions can be assigned to a given nuclear body in a given cellular condition. This question was central to my thesis and led me to concentrate on one of the most elusive and multifunctional nuclear bodies, the PML body.

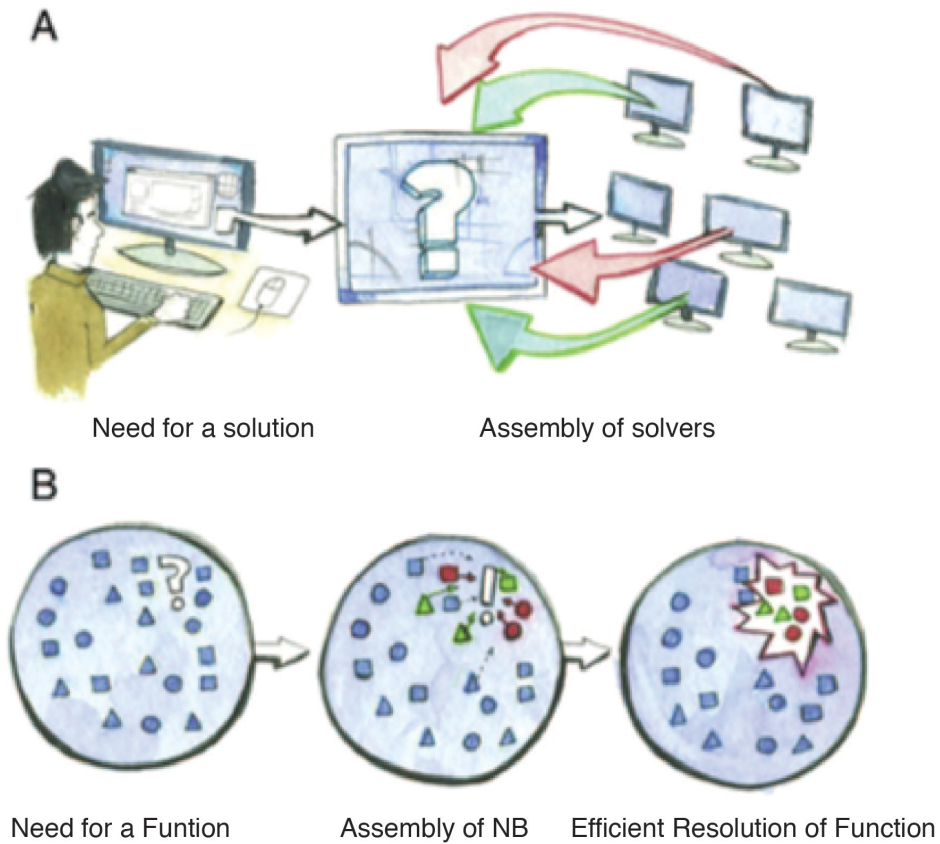


Figure 1.1 Illustrative interpretation of NB assembly. (A) A crowdsourcing model describes a stochastic assembly of problem solvers called upon by someone in need of a solution. The problem efficiently solved through collective action. (B) The crowdsourcing model is applied to functional nuclear organization in which nuclear functions are condensed in spaced for efficient resolution. Adapted from Wood et al. 2014 (21). Illustration by Scott Holterhaus.

1.2 Form and function of Promyelocytic Leukemia (PML) bodies

1.2.1 Formation of PML bodies

A prominent group of nuclear bodies, termed PML bodies or nuclear domain 10 (ND10), are multifunctional sub-organelles consisting of its signature protein, PML/TRIM19, and a heterogeneous composition of protein binding partners as well as nucleic acids. The PML protein itself is part of the tripartite motif-containing (TRIM) family of proteins that has a conserved TRIM region on the N terminal end, an NLS sequence, and a variable region at the C terminal end. The TRIM region of PML contains a ring finger domain, two B-box zinc finger domains, and a coiled coil domain (22). TRIM family proteins are all induced by interferons and play roles in cellular stress response. The variable C-terminus is responsible for at least 9 isoforms of the PML protein, all formed by alternative splicing. PML isoform IV is the best studied of the PML proteins, though all of the isoforms are able to nucleate a nuclear PML body. It is important to distinguish between PML bodies and free PML protein, since there is a high percentage of non-NB associated PML protein in the cell. Some isoforms of PML shuttle between the cytoplasm and the nucleus, while others are mainly nuclear. One isoform is cytoplasmic since the NLS is removed from splicing (23). All PML isoforms are themselves small ubiquitin-like modifier (SUMO) E3 ligases and have an ability to SUMOylate themselves as well as other proteins (24).

PML proteins, when SUMOylated, self-associate to form a shell around its interacting partners, forming a PML body. SUMOylation is necessary for PML body formation. PML bodies exist as 5-30 punctate structures in most mammalian cell lines and tissues (25). Surprisingly, however, PML bodies are not essential for cellular survival or organismal survival.

Among the over 200 documented PML interacting partners include those that function in tumor suppression, post-translational modification of proteins, immune surveillance, and apoptosis (26). Some of the most prominent and well-studied PML body components include Daxx, ATRX, and Sp100, each of which function in anti-tumor and DNA regulation. Most proteins that associate with PML are able to be SUMOylated (27). Additionally, PML bodies associate with some RNAs, though the identity of such RNAs is not yet defined and the function of RNA association is unclear (28). PML bodies are proposed to be important for virtually all cell regulatory processes due to their association with the myriad of protein binding partners.

PML nuclear bodies were originally characterized by their involvement in acute promyelocytic leukemia (APL), caused by the t(15;17) translocation of PML gene locus with retinoic acid receptor-alpha gene (RARA). The resulting PML/RAR- α fusion protein disrupts the localization of PML bodies. Treatment with all trans retinoic acid or arsenic trioxide rescues PML body formation by restoring PML's capacity to be SUMOylated (29).

1.2.2 Disparate Functions of PML bodies

Like other nuclear bodies discussed in Chapter 1.1, PML bodies are largely multifunctional and depend on their associated protein and nucleic acid binding partners. PML body composition dynamically changes depending on cell type and condition. In the current literature, the composition of PML bodies during varied cellular conditions is ill defined. In fact, the large number of PML body-associating proteins can be explained by the varying interactions during different conditions or even within one cell. Studies have shown PML to have functional capacity in DNA damage repair, transcriptional regulation, tumor suppression, senescence, apoptosis, antiviral response, innate immune response, and post-translational modification and

regulation of proteins (30). *Importantly, PML bodies are important components of the cellular stress response.* Below is a selection of PML body functions.

PML bodies are sensitive to stressors that cause DNA damage, such as ultraviolet (UV) irradiation. PML bodies disperse somewhat during UV irradiation, forming smaller bodies at greater numbers (22). PML bodies respond to this cell stress promoting double strand break (DSB) repair. Binding partners of PML bodies include ATM, ATR, MRN (Rad50/Mre11/NBS1), and Rad51/52 complexes, among many other repair proteins such as RecQ helicases WRN and BLM (31, 32). Upon UV irradiation, PML bodies are recruited to damaged DNA foci, where they associate with DSB repair proteins. Localization of PML bodies to damaged DNA is dependent on clustering of repair proteins, as tethering repair proteins to chromatin in the absence of DNA damage is sufficient to recruit a PML body (33). A recent study revealed that PML bodies are important for the later stages of DSB repair, as PML knock-down cells have 10-fold less DSB repair even with sufficient phosphorylation of H2AX (34). These studies highlight PML's ability to sense and respond to UV irradiation stress.

Several other studies indicate that PML bodies respond to a variety of stresses, such as oxidative stress. PML body morphology changes from several small nuclear dots to few large ring-like structures when exposed to oxidative stress. One main way PML responds to the cellular reactive oxygen species (ROS) environment is by the regulation of the ROS detoxification transcription factor NRF2. PML bodies sense the level of ROS toxicity by regulating the level of NRF2 in the nucleus. In cells with suppressed expression of PML, NRF2 expression increases (35). These studies indicate that PML bodies can regulate the expression of ROS detoxifying genes through the degradation of NRF2.

Several studies show PML interaction with sites of active gene loci and nascent mRNA transcription (25). Notably, PML bodies nonrandomly interact with the major histocompatibility complex (MHC) locus and this interaction is strengthened upon interferon-gamma (IFN- γ) stimulation (36). A prominent study depicted that PML bodies co-regulate IFN- γ mediated MHC class II expression through stabilization of a MHC transactivator, suggesting that PML bodies regulate transcription at the MHC locus (37). Another study using immuno-TRAP technology uncovered direct PML body interactions with the promoter regions of TP53, TFF-1, ABCA, and surprisingly, the PML gene loci (38). Overall, evidence suggests PML bodies regulate and promote transcription at certain transcriptionally active genomic loci and participate in innate immune protection of the cell.

Several studies show PML bodies are essential in the anti-viral response as well as the general innate immune response. The largest evidence for this is the interferon response element in the promoter region of the PML gene (30). Additionally, PML bodies are shown to associate with, and regulate the growth of RNA and DNA viruses such as SV-40 and adenovirus E4-ORF3 (39). PML bodies are shown to repress viral replication through epigenetic silencing of viral nucleic acid. Several viruses disrupt PML body formation, such as human cytomegalovirus (CMV) and herpes simplex virus (HSV), showing that disruption of PML bodies is a necessary evolutionary function of some viruses for survival and providing evidence for PMLs protective role in the innate immune system (40, 41).

1.2.3 PML bodies in protein quality control

Probably the most well defined function of PML bodies is the post-translational modification and regulation of proteins. This function relies on PML's capacity as a SUMO E3

ligase and it is postulated that PML post-translational modification of proteins contributes to its multifunctionality. PML itself also has a SUMO-interacting motif, forming structured multimers through SUMOylation (29). Beyond PML protein itself, several PML binding partners function in acetylation, ubiquitination, and SUMOylation of proteins. Additionally, PML associates with proteases (42). Specifically, PML bodies are hypothesized to sequester, modify and sometimes degrade partner proteins (43). These functions make PML an essential component of protein quality control (PQC) in the nucleus. For example, PML modulates p53 activity through post-translational modification of several proteins that stabilize p53. PML interacts with p53-ubiquitin ligase, MDM2 and sequesters it to the nucleolus during DNA damage, causing the stability of p53. PML also physically associates with p53, promoting its activation (44, 45). Because of this function, PML is known as a promoter of senescence and apoptosis, giving it the ability to be a strong tumor suppressor in these conditions.

PML bodies are shown to regulate and degrade misfolded proteins as part of its protein quality control functionality. Several studies indicate that PML specifically functions in the post-translational modification and subsequent degradation of aggregation prone proteins through PML-associated proteasomes. An example of this type of protein heavily cited in the literature is Ataxin, a family of large proteins prone to misfolding and aggregation when mutated (see section 1.3 for a detailed description of Ataxin). PML bodies strongly associate with nuclear aggregated proteins such as mutated Ataxins and intrinsically contribute to their degradation (46).

Overexpression of PML leads to the increased degradation of Ataxins while disruption of PML expression increases Ataxin expression (47). Additionally, induction of PML expression via the interferon response leads to increased degradation of Ataxins. An additional study showed that

increased expression of PML *in vivo* contributes to improved clearance of the misfolded and aggregated Ataxin protein (48). These studies introduced PML bodies as a site for regulation of dysfunctional proteins specifically localized to the nucleus.

A comprehensive 2014 study detailed a mechanism behind PML's function in degrading misfolded proteins. PML protein's SUMO E3 ligase activity works in concert with a SUMO dependent ubiquitin ligase, RNF4, to tag Ataxin type 1 (Atxn1) proteins for degradation. Specifically, PML directly tags Atxn1 with SUMOs for recognition by RNF4. Then RNF4 tags the SUMOylated protein and targets it for proteasomal degradation (Fig. 1.2). This mechanism can be applied to other misfolded proteins such as expanded mutant Huntington (Htt) (49). This study illustrated a unique nucleus-localized system for degrading misfolded proteins and highlighted the importance of the nuclear compartment for protein quality control.

The evidence for PML in protein quality control is mounting and convincing, though the mechanism for PML regulation of aggregation-prone proteins like Ataxin is incomplete. Additionally, how PML's protein quality control function is incorporated into the multiplicity of PML bodies' functions is unresolved. How does PML's protein quality control function relate to PML's role in regulating cell stress in general? It is PML body's function in protein quality control that was a main focus of my thesis work, expanding on the function of PML bodies in regulation of Ataxin as well as PML's role in the cellular response to stress. For the majority of my thesis work, I used the model system of Ataxin-based cell stress to define PML's role in regulating cellular stress. The following section is a description of the model system.

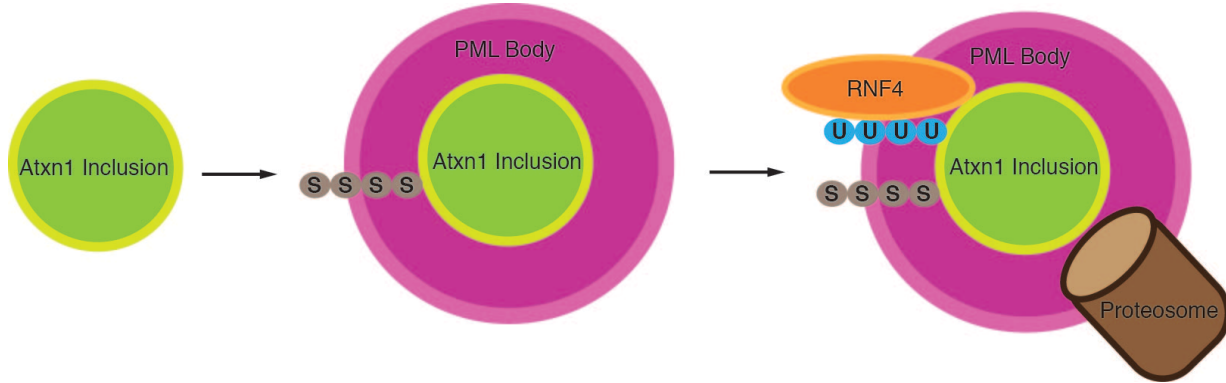


Figure 1.2 PML bodies are sites of protein quality control. Accumulated misfolded Atxn1 protein forms inclusions that colocalize with PML bodies. PML's SUMO E3 ligase activity leads a SUMO-dependent ubiquitin ligase RNF4 to function in the proteasomal degradation of Atxn1 protein at PML bodies.

1.3 SCA1: a model system for RNA and proteotoxic stress

Spinocerebellar Ataxia Type 1 (SCA1) is a polyglutamine (or polyQ) disease, an autosomal dominant genetic disorder caused by an expansion of CAG microsatellite repeats somewhere within the affected gene. SCA1 manifests as a neurological disorder and causes deterioration of neurons and Purkinje in the brain stem and cerebellum. SCA1 patients progressively lose control of their bodily movements and the disease is ultimately fatal (50). Polyglutamine diseases are also known as CAG repeat disorders. Polyglutamine diseases are in the family of trinucleotide repeat disorders (also termed triplicate repeat expansion disorders, trinucleotide repeat expansion disorders, and codon reiteration disorders). Over half of the known trinucleotide repeat disorders are CAG repeat expansion/polyglutamine diseases, including several SCAs as well as Huntington's disease- 9 CAG repeat expansion disorders are clinically described (51). The other trinucleotide repeat disorders, such as fragile X syndrome or myotonic dystrophy are caused by other triplicate repeats. Trinucleotide-repeat disorders are rare and no cure or affective treatment for any of the diseases exists currently. These disorders collectively share several molecular and cellular pathologies with the broader list of repeat-associated diseases, such as amyotrophic lateral sclerosis (ALS) (52).

SCA1 specifically is caused by the expansion of CAG repeats in the coding region of the Ataxin-1 (ATXN1) gene. Normally, the ATXN1 gene contains about 4-30 CAG repeats. SCA1 and other CAG repeat expansion mutations are hypothesized to be caused by error-prone replication machinery and/or error-causing mutations in DNA-repair machinery. Overtime and across generations, the number of CAGs gradually increases until a disease threshold of about 40 CAG codons is reached. The number of repeats in patients can expand beyond 80, depending on

inheritance and severity. An increasing number of repeats is associated with earlier symptoms and a poorer disease outlook (50).

1.3.1 SCA1 RNA toxicity

SCA1 manifests itself in the cell by both RNA toxicity and proteotoxicity. When mutated ATXN1 is transcribed, the resulting mRNA contains a long stretch of CAG repeats. These repeats create a long, stable stem loop within the transcript. The longer the repeat is the longer and more stable the CAG RNA stem loop (53). Additionally, the number of non-CAG codons in the expanded CAG tract is inversely associated with toxicity (54). RNA cytotoxicity is a newly described phenotype shared by several repeat expansion disorders.

Several gain-of-function toxicities are associated with the repeat-expanded cytotoxic mRNA. First, these disordered mRNAs aggregate and form aberrant nuclear foci. These foci are visible via microscopy in several patient cell lines as well as *in vitro* (55). One study suggested these RNA foci have liquid droplet properties. The study demonstrated that multivalent base-pairing cause these transcripts to condense in space. Interestingly, these foci associated with RNA-rich nuclear speckles (56). Additionally, these foci have been shown to sequester away several important RNA-binding proteins from their normal functions. For example, the splicing factor SRSF6 binds to the CAG repeats in the expanded mutant Huntington transcript, causing altered splicing of the transcript (57). Disruption of normal nuclear function by protein sequestration may be a major source of cytotoxicity from trinucleotide repeat disorders.

Additional forms of RNA toxicity arise from abnormal bidirectional transcription of the CAG tract, creating a noncanonical anti-sense RNA transcript that in turn can translate into repeat-containing polypeptides. Both the sense and anti-sense mRNAs can be translated through

a pathogenic repeat-associated non-AUG (RAN) translation. This type of translation uses the expanded repeat to dock the translation initiation machinery (58). RAN translation was first reported by Zu et al. using ATXN8 constructs with expanded CAG repeats lacking the start codon (59, 60). They demonstrated that long hairpin structures formed by CAG repeats induce RAN translation and result in the expression of poly-serine or poly-alanine tract proteins in addition to poly-glutamine. RAN translation has now been observed in multiple nucleotide repeat expansion disorders, including Huntington disease, and fragile X syndrome (61, 62). Though, the mechanism and required translation machinery for RAN translation, in addition to the toxicity of the resulting polypeptides is currently unclear. RNA toxicity is an emerging field of study within several neurological disorders and its implications for potential therapeutics is encouraging.

1.3.2 SCA1 proteotoxicity

In addition to RNA phenotypes, SCA1 manifests in disordered Atxn1 proteins. Translation, by canonical AUG-dependent or RAN mechanisms, of the ATXN1 transcripts creates a protein with an expanded polyglutamine tract (60). Studies hypothesize that SCA1 can arise from either loss-of-function of the wild-type Atxn1 protein, gain-of-function of the expanded mutant, or both. The function of the wild-type Atxn1 protein is still under investigation, though it is shown to be a transcriptional regulator of Notch signaling and may be involved in RNA processing (63). Some studies indicate that loss-of-function of Atxn1 protein contributes to disease, because Atxn1-null mice display decreased motor neuron function (64). However, the correlation between the number of repeats and the severity of SCA1 indicates that a gain-of-function of the mutant transcript and protein is the primary mode of pathogenicity (50).

One recent study identified that mutant Atxn1 association with its binding partner capicua (CIC) is the major source of the gain-of-function pathology of SCA1 (65). This study highlights the importance of clearance of the mutant form of Atxn1.

The expanded protein tract in Atxn1 causes the protein to misfold and aggregate in the nucleus. Atxn1 aggregates are extremely difficult to degrade due to their insolubility. Overtime, these protein aggregates accumulate and eventually, these aggregates form large inclusion bodies visible by microscopy (46). In addition, RAN-translated proteins may contribute to the aggregates although more research is needed to confirm this (60). Neurons, post-mitotic cells incapable of distribution of Atxn1 protein through cell division, cannot clear the Atxn1 proteins faster than the rate of their accumulation, resulting in more aggregation of Atxn1 proteins in these specific cells (depending on relative expression in neuron cell type) (66). Protein aggregation is a common phenotype of most repeat expansion disorders, and research on the regulation and clearance of aggregates is a large area of study. However, controversy remains over if protein aggregation in mammalian cells causes toxicity or if it is a defense mechanism of the cell to sequester the misfolded proteins (67).

ATXN1 is expressed in several tissues, most significantly in the neural tissues described, where pathogenic expression of the gene is of primary concern. Primary cells and tissues expressing repeat expanded ATXN1 contain RNA foci, but not large protein aggregates. This is due to the cells ability to divide and distribute the aggregated proteins. An exception of this is in late-stage diseased brain stem neurons, where large inclusion bodies were found in patient tissue. These neurons cannot distribute the aggregated proteins through cell division because they are post mitotic (50).

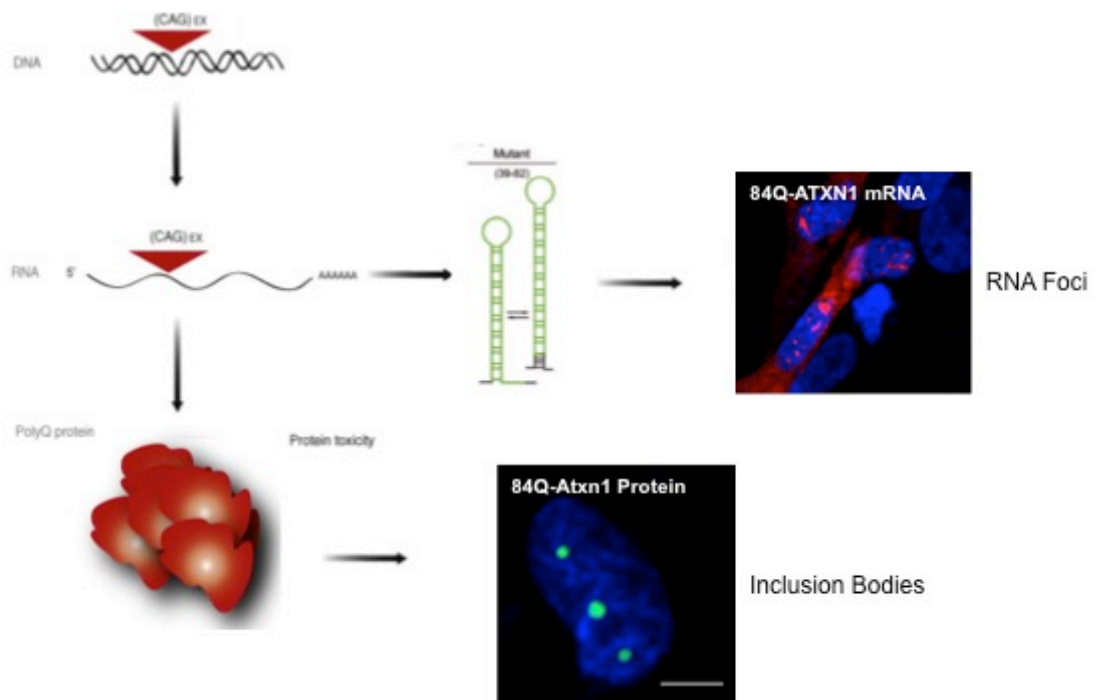


Figure 1.3 Expanded-mutant Atxn1 causes both mRNA foci and aggregated protein products. SCA1 is caused by an expansion of CAG repeats in the coding region of the *ATXN1* gene. Transcription of expanded mutant *ATXN1* leads to highly structured CAG mRNAs that sequester RNA binding proteins. When translated, the protein contains a long polyglutamine tract that causes it to misfold and aggregate. Adapted from Galaka-Marciniak 2012 and Wood M Trends in Genetics 2009.

As described in section 1.2.3, studies of PML's role in the regulation and clearance of Atxn1 proteins are robust. However, the role of PML or any other nuclear component in the regulation of ATXN1 mRNA remains limited. Since RNA toxicity is newly described as a major contributor to the SCA1 disease phenotype, it is crucial to understand the regulatory mechanisms of the cell that combat mutated mRNAs. A large goal of my thesis was to determine if there is a relationship between PML bodies and ATXN1 mRNA and determine if a regulatory mechanism exists that defines this relationship. Below are mechanisms that we hypothesize may contribute to the nuclear and/or PML-based regulatory function that controls mutated ATXN1 gene products.

1.4 mRNA surveillance mechanisms

A functional proteome relies on the sequence accuracy of the mRNA transcripts as well as the folding accuracy of the newly synthesized proteins. Misregulation of protein production over time can cause proteopathies including most of the major neurodegenerative disorders, as well as cancer and other age related diseases (66). SCA1 for example, described in detail above, is caused by a major defect in quality control mechanisms. For this reason, quality control mechanisms exist at every step of the central dogma of molecular biology, from replication of DNA, transcription of mRNAs, to protein synthesis and degradation. Quality control functions are crucial for normal protein homeostasis, and they can act as a first defense for pathologies. Numerous protein quality control mechanisms exist at the level of the ribosome, including mRNA surveillance and co-translational modification of peptides (68, 69). One study predicts that up to 30% of nascent polypeptides are subject to proteasomal degradation. Longer, more

complex proteins are more likely to be subject to regulation at the level of translation (69). These ribosome-based mechanisms are defined by non-canonical translation and may be a major source of post-transcriptional quality control. Specifically, mRNA surveillance mechanisms may represent a significant source of mRNA and protein regulation (70). Here I will briefly describe the state of the literature of mRNA surveillance mechanisms that specifically relate to polyglutamine disorders.

mRNA surveillance spans the gap between RNA and protein quality control. In general, RNA surveillance is a group of mechanisms that monitor mRNA health at the level of translation. In the presence of an aberrant mRNA transcript, ribosomes stall. This causes the dissociation of the ribosome from the transcript and leads to the degradation of the transcript and the nascent polypeptide. There are three known mechanisms of mRNA surveillance; nonsense-mediated decay (NMD), non-stop decay (NSD), and no-go decay (NGD). NMD is the best studied of the mRNA surveillance mechanisms. Most studies of mRNA surveillance mechanisms are performed in yeast models. Only a handful of studies on NMD and even less studies on NSD and NGD currently exist in the literature (71). Because of these limitations in the literature, there are several questions yet to be answered about the specificities of mRNA surveillance. However, the importance of these mechanisms for the regulation of protein synthesis in higher eukaryotes is becoming apparent with each new study.

Briefly, NMD occurs when an mRNA transcript contains a premature termination codon (PTC). This arises from either any nonsense mutation that arises from a missense, addition, or frameshift mutation. If the premature stop/termination codon occurs before an exon junction, communication occurs between the exon junction complex and the upstream terminated

ribosome via the protein Upf1. This signals for the cell to recycle the ribosome and degrade the mRNA transcript and nascent polypeptide (72).

NSD and NGD are related in cellular recognition and potential mechanism, but are caused by different aberrations. NSD occurs when a mutation results in the lack of a stop codon. The ribosome then stalls in the poly-a tract of the transcript. NGD occurs from a range of mutations or defects that cause a stall of a ribosome in the coding region of mRNA. This could be from a defect on the growing polypeptide chain or an aberrant mRNA structural feature. The two proteins HBS1L and Pelota (HBS1 and Dom34 in yeast respectfully), bind to the A site of the stalled ribosome, causing dissociation and recycling of the ribosome. HBS1L and Pelota (PELO) are related to the canonical translation termination factors eRF1 and eRF3 respectfully. Binding of the dimer also triggers endo- and exo-nucleolytic cleavage of the mRNA as well as degradation of the nascent polypeptide. Though the mechanism of this action in eukaryotes remains unknown (71, 73).

We became interested in NGD specifically because it is the mechanism that could be the basis of translation-based regulation of structured mRNAs such as those caused by triplicate repeat disorders. Specifically, NGD is shown to respond to abnormally stable stem-loops that cause ribosomal pauses (74). Since mutated ATXN1 has the hallmark phenotype of a stable stem-loop, we proposed to probe the possibility of NGD occurring in the nucleus and possibly at PML bodies. We hypothesized that NGD was part of PML bodies' protein quality control function and represented a major source of regulation both during cellular homeostasis and during disease. The possibility of NGD occurring at PML bodies as a continuation of its protein quality control raises the possibility of the controversial phenomenon of nuclear translation.

Below is a description of the current literature that is most convincing of this unique phenomenon.

1.5 Evidence for peptide synthesis in the nuclear compartment

Nuclear translation has a long history of controversy. Nuclear translation was first described in the 1950's and again in the 1970's (75, 76). These studies, respectively, showed incorporation of radioactive amino acids into nuclear proteins and the isolation of polyribosomes from the nucleus. Although this evidence was compelling, most biologists dismissed nuclear translation altogether. In 2001, the Cook laboratory breathed new life into the contentious hypothesis of nuclear translation (77). However, this study garnered more controversy than clarity, and the findings were later attributed to contamination by cytoplasmic ribosomes (78-80). Despite earlier criticisms, in 2012 the Yewdell group concretely demonstrated that nuclear translation can be detected using the novel ribopuromycylation (RPM) method. RPM uses inhibitors of translation elongation to stall polyribosomes with nascent polypeptides on mRNA transcripts (81). RPM is followed by ELISA or immunofluorescence microscopy and can be used to detect the localization patterns of cytoplasmic and nuclear translation in several cell types (82). This research demonstrates that nuclear translation occurs in immortalized and primary cell lines and is enriched in the nucleolus.

Since the development of RPM, several independent studies have utilized the technique to detect active peptide synthesis both in the nucleolus (83, 84). The flagship study using the RPM method primarily detected protein synthesis in the nucleolus and hypothesized that nucleolar translation occurs to test the functionality of newly synthesized ribosomes (81).

Translation in the nucleolus of live cells was also observed using a highly sophisticated imaging technique: vibrational imaging of newly synthesized proteins by stimulated Raman scattering microscopy (85). However, RPM signal and actively translating ribosomes have also been described in the nucleoplasm in multiple studies. One such study used a variation of FRAP called BiFC to elegantly demonstrate the assembly of 80S polysomes within the nucleus. This study found the 80S ribosomes to be translationally active and localized to both the nucleolus and the nucleoplasm. They hypothesized the role of nuclear translation in “test-translating” nascent mRNA transcripts before they were exported to the cytoplasm for canonical translation (86). Another study reported detecting nuclear protein synthesis following protein degradation with pulses as short as 5 sec using 3 different labeling techniques: RPM, L-azidohomoalanine (detected after attaching fluorophores using ‘click’ chemistry), and ‘heavy’ amino acids (detected using secondary ion mass spectrometry) (87). This study suggested that this extremely short turnover of newly synthesized peptides suggests a regulatory role for nuclear translation.

Other studies postulated regulatory roles for non-canonical nucleus-localized translation. The detection of nuclear translation in cells from both flies and mammals suggests this is a conserved regulatory process. One study demonstrated that nuclear translation as a way to produce antigens for the MHC class one pathway (83). They showed that scanning ribosomes were translating pre-spliced mRNAs in the nuclear compartment, producing small intronic peptides. This study highlighted a physiological role of nuclear translation in the regulation of newly transcribed mRNAs. Another study suggested that NMD could occur in the nuclear compartment (88). They found that mRNA transcripts that contained a PTC were sequestered in

the nuclear compartment and were translated by ribosomes that associated with the NMD factor Upf1. They suggested this as a mechanism for proofreading potentially cytotoxic mRNAs.

My thesis work expands upon these studies, suggesting that in addition to NMD, NGD may be an important physiological function of the nuclear compartment. Using the model system of ATXN1, and expanding the possibility of translation functioning during different cell stressors, I will describe a novel function of PML bodies during cell stress. This work will add to the multiplicity of PML body function to include a novel nuclear regulatory mechanism at the level of peptide synthesis that prevents proteotoxicity.

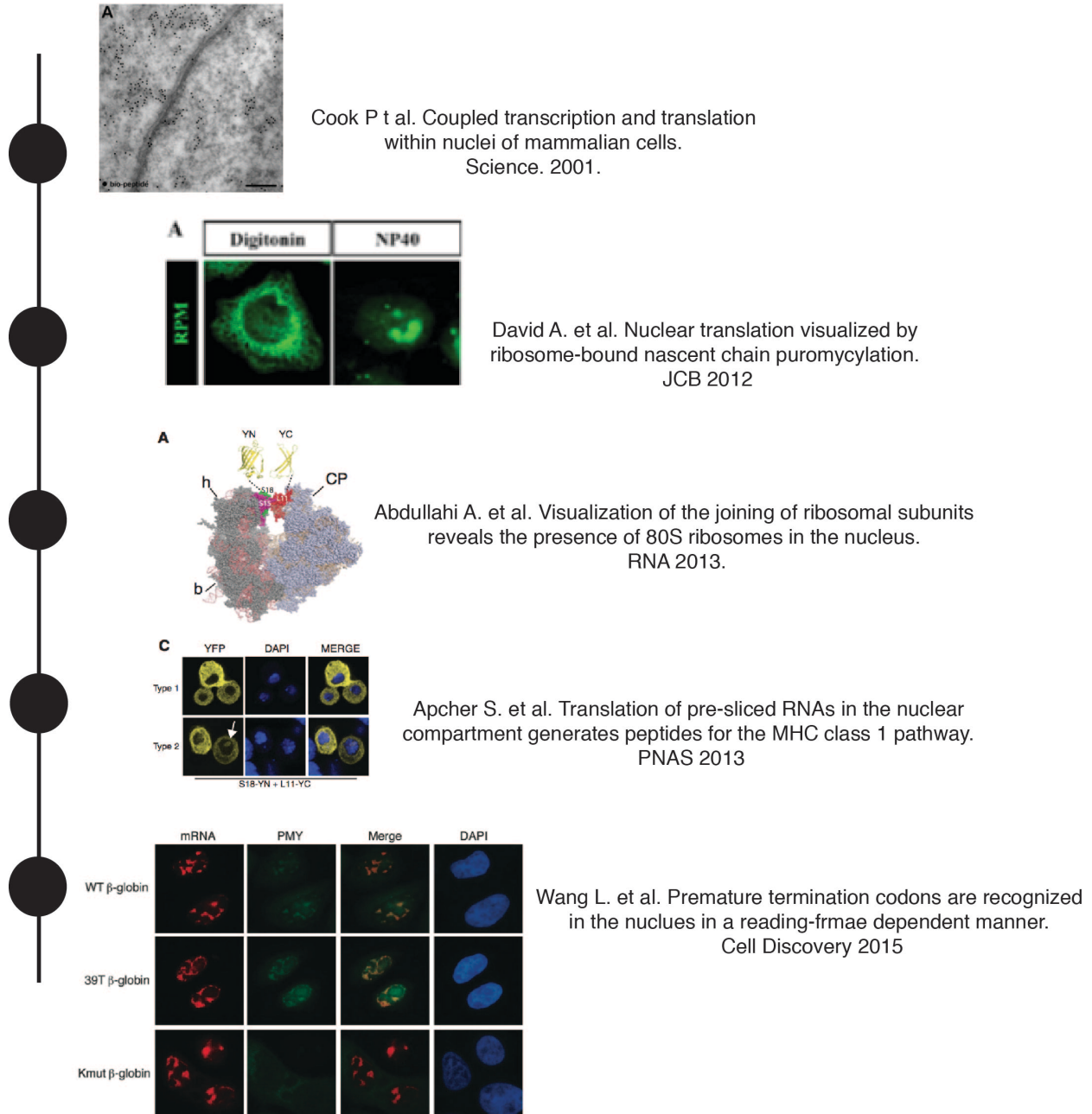


Figure 1.4 A collection of recent reports support the possibility of peptide synthesis in the nucleus. These recent inquiries began in 2001 with Peter Cook who proposed coupled transcription and translation. Then in 2012, The Yewdell group designed a method of detecting active translation by fluorescence microscopy. Also in 2013, the Abdullahi group found a portion of 80S ribosomes resided in the nucleus. Other studies proposed mechanisms for nuclear peptide synthesis as a way to generate peptides for the MHC class 1 pathway or as nonsense mediated decay. Adapted from the titles above (77, 81, 86, 88, 89).

1.6 Significance

The vast majority of cellular functions are highly coordinated processes that are subject to many levels of regulation. This is apparent when we consider the numerous ways in which a cell ensures proper function, such as cell cycle check-points, pathways that degrade defective transcripts and proteins, and the physical separation of cellular processes by membrane bound organelles. This suggests that very little is left to chance within the cell, and therefore it is not surprising that nuclear organization, which was once thought to be relatively random due to its lack of membrane bound organelles, is now known to be highly structured (90, 91). This organization occurs through the non-random positioning of chromatin within the nucleus and the formation of sub-nuclear bodies. Many nuclear activities are detected as discrete foci or structures, from replication foci and transcription factories. For many of these nuclear bodies, the protein components are well-characterized, but their coordinated function(s) remain elusive (90, 91).

Ribosomal proteins and translation factors have long been known to associate with NBs. Indeed, ribosome biogenesis takes place in the nucleolus, a canonical nuclear body and the primary site of nuclear translation described in the above studies (81). However, proteins involved in translation are also found outside of the nucleolus. PML bodies harbor multiple components of translation, including eIF4E, eIF3, and ribosomal proteins (92-96). PML bodies have many proposed functions, including the antiviral response, protein homeostasis, and apoptosis, but whether these pathways may be integrated through their PML association remains poorly understood (25). Multiple lines of evidence suggest that the PML NB plays a centralized role in the response to intrinsic and extrinsic cell stress (22, 25, 97-99). For example, PML

bodies co-localize with nuclear inclusions formed by proteotoxic neurodegenerative conditions such as SCA1 (100), and are found to function in the clearance of mutant Atxn1 proteins (101, 102). There is a growing body of evidence suggesting that protein degradation pathways are often coupled with translation-based mRNA scanning mechanisms (69). Despite the evidence that PML bodies contain translation factors and ribosomal proteins, no studies have directly examined whether protein synthesis occurs at this nuclear body as part of its function in protein homeostasis. *Our group hypothesized that PML bodies function as organizational hubs during cellular stress to coordinate the co-translational surveillance of structurally aberrant mRNAs and their encoded protein products, targeting them for degradation.*

Recent studies underscore the significance of non-canonical translation in both physiological and pathological conditions (103-105). For example, the co-translational nature of mRNA surveillance is being given greater consideration as a housekeeping mechanism for proteome health. Nuclear mRNA surveillance may represent another form of regulatory translation, testing specific transcripts that may induce proteotoxicity or cellular stress upon translation, and thereby linking mRNA surveillance with nuclear protein degradation pathways. These mechanisms, when characterized, can be harnessed through therapeutic intervention for several types of diseases that result in the loss of protein homeostasis. These diseases are largely age associated, including cancers and neurodegenerative diseases but can also include viral infections and other infectious diseases that manipulate PML body function or the cell's protein homeostasis. For example, increasing the expression of PML through interferon treatment may enhance PML's capability for Atxn1 protein regulation, thus alleviating the cell of Atxn1 protein accumulation (48). Additionally, characterizing different types of translation can allow us to

target pathological translation specifically, while leaving vital canonical translation alone.

Importantly, diseases such as cancers, that are intrinsically associated with a disruption in protein homeostasis, can be targeted through translation or PML body-specific therapies.

In the following studies, I test the hypothesis that PML bodies function as an organizational hub during cellular stress that coordinates the co-translational surveillance of structurally aberrant mRNAs and their encoded protein products, targeting them for degradation. I also employ proteomics techniques to identify proteins associated with PML bodies, and determined the dynamic changes in the composition of PML bodies as a function of stress. Then I explicate a possible mechanism of co-translational mRNA surveillance and protein quality control in regulating expression of genes encoding nucleotide-repeat expansions. This body of work contributed to our understanding of an underappreciated process, nuclear translation, and elucidate a novel, important function of the PML nuclear body with broad implications in human disease, including neurodegenerative disorders, cancer, and aging.

Chapter 2: Materials and Methods

2.1 Cell propagation and manipulation

2.1.1 Plasmids and oligonucleotides

pLEX-ATXN1 constructs with either 32Q-ATXN1 and 84Q-ATXN1 fused C-terminally to GFP in the pLEX-MCS cloning vector (Open Biosystems) were generously provided by Dr. Puneet Opal (Northwestern University). PMLIV and PMLV constructs in the pCDNA3.1 vector were generous gifts from Dr. Kun-Sang Chang (University of Texas MD Anderson Cancer Center). Myc-BirA-PMLIV was generated by PCR amplification of the PMLIV sequence from pCDNA3.1-PMLIV and insertion into pCDNA3.1 mycBioID construct (generously provided by Dr. Kyle Roux, Addgene #35700) between Xho1 and Not1 using standard cloning methods. Plasmids for expressing LacI fused human ribosomal proteins were generated by genomic DNA extraction of RPLP0, RPLP1, and RPLP2 from hematopoietic stem cells using DNeasy blood and tissue kit (Qiagen), amplification by PCR, and insertion between EcoR1 and Kpn1 of a GFP-LacI-NLS or mCherry-LacI-NLS (C1 backbone) construct (courtesy of Dr. Sui Huang). pFLAG-HBS1L and pFLAG-PELO constructs were a generous gift of Dr. Shinichi Hoshino (Nagoya City University).

siRNAs for target genes are as follows: Hs_PML_9, CACCCGCAAGACCAACAACAT; Hs_PELO_5, CTGAAGAGGATTAATGATTGA; Hs_HBS1L_7, CGAGGCTATAACTACGATGAA (Qiagen). Allstars Negative Control siRNA (Qiagen) was used as a negative control in all experiments.

2.1.2 Cell culture

IMR-90 normal human primary lung fibroblasts (ATCC), human Spinocerebellar Ataxia 1 fibroblasts (GM06927, Coriell Cell Repositories) with 52 CAG repeats on the affected allele, and human Huntington Disease fibroblasts (GM04287, Coriell Cell Repositories) with 50 CAG repeats on the affected allele, were cultured in Minimum Essential Medium alpha (MEM α , Invitrogen) supplemented with 15% fetal bovine serum (Atlanta Biologicals), 1% penicillin/streptomycin (Invitrogen), and 1% L-glutamine (Invitrogen). IMR-90 hTert passage-elongated fibroblasts, generated previously (Neems, D et al 2016), were cultured in MEM α supplemented with 10% fetal bovine serum, 1% penicillin/streptomycin, and 1% L-glutamine. HeLa-LacO cells with the stably integrated LacO array on chromosome 7 were kindly provided by Dr. Sui Huang (Northwestern University) and were cultured in DMEM (Invitrogen) supplemented with 10% fetal bovine serum, 1% penicillin/streptomycin, and 1% l-glutamine. HEK293 cells were cultured in DMEM (Invitrogen) supplemented with 10% fetal bovine serum, 1% penicillin/streptomycin, and 1% l-glutamine. All cells were cultured at 37°C in a humid 5% CO₂ incubator. All primary and primary-derived fibroblasts were split at 1:3 every 4-6 days. All transformed cell types were split 1:10 every 4-6 days. Cells were frozen in 10% DMSO in a liquid nitrogen tank for preservation.

2.1.3 Transfection of cells

DNA plasmids were transfected into cells after seeding on coverslips or plates using the PolyJet Transfection system (SignaGen) according to manufacturer's instructions. Briefly, cells were seeded so that cells were 50-90% confluent at the time of transfection (dependent on cell type). Culture media was replaced with half volume of fresh complete media. Plasmids were mixed with media without antibiotics or serum at the equivalent of 0.8 μ g DNA in 50 μ L media.

3 μ L PolyJet were mixed with 50 μ L media (no serum, no antibiotics) and immediately added to DNA and mixed. DNA mixture was incubated for 15 min at RT then added drop-wise to cells. Cells were incubated in DNA mixture for 5-18 hours then replaced with the full volume of fresh complete media. Cells were harvested or processed 18-24 hours after transfection of plasmids unless otherwise specified.

siRNAs were transfected into cells using the Pepmute Transfection System (SignaGen) according to the manufacturer. Culture media was replaced with half volume of fresh complete media. Plasmids were mixed with 100 μ L Pepmute transfection buffer at the equivalent of 5 nM siRNA for transformed cells and 30 mM siRNA for primary fibroblasts in a 6 well format. 2.4-3.6 μ L Pepmute were mixed with siRNA mixture and incubated for 15 min at RT. The siRNAs were then added drop-wise to cells. Cells were harvested or processed 72 hours after siRNA knock-down. For co-knock down of multiple genes, equal molar ratios of each siRNA were used. For co-transfections of siRNA and DNA, cells were incubated in siRNA for 48 h before co-transfection with DNA and incubated with siRNA/DNA for an additional 18-24 h.

2.1.4 Generation of stable cell lines

HEK293 cells stably expressing either myc-BirA* or myc-BirA*-PMLIV were generated by Geneticin selection following transfection (Thermo-Fisher Scientific). Briefly, HEK293 cells were tested for sensitivity to Geneticin before transfection of plasmids. A kill curve was generated by incubating HEK293 cells in normal media supplemented with 100 μ M, 200 μ M, 400 μ M, 600 μ M, and 800 μ M Geneticin for one week with a change of media every 2-3 days. 400 μ M was the optimal amount for Geneticin for selection. HEK293 cells were seeded onto 6 well plates 24 h before transfection at 30% confluency. Then cells were transfected with BirA*

constructs as described in section 2.1.3. 24 h after transfection, cells were expanded onto 10cm plates and 400 μ M Geneticin was added to media. Cells were cultured for 2-3 weeks and media with Geneticin was replaced every 2-3 days. Any visible colonies were harvested by washing once with PBS then replacing media with 0.05% trypsin in PBS. Single colonies were picked by manual aspiration using a pipet and careful scraping and aspiration under an inverted light microscope. Colonies were re-plated onto 12 cm plates. Approximately 1 week after re-plating, clones were split so that 1/3 of cells were seeded onto coverslips on 24 well plates and 2/3 were re-plated onto 12 well plates. Clones on coverslips were verified for correct localization patterns and ability to be biotinylated by 24 h incubation in media supplemented with 50 μ M biotin followed by immunofluorescence analysis (see section 2.2.2). Clones with correct localization in all visible cells were propagated in media with 200 μ M Geneticin and frozen down in liquid nitrogen for preservation.

2.1.5 Extrinsic stress and drug treatment

IMR90 cells were subjected to multiple extrinsic stresses including serum starvation in MEM alpha media without FBS for 24 hours, UV-C exposure for 25 minutes UV-C light in PBS, with 1 hour recovery, heat shock at 1 hour at 43°C followed by 30 minute recovery, and oxidative stress for 1 hour in 100 μ M H₂O₂ followed by 15 min recovery. For UV-C, heat shock, and oxidative stress experiments cells were allowed to recover in complete MEM alpha (MEM alpha with 15% FBS). Interferon beta treatment was done at 100 U/mL for 48 h.

2.2 Cell and molecular biology experiments

2.2.1 Antibodies

The following primary antibodies were used in immunofluorescence and western blotting: PML (rabbit, H-238; goat A-20 Santa Cruz 1:200 IF, 1:500 western), SC35 (mouse, s4045 Sigma, 1:1000 IF), Nucleolin (rabbit, ab22758, 1:2000 IF), C23 (goat, sc-9893, 1:25 IF), RiboP (human, ImmunoVision, 1:200 IF), Daxx (rabbit, M-112 Santa Cruz, 1:100 IF, 1:200 western), HBS1L (rabbit, HP A029729 Atlas, 1:100 IF, 1:200 western), PELO (mouse, F-8 Santa Cruz 1:50 IF, 1:100 western), Puromycin (mouse, MABE343 Millipore, 1:100 IF), Myc (rabbit, 9e10 Santa Cruz, 1:500 IF, 1:500 western), FLAG (mouse, sigma F1804 1:1000 western/IF), GFP (mouse, ab1218 Abcam, 1:500 western), Biotin (goat 1:10,000 western), alpha-tubulin (1:4000 western), HSP90 Lamin A/C (mouse, generous gift from Dr. Robert Goldman and Dr. Stephen Adam, Northwestern University, 1:1000 Western).

The following secondary antibodies were used for detection in immunofluorescence at 1:250 (Invitrogen): Donkey anti-rabbit Alexa Fluor[®] 594, donkey anti-rabbit Alexa Fluor[®] 647, donkey anti-mouse Alexa Fluor[®] 488, donkey anti-mouse Alexa Fluor[®] 594, donkey anti-mouse Alexa Fluor[®] 647, and donkey anti-human Alexa Fluor[®] 594 (Jackson ImmunoResearch). Biotin-conjugated goat anti-rabbit or anti-mouse was used for DNA FISH. For Western blotting the following antibodies were used for detection at 1:2000 to 1:10,000 (Abcam): goat anti-mouse-HRP and goat anti-rabbit-HRP and donkey anti-goat HRP.

2.2.2 Immunofluorescence

Cells of all types on coverslips were rinsed with PBS⁺⁺ and fixed with 4% paraformaldehyde (PFA) in PBS for 10 minutes at room temperature. Then cells were rinsed with PBS⁺⁺ and permeabilized for 15 minutes in 0.5% Triton X-100 in PBS⁺⁺ at room temperature (RT). Cells were then blocked in 10% goat or donkey serum for 30 minutes at room

temperature before incubation in primary and secondary antibodies diluted in blocking solution for 1 hour each at room temperature with 3 PBST (0.1% Triton X-100 in PBS⁺⁺) washes for 5 min in between antibody incubations. Cells on the coverslips were mounted on slides in Pro-Long Diamond Anti-Fade with DAPI (Invitrogen). Slides were cured overnight at RT before being sealed with clear nail polish.

2.2.3 Nuclear Ribopuromycylation (RPM)

Nuclear ribopuromycylation method was performed as described in (106) IMR-90, SCA1, HD, and HeLa-LacO cells on coverslips were incubated for 5 minutes in puromycin labeling media (complete MEM alpha with 45 μ M emetine and 91 μ M puromycin) in the 37°C incubator then rinsed with cold PBS. Pre-incubation of cells with anisomycin at 10 μ g/mL for 15 min or harringtonine at 2 μ g/mL for 15 min before labeling media was implemented for RPM controls. Other optional RPM controls were 15 m pre-incubation with emetine or a puromycin-only labeling media control. Cells were transferred to ice very carefully. The rest of the following steps were done with extreme caution as the cells were fragile and not well adherent to the coverslips well once the cytoplasm was removed. A 1 mL pipetman and 1 mL pipette tips were used to slowly add and remove buffers. The plate was not tilted or moved until buffer was removed from the wells. Permeabilization was performed for 5 minutes in permeabilization buffer with NP-40 (50 mM Tris-HCl, 150 mM NaCl, protease inhibitors, and 1% NP-40/IPGAL) in ice and washed with permeabilization buffer without NP-40 on ice. A no NP-40 control was included in all experiments. Cells were then fixed in 4% PFA at RT. Cells were washed with PBS after PFA incubation. Prior to primary antibody incubation, cells were blocked in RPM staining buffer (0.05% saponin, 10mM glycine, 5% FBS, in PBS). Primary and secondary

antibodies diluted in staining buffer were added to cells and incubated at 37°C for 1 hour or 45 minutes, respectively. Between antibodies and after the secondary antibody, cells were carefully washed with PBS 3 times. All steps starting with the secondary antibody were performed in the dark and the wells were shielded from light using foil during all incubations. Coverslips were mounted onto slides in Pro-Long Diamond Anti-Fade with DAPI (Invitrogen) and cured overnight at RT before being sealed with clear nail polish.

2.2.4 Immuno-RNA fluorescence in situ hybridization (FISH)

Cells on coverslips were rinsed with DEPC treated PBS and fixed with 4% PFA for 10 minutes at room temperature. Then cells were rinsed and permeabilized for 15 minutes in 0.5% TritonX-100 with 2 mM Ribonucleoside Vanadyl Complex (VRC, NEB) in DEPC-PBS at room temperature. Cells were rinsed with DEPC-2X SSC and incubated in 30% formamide in 2X-SSC for 30 minutes. The coverslips were inverted onto slides with 10 µL RNA hybridization buffer (30% formamide, 200 ng/ml salmon sperm DNA, 0.02% BSA, 10% dextran sulfate, 2 mM VRC, in 2X SSC) and 250 nM LNA oligonucleotide probe with a 5TYE563 fluorophore modification with the following sequence: /5TYE563/C+TGC+TGC+TGCTG+CTG+CTG+CT adapted from (107). Slides were sealed with rubber cement and incubated in a humid chamber at 37°C overnight. All steps starting on day two were performed in the dark and the wells were shielded from light using foil during all incubations. Cells were transferred into wells and washed with 2X SSC in 30% formamide two times for 10 minutes each at room temperature. Then cells were washed with 1X SSC for 10 minutes at room temperature. Cells were rinsed with PBS and fixed again in 2% paraformaldehyde for 10 minutes at room temperature. Cells were then processed for immunofluorescence detection of proteins as described above. For RNA FISH without

immunofluorescence, cells were mounted onto coverslips as described in the IF protocol after SSC washes on day 2. All coverslips were cured for 2-4 h at RT before sealing with clear nail polish. Slides were then transferred over to -20°C to prevent RNA signal fading or ideally imaged right away.

2.2.5 RPM-RNA FISH

Cells on coverslips were incubated for 5 minutes in puromycin labeling media then rinsed with cold DEPC-PBS on ice. The rest of the following steps were done with extreme caution as the cells were fragile and not well adherent to the coverslips well once the cytoplasm was removed. A 1 mL pipetman and 1 mL pipette tips were used to slowly add and remove buffers. The plate was not tilted or moved until buffer was removed from the wells. Permeabilization was performed for 5 minutes in permeabilization buffer with NP-40 and VRC on ice and washed with permeabilization buffer without NP-40 on ice. Cells were then fixed in 4% PFA at RT. Then cells were washed once with PBS, then incubated in DEPC 2X SSC for 20 minutes. Cells were inverted onto slides with 10 µL hybridization buffer and 250 nM LNA oligonucleotide probe with a 5TYE563 fluorophore modification. Slides were sealed with rubber cement and incubated in a humid chamber at 37°C overnight. All steps starting on day two were performed in the dark and the wells were shielded from light using foil during all incubations. Cells were transferred into wells and washed with 2X SSC one time for 10 minutes and washed with 1X SSC for 10 minutes both at room temperature. Then cells were washed with PBS and incubated for 15 minutes in RPM staining buffer with VRC. Cells were then incubated in primary and secondary antibodies as described in the RPM method. As will regular RNA FISH, all coverslips were

cured for 2-4 h at RT before sealing with clear nail polish. Slides were then transferred over to -20°C to prevent RNA signal fading or ideally imaged right away.

2.2.6 *L-homopropargylglycine Protein Synthesis Assay*

Cells on coverslips were labeled with L-homopropargylglycine (HPG) using the Click-iT[®] HPG Alexa Fluor[®] 594 Protein Synthesis Assay Kit (Thermo Fisher Scientific) according to the manufacturer's instructions with the following modifications: cells were rinsed with PBS once, then incubated in methionine free media with 50 µM HPG metabolic labeling reagent for 15 minutes. The cells were then rinsed with PBS and fixed with 4% paraformaldehyde for 15 minutes, followed by rest of the manufacturer's protocol.

2.2.7 *3D DNA immunoFISH*

DNA probes were generated from the pLEX-GFP-84QATXN1 plasmid by nick translation with the Roche nick translation kit and the DIG-11-UTP conjugation for 1 hr and 15 min. Probes were purified via the illustra[™] ProbeQuant[™] G-50 Micro Columns (GE Healthcare). Then probes were ethanol precipitated by adding 5 µL nick translated probe with 5 µL salmon sperm DNA, 1 µL human Cot1 DNA, 1.1 µL 3 M potassium acetate, and 22.5 µL ethanol. The precipitate was incubated at -80°C for 30 min, spun down at 4°C at max speed for 30 min, and speed vac'ed for 5 min. 10 µL DNA hybridization buffer per slide was added to the probe mixture and incubated at 37°C for 1 hr. Cells of all types on coverslips were rinsed with PBS⁺⁺ and fixed with 4% PFA in PBS for 10 minutes at room temperature. Then cells were rinsed with PBS⁺⁺ and permeabilized for 15 minutes in 0.5% Triton X-100 in PBS⁺⁺ at room temperature. Cells were then blocked in 4% BSA in PBST for 10-30 min at RT. Primary antibody was incubated at 37°C for 1 hr and washed three times with PBST for 5 min each.

Biotin-conjugated secondary antibody was incubated for 45 min at 37°C and washed 2 times with PBST. Cells were then post-fixed in 1% PFA for 10 min at RT, then incubated in 0.1 N HCl for 10 min. Cells were permeabilized again in 0.5% Triton/PBS for 5 min and then incubated in 20% glycerol in PBS⁺⁺ for 45 min at RT. Then slides were frozen in liquid nitrogen and thawed for 4 cycles. Then cells were washed in 2X SSC for 5 min and then stored in 50% formamide in 2X SSC for at least 24 h. DNA probes were generated from the pLEX-GFP-84QATXN1 plasmid by nick translation with the Roche nick translation kit and the DIG-11-UTP conjugation for 1 hr and 15 min. Probes were purified via the illustraTM ProbeQuantTM G-50 Micro Columns (GE Healthcare). Then probes were ethanol precipitated by adding 5 μ L nick translated probe with 5 μ L salmon sperm DNA, 1 μ L human Cot1 DNA, 1.1 μ L 3 M potassium acetate, and 22.5 μ L ethanol. The precipitate was incubated at -80°C for 30 min, spun down at 4°C at max speed for 30 min, and speed vac'ed for 5 min. 10 μ L DNA hybridization buffer per slide was added to the probe mixture and incubated at 37°C for 1 hr.

2.2.8 Fluorescence microscopy and image analysis

All images were generated using a Nikon A1R Confocal Microscope with the Nikon Elements software or a Leica DMI6000 fluorescence microscope with both with a 60x objective lens. Z-stack images for both analysis and representative images were taken at .125 μ m step sizes in a range of 5-10 stacks on average. Depending on the resolution required, images were taken of single cells or up to 10 cells per field. For analysis, normal scan rates were used. For representative images, 4X pixel linger was used to increase resolution of the image. Colocalization analysis was performed in FIJI/ImageJ using the Coloc2 plugin and the Mander's correlation coefficient. First, the images were dropped into FIJI and Z-projections (max

projections) were made. The projections were split into color channels using the color tab. The DAPI channel was selected to threshold the nucleus as an ROI. DAPI was thresholded using the threshold toolbar. In the analyze tab, under tools, the ROI manager was used to select each nucleus. Using the wand tool, each nucleus was selected and added using the + button. In the ROI manager, all of the nuclei were selected, then in the more tab in the ROI manager, the nuclei were combined. The other channels were thresholded as necessary, depending on the diffuseness of the channel. Each channel was in 16 bit if required. Then in the analyze tab, coloc2 in the colocalization option was chosen. Each channel to be colocalized was selected, and the ROI manager was used as the ROI. Mander's correlation was selected. The results of each nucleus was copied and pasted onto an excel workbook. Using the text to columns tool in the data tab, values of each result were separated from their titles. The values were copied and pasted using paste special- transpose so that cells were horizontal. The thresholded Mander's correlation M1 or M2, depending on the channels used, was calculated. Colocalization of PMY and PML/nucleolin was statistically evaluated using the average of averages of the three trials and a one-way analysis of variance followed by student's t-tests. For colocalization of CAG repeat mRNA and nuclear bodies or PMY, 150 whole nuclei were analyzed for total percent overlap between channels and were binned into percent of nuclei with the indicated overlap to indicate variations in overlap. These analyses were statistically evaluated using chi square statistic at 0.05 significance level.

PMY intensity analysis was evaluated using Analyze Particles function on ImageJ using the maximum pixel intensity measurement of each nuclear particle. First, the images were dropped into FIJI and Z-projections (maximum projections) were made. The projections were

split into color channels using the color tab. The DAPI channel was selected to threshold the nucleus as an ROI. DAPI was thresholded using the threshold toolbar. In the analyze tab, under tools, the ROI manager was used to select each nucleus. Using the wand tool, each nucleus was selected and added using the + button. In the ROI manager, all of the nuclei were selected, then in the more tab in the ROI manager, the nuclei were combined. The other channel was thresholded as necessary within the ROI. Then, in the analysis tab, the analyze particles option was selected. The particle size limitations were selected to be between 0.1 μm and infinity. Atxn1 inclusion size analysis was also performed with ImageJ analyze particles function using area of each particle as a measurement of Atxn1 area. The maximum of signal intensity was recorded for each nuclei and all data from the particle analysis was transferred into excel for calculations. Then the average of all maximum pixel intensities of the trials was calculated and used for graphical comparison. The analysis was statistically evaluated using the one-way analysis of variance via student's t-tests.

For representative images, all z-stacked maximum projected channels in ImageJ were made into a composite and converted into RGB color images in the image-type tab. Scale bars and DAPI were added to composite images (bar = 5 μm) and the image was saved as a TIFF file. All other single channels excluding DAPI were processed as RGB colors by unchecking all channels but the wanted channel. No scale bars were added to single channels before saving as TIFF files.

2.2.9 Super Resolution Microscopy

RPM immunofluorescence was performed in transfected cells as described above; however cells were incubated in Hoescht (1:5000) for 5 minutes after secondary antibody

incubation and mounted in ProLong Gold (Invitrogen). Super-resolution images were acquired on a Nikon N-SIM microscope with a 100X 1.49 NA Plan Apo TIRF objective lens (Nikon) and an Andor DU-897 EMCCD camera using 405nm, 488nm, 561nm, and 640nm diode lasers. 3D-SIM stacks were acquired using five phases and three rotations for a total of 15 wide field images per plane, and images were reconstructed using Nikon Elements software.

2.2.10 RNA isolation, cDNA preparation, and qPCR

At time of cell harvest, cells were trypsinized from 6 well plates (1-2 wells per condition), scraped off with a cell scraper for assurance of cell detachment, and pelleted by centrifugation at 1000 X g for 5 min. Cell pellets were washed once with 1X PBS⁺⁺ and spun again. After washing, all cellular RNA was isolated with the TRIzol reagent (Thermo Fischer Scientific) at 1 mL of Trizol per $0.5-1 \times 10^7$ cells and mixed by pipetting. The cells were incubated in Trizol for 5 min at RT, then 200 μ L choloform per mL of Trizol and shaken by hand for 15 s. Lysates were incubated for 2-3 min and then centrifuged at 12,000 x g for 15 min at 4°C. RNA in the aqueous layer was precipitated with 0.5 mL isopropanol per mL of Trizol for 10 min at RT, centrifuged for 10 min at 4°C and washed with 1 mL ethanol. The pellets in ethanol were centrifuged for 5 min at 7500 x g at 4 then resuspended in 20-44 μ L water.

RNA was measured using a nanodrop and cDNA was synthesized from the RNA using the SuperScript[™] IV First-Strand Synthesis System (Thermo Fischer Scientific). Briefly, DNA was removed with amplification grade Dnase I (Thermo Fischer Scientific), and cDNA was made via the reverse transcriptase in the kit. Remaining RNA was removed with RnaseH. qPCR analysis was performed with the LightCycler[®] 480 (Roche, Basel Switzerland) using the 480 SYBR Green 1 Master reagent (Roche). Triplicates of each condition were prepared and

GAPDH was used as a universal reference gene. Primer sequences for the target genes are as follows: ATXN1 fwd, TACAAGCACCAAGCTCCCTG; ATXN1 rev, TCACTATGCTCCAGTATGCTGAC; HTT fwd, CATAGCGATGCCAGAAAGTT; HTT rev, GCTACCAAGAAAGACCGTGTG, GAPDH fwd, GTCAGTGGTGGACCTGACCT, GAPDH rev, AAAGGTGGAGGAGTGGGTGT. All primers were analyzed for efficiency through standard curve analysis of IMR90 cDNA using triplicates of 5 serial dilutions. ATXN1 primer efficiency is 2.068, HTT primer efficiency is 2.343, and GAPDH primer efficiency is 2.57. qPCR analysis was performed on the Roche LightCycler[®] 480 software. On the sample editor tab, relative quantification was chosen. The control triplicate sample was labeled as Positive control/calibrator. The variable samples were labeled as unknowns. Target primer was the experimental primer and the reference primer was GAPDH. Efficiency was recorded for all primers. Then all samples were selected and auto replicates were made. In the analysis tab, basic relative quantification was used to determine fold changes in cDNA. Melting curves and S curves were checked for triplicate precision and the relative quantification of samples was recalculated as necessary.

2.2.11 Cell lysis and nuclear-cytoplasmic isolation

For whole cell lysates, at time of cell harvest, cells were trypsinized from 10cm plates and pelleted by centrifugation. Cell pellets were washed once with 1X PBS⁺⁺ followed by lysis in harsh lysis buffer (50 mM Tris, 300 mM NaCl, 50 mM sodium fluoride, 1% Triton-X100, 0.5% deoxycholic acid, 0.1% SDS). Cells were incubated in the lysis buffer on ice for 40 min and centrifuged at 150000 x g for 10 min.

For nuclear-cytoplasmic isolation, at time of cell harvest, cells were trypsinized from 10cm plates and pelleted by centrifugation. Cell pellets were washed once with 1X PBS⁺⁺ followed by nuclear and cytoplasmic extraction with the NE-PERTM reagents (Pierce) according to manufacturer's instructions and scaled according to cell count. Briefly, cells were incubated on ice in CER1 for 10 min or more before addition of CER2. Then cells were vortexed and centrifuged at 150000 x g for 5-10 min. Soluble cytoplasmic proteins were isolated into separate tubes. Remaining lysates were washed with CER1 and incubated in CER2 for 40-120 min. Cells were centrifuged again for 10 min and soluble nuclear lysates were collected in separate tubes. Remaining pellets were saved for aggregated proteins and cellular debris. Soluble nuclear and cytoplasmic protein fractions were quantified by Pierce 660nm protein assay reagent (Thermo Fisher Scientific, Waltham, MA, USA) and nano-drop (Thermo Fisher Scientific).

2.2.12 Western Blot

Equal cytoplasmic and nuclear protein, or whole cell lysate concentrations were loaded and run on 4-12% SDS-PAGE gels (Invitrogen) for 2h at 120V. Proteins were transferred onto nitrocellulose membranes at 4°C for 1hr 20min at 30V. Membranes were blocked in 5% block (milk or BSA) in 1X TBS + 0.1% Tween-20 (TBST) while rocking/shaking. Membranes were incubated in primary and secondary antibodies diluted in 1% block in TBST while rotating for 1h at RT or overnight at 4°C. Western blot signal was resolved with Super Signal West Pico HRP detection reagent (Thermo Fisher Scientific) and imaged using the luminescent image analyzer, LAS-4000 (Fujifilm, Minato, Tokyo, Japan). Membranes were stripped with 25 mL harsh stripping buffer (2% SDS in 62.6 mM Tris-HCl pH 6.8 with 200 µL beta-mercaptoethanol per 25 mL buffer added fresh) at 50°C for 30 min. After stripping, membranes were rinsed under

constantly running distilled water for 30-60 min then washed with TBST 3 times for 5 min each before incubating in the new antibody.

Quantification of westerns was performed with ImageJ gels tool and all values were normalized to loading control.

2.3 BioID Proteomics Analysis

All BioID analyses were performed according to (108). Please see the publication for detailed protocols in BirA* fusion protein design, stable cell line generation, validation of the fusion protein in stable cells, immunoprecipitation and preparation of samples for BioID analysis.

2.3.1 Immunoprecipitation and preparation for mass spectrometry

HEK293 cells stably expressing the BirA* fusion proteins were seeded onto four to five 10 cm dishes of per condition. All conditions were supplemented with 50 μ M biotin (Sigma) 18-24 h after seeding and for 24 h before lysis. UV irradiated cells were subject to irradiation at the beginning of biotin supplementation (see 2.1.5 for UV irradiation conditions). Proteomic stressed cells were transfected with 5 g per plate of 84Q-ATXN1 with a 32Q-ATXN1 control at the beginning of biotin supplementation. At the time of cell harvest, plates were rinsed twice with PBS and harvested with BioID lysis buffer (0.2% SDS, 50 mM Tris HCl pH 7.4, 500 mM NaCl, 1X protease inhibitor (Roche), 1 mM DTT). Triton X-100 was added at 2% and lysates were incubated on ice. Lysates were subject to two session of sonication (Qsonica 1 s on 1 s off for 20 s at 40-50% amp). Then lysates were diluted with 50 mM Tris HCl and subject to an addition sonication session. Samples were centrifuged at 16000 x g and soluble proteins were incubated

in magnetic streptavidin beads (MyOne DynaBeads, Life Technologies) overnight at 4°C. Then samples were washed with wash buffer 1 (2% SDS), Wash buffer 2 (0.1% deoxycholic acid, 1% Triton X-100, 1 mM EDTA, 500 mM NaCl, 50 mM HEPES, pH 7.5), and wash buffer 3 (.5% deoxycholic acid, 0.5% NP-40, 1 mM EDTA, 250 mM LiCl, 10 mM Tris-HCl, pH 7.4). Beads were finally washed with 50 mM Tris-HCl. Beads were collected via centrifugation and washed with 100 mM ammonium bicarbonate. Small aliquots were saved for Western blot analysis.

Cells were then subject to on-bead trypsin digestion according to the Northwestern Proteomics core protocol. Briefly, proteins were reduced with 10 mM DTT in 100 mM ammonium bicarbonate at 50°C for 30 min, then alkylated with 100mM iodoacetamide for 30 min at RT in the dark. Then proteins were washed with bicarb and trypsinized overnight with 1 µg trypsin at 37°C. Trypsin was stopped with 2% formic acid and proteins were isolated from beads and flash frozen in liquid nitrogen. Proteins were submitted to NU Proteomics core for mass spectrometry analysis on a LTQ Orbitrap and resulting spectra results were reported on Scaffold 4.

2.3.2 Proteomics analysis

Protein reports were exported Scaffold into excel files and each condition was separated into separate sheets in the workbook. Contaminating proteins were excluded from the dataset including endogenously biotinylated proteins, keratins, limited ribosomal proteins, histones and a small pool of other proteins. These proteins were identified by Roux *et al.* in the parent HEK293 cell line with no fusion protein. Any proteins that overlap with our dataset were labeled as contaminants. However, any proteins in this pool that were known PML interaction partners were excluded from the contamination list. This provided stringent inclusion criteria for downstream analysis.

Resulting proteins were analyzed for overlap on Venny 2.1.0 Venn diagram calculator between samples as well as with the BioGRID database. In the STRING platform, the identified proteins in each sample were visually represented in a network. Then the following analyses were completed in STRING. Each condition was analyzed for gene ontology functional classification by protein class based on the PANTHER database. Then, proteins found exclusively in the stress conditions of UV irradiation and 84Q-ATXN1 expression samples were subject to gene ontology statistical overrepresentation test by molecular function, biological process, and cellular component, based on the STRING database PANTHER analysis type.

Quantitative proteomics analysis was performed by preparation and submission of 3 trials of samples containing normal conditions, expression of pCDNA empty vector, 30Q-ATXN1, and 85Q-ATXN1 overtime. A label-free intensity analysis using MaxQuant software was performed, followed by a pairwise test between each sample set for statistical enrichment, was performed by the proteomics core and the resulting analysis were visualized by volcano plots.

Chapter 3: Results

3.1 Regulatory peptide synthesis at PML bodies during cellular stress

3.1.1 Background

Cellular homeostasis requires the maintenance of genomic and proteomic integrity, with highly coordinated and redundant quality control mechanisms existing at every step of gene expression. Many of these mechanisms are dynamically organized in the nuclear compartment at nuclear bodies (NBs), non-membranous self-organizing assemblies whose functions are largely determined by their four-dimensional protein composition (21). Promyelocytic leukemia (PML) bodies exemplify nuclear localized quality control with a centralized role in the cellular response to intrinsic and extrinsic stress through multiple disparate mechanisms (30). For example, PML bodies function in a SUMO-dependent ubiquitin degradation mechanism of misfolded proteins common to neurodegenerative disorders such as SCA1 (49).

SCA1 belongs to a class of polyglutamine (polyQ) disorders associated with both proteotoxicity and RNA toxicity caused by the expansion of CAG repeats in the coding region of *ATXN1* (46, 54). A growing body of evidence suggests protein degradation pathways are often connected with mRNA regulation mechanisms coincident with translation (109). Despite evidence that PML bodies associate with mRNAs as well as various factors required for protein synthesis, including eIF4e, eIF3, and ribosomal P proteins, an examination of the functional relationship between PML bodies and these particular binding partners remains unresolved (95, 110, 111). In the current study, we demonstrate that the disparate functions attributed to PML

bodies are linked to an integrated response to cell stress, involving mRNA localization, polypeptide synthesis, and protein degradation.

3.1.2 Results

Expanded-mutant *ATXN1* mRNA foci localize with PML bodies. It is known that proteins with expanded polyQ tracts can aggregate at PML bodies. Although the corresponding CAG repeat-expanded mRNA also form nuclear foci (56), whether they localize with PML bodies remains untested. We performed RNA fluorescence *in situ* hybridization (FISH) on normal human fibroblasts (IMR-90s) ectopically expressing a pathogenic form of *ATXN1* with 84 CAG repeats (84Q-*ATXN1*) and a nonpathogenic 32Q-*ATXN1* control. Under control conditions, CAG repeat RNA was predominantly localized in the cytoplasm 12 hr post transfection and largely degraded by 48 h. Conversely, in 84Q-*ATXN1* expressing cells, CAG repeat RNA was significantly retained in the nucleus, forming large nuclear foci by 12 h that remained observable at 48 hr (Fig. 3.1). These foci demonstrated a significant overlap with PML bodies when compared to nucleoli (Fig. 3.2), as seen by immuno-RNA-FISH. Moreover, the colocalization between PML and 84Q-*ATXN1* mRNA was comparable to nuclear speckles, NBs shown to colocalize with RNA foci (Fig. 3.3A, B) (56). However, knocking down PML in IMR-90 cells expressing 84Q-*ATXN1* via RNAi did not change the average number or signal intensity of the RNA foci (Fig 3.4). Follow-up of this experiment using a higher number of cells per condition is required for confirmation of the result. These results demonstrate an interaction between PML bodies and CAG repeat-expanded mRNA foci.

To test whether PML body association with repeat-expanded *ATXN1* mRNA foci can be observed endogenously, we performed immuno-RNA-FISH on CAG repeat RNA in SCA1

patient fibroblasts compared to a control cell line (IMR-90). We detected RNA foci only in SCA1 cells, consistent with previous reports (107), and a significant overlap between PML bodies and CAG repeat RNA compared to the control (Fig 3.5A, B). Yet, we observed no significant difference in association between nuclear speckles and CAG repeat RNA between SCA1 cells and the control (Fig. 3.3C, D), while nucleoli were largely void of CAG repeat RNA in both cell types (Fig. 3.6). Knocking down PML expression with RNAi resulted in a significant increase in *ATXN1* mRNA in SCA1 cells compared to the IMR-90 control (Fig. 3.5C). However, knocking down PML in SCA1 cells did not increase Atxn1 protein levels (this result will need to be further tested with an updated PML siRNA and a verified antibody for Atxn1) (data not shown). These results suggest repeat-expanded mRNA in *ATXN1* can associate with PML bodies in a disease-specific manner.

To expand upon our results beyond one repeat-expansion disorder, we analyzed an additional polyQ disorder—Huntington’s disease (HD). Huntington’s disease contains arises from a CAG repeat expansion in the Huntington (*HTT*) gene. Since the *HTT* gene and CAG expansion is larger, the phenotype of the RNA foci and misfolded protein are often more pronounced than that of mutant *ATXN1*. Again, we performed immuno-RNA-FISH in HD patient cells and observed a significant overlap between PML bodies and CAG-repeat RNA in HD cells, similar to that of nuclear speckles. Nucleoli were again mainly void of the RNA. When we knocked-down PML expression with RNAi we observed a significant increase in *HTT* mRNA in HD cells compared to the IMR-90 control. These results in HD cells support our hypothesis that PML bodies play a larger role in the physiological response to the cellular stress caused by repeat-expanded mRNA (Fig. 3.7).

Polypeptide synthesis occurs at PML bodies during proteotoxic stress. Our observation of PML body association with repeat-expanded *ATXN1* mRNA foci coupled with their known association of Atxn1 protein aggregates led us to consider whether this association underlies a shared mechanism. It has been demonstrated that both aberrant mRNAs and misfolded proteins can be co-translationally regulated, and recent studies indicate aberrant mRNAs are recognized by translating ribosomes in the nucleus (87, 88, 112). Thus, we hypothesized that PML bodies, which contain multiple factors involved in translation, may represent a site of regulatory polypeptide synthesis. The phenomenon of nuclear translation—first described in 1954—remains both highly divisive and enigmatic, not least due to its unknown physiological role. However, several groups have now provided compelling evidence for nuclear translation using diverse experimental approaches (75, 81, 86, 113). Therefore, we tested the possibility of polypeptide synthesis at PML bodies in response to proteotoxic stress.

In order to visualize active peptide synthesis in the nuclear compartment, we employed the ribopuromylation (RPM) method. The RPM method employs two translation inhibitors, puromycin (PMY) and emetine. PMY incorporates into the ribosomal A site and binds the elongating chain, causing premature translation termination. Emetine binds the 40S ribosomal subunit and inhibits transpeptidation during elongation. This combination effectively freezes the puromycylated peptides on polyribosomes, which can be visualized in the nucleus, after detergent extraction of the cytoplasm, with an antibody to PMY (23). Under normal conditions nuclear localized polypeptide synthesis occurs in nucleoli, which may function to test the translational capacity of newly synthesized ribosomal proteins prior to their cytoplasmic export. The effect of stress on nuclear translation as visualized by RPM has not yet been resolved.

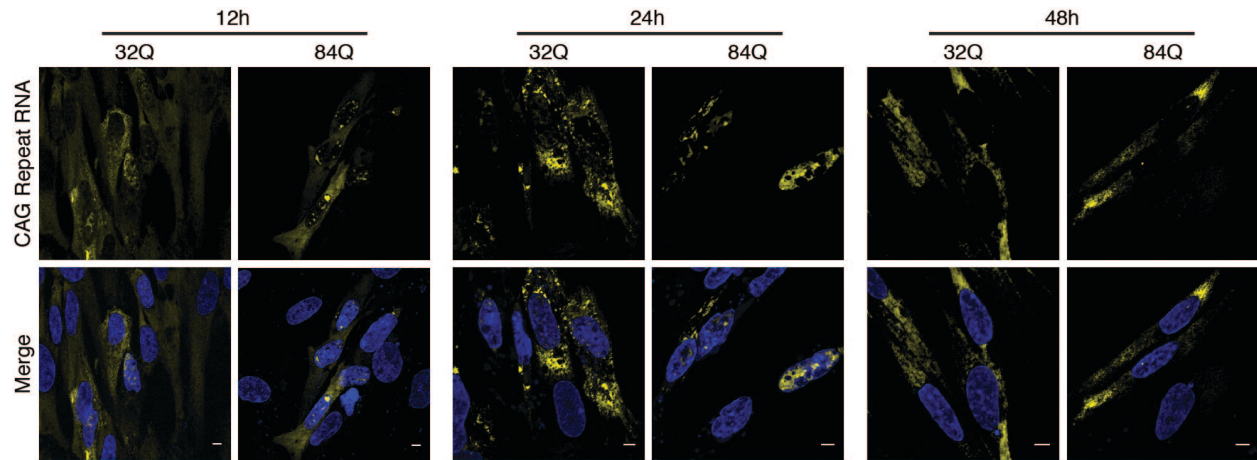


Figure 3.1 84Q-ATXN1 mRNA is retained in the nucleus. Confocal microscopy images of immuno-RNA-FISH using a CAG-repeat FISH probe on IMR-90s 12, 24, and 48 hours after transfection of either 32Q-*ATXN1* or 84Q-*ATXN1*. At 12 h post transfection, 38% of 84Q-*ATXN1* mRNA was retained in the nucleus (n = 104), while only 8% of 32Q-*ATXN1* mRNA was nuclear (n = 45).

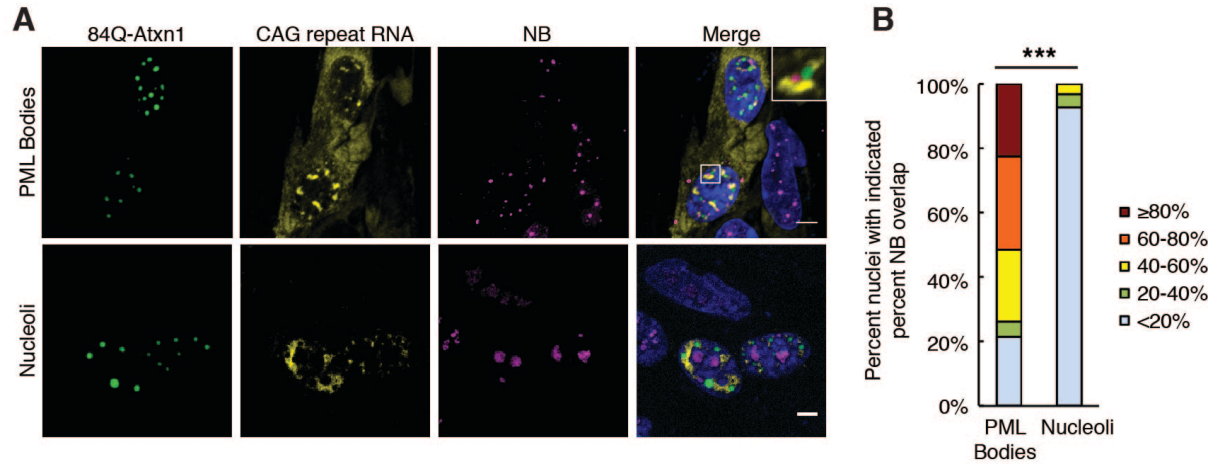


Figure 3.2 84Q-ATXN1 mRNA associates with with PML bodies. (A) immuno-RNA-FISH in IMR-90s 18 h post-transfection of 84Q-*ATXN1*, stained with a CAG repeat probe and PML or nucleolin, quantified in (B) as percent nuclei with indicated percent overlap between NBs and CAG repeat RNA (n = 107 and 101 respectfully, from 3 independent experiments, chi square test analyzed with an unpaired t test, *** = p < .001).

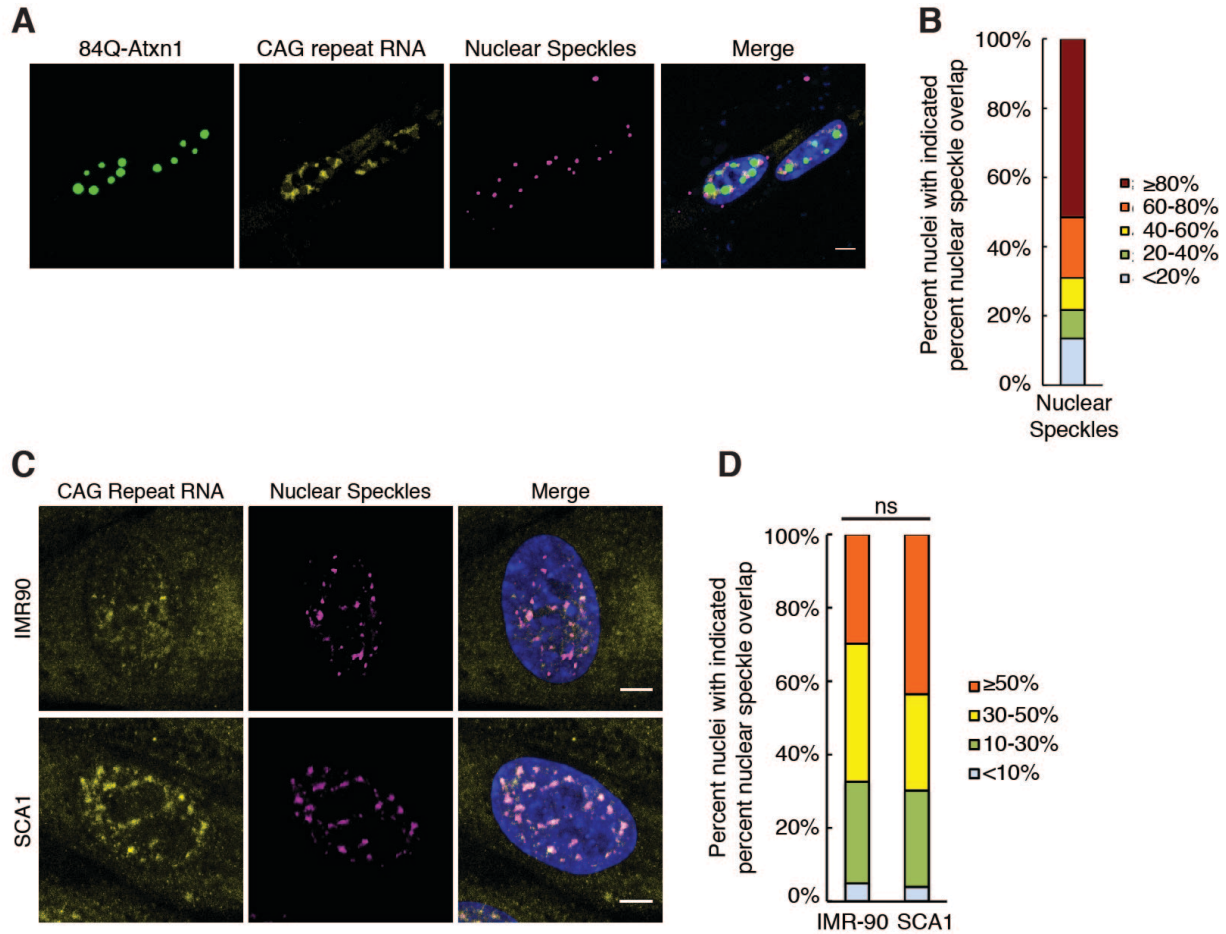


Figure 3.3 Nuclear speckle interaction with CAG repeat RNA remains constant in SCA1. (A) immuno-RNA-FISH in IMR-90s transfected with 84Q-*ATXN1* stained with a CAG repeat probe and SC35 antibody, quantified in (B) as percent nuclei with indicated percent overlap between nuclear bodies and CAG repeat RNA (n = 98 from 3 independent experiments). (C) immuno-RNA-FISH of CAG repeat RNA and SC35 in IMR-90s or SCA1 patient fibroblasts, quantified in (D) (n = 148 and 136 respectively from three independent experiments, chi square test, analyzed with unpaired t test, ns = $p > 0.05$). Analysis for (D) performed by Chelsea Strojny-Okyere. Scale bar, 5 μ m.

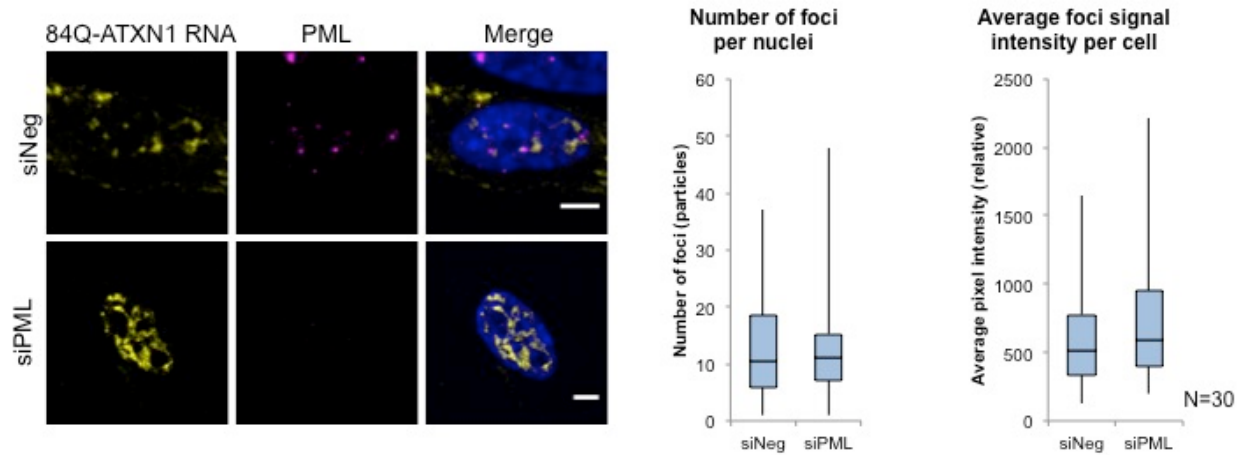


Figure 3.4 Knock-down of PML does not significantly alter *ATXN1* foci. Confocal images of IMR-90 cells expressing 84Q-*ATXN1* and immunostained for PML after incubation in a PML siRNA or a negative control siRNA. RNA foci are quantified for average number per nuclei and average pixel intensity per cell in each condition.

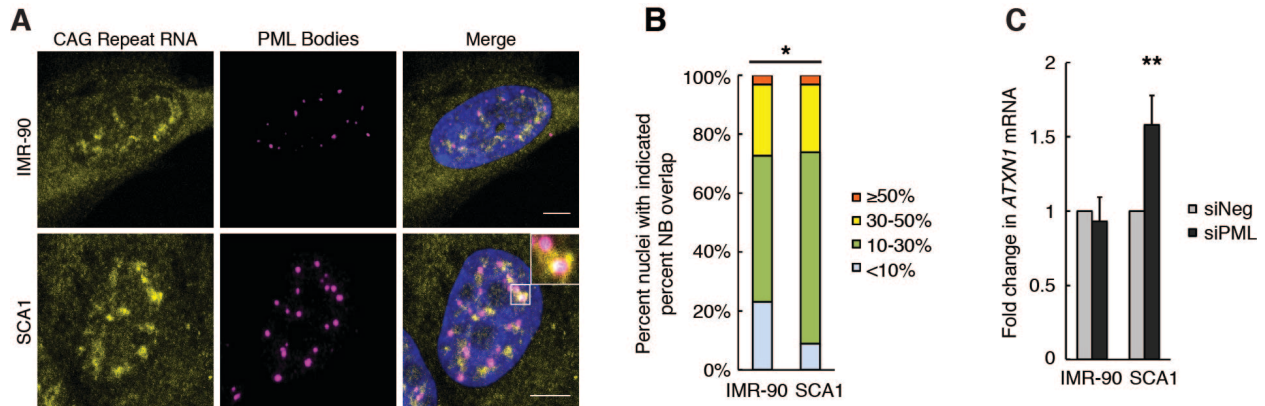


Figure 3.5 CAG-Repeat mRNA significantly associated with PML bodies in SCA1 patient cells. (A) immuno-RNA-FISH of CAG repeat RNA and PML in IMR-90s or SCA1 patient fibroblasts, quantified in (B) ($n = 150$ per condition from 3 independent experiments, chi square test analyzed with an unpaired t test, $* = p < .05$). Scale bar, $5\mu\text{m}$. Analysis in (C) performed by Chelsea Strojny-Okyere. (C) qRT-PCR analysis of endogenous *ATXN1* in either IMR-90s or SCA1 patient fibroblasts after siRNA knock-down of PML or a negative control. Values normalized to *GAPDH*, analyzed with an unpaired t test ($** = p < .01$).

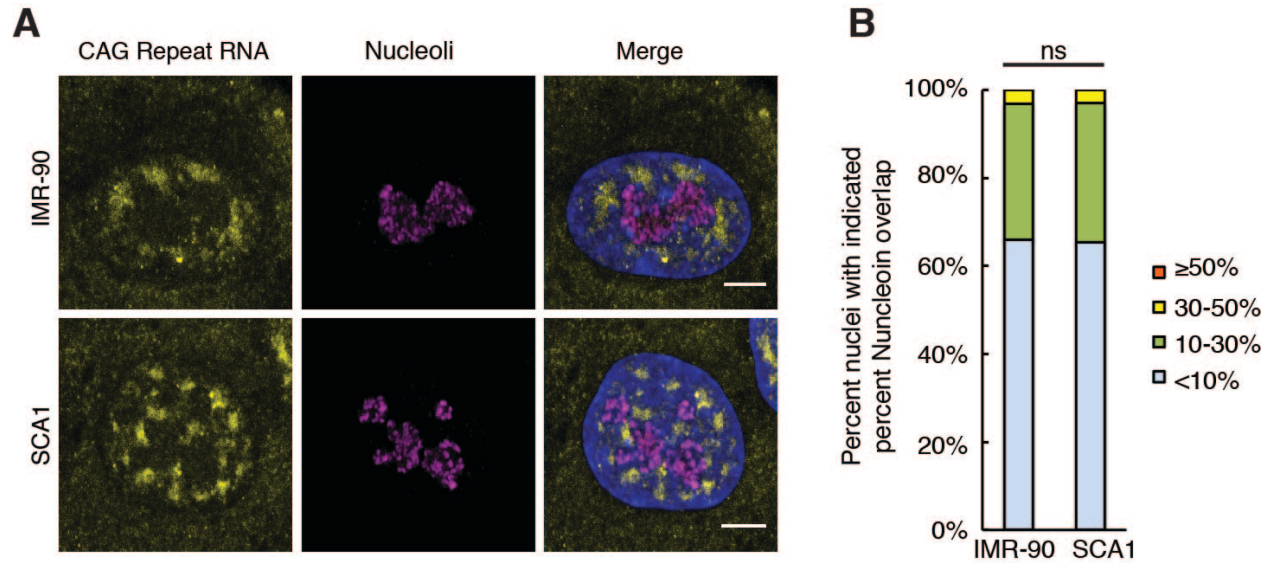


Figure 3.6 Endogenous repeat expanded ATXN1 mRNA is absent from nucleoli. (A) immuno-RNA-FISH of CAG repeat RNA and nucleolin in IMR-90s or SCA1 patient fibroblasts, quantified in (B) ($n = 149$ per condition from three independent experiments, chi square test, analyzed with unpaired t test, $ns = p > 0.05$). Scale bar, $5\mu\text{m}$.

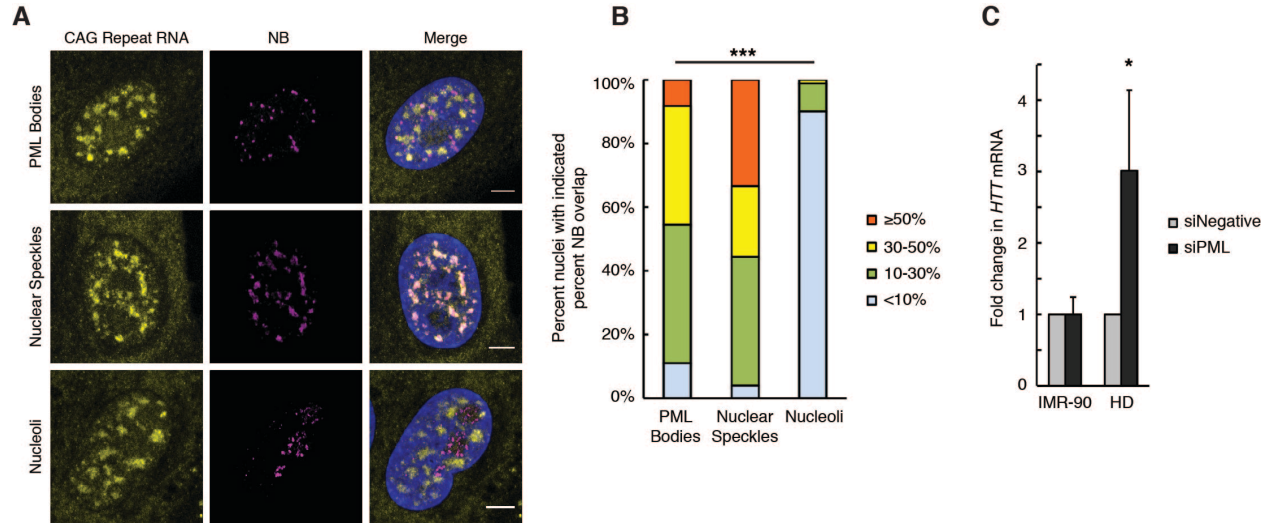


Figure 3.7 PML bodies interact with expanded repeat HTT mRNA foci. (A) immuno-RNA-FISH of CAG repeat RNA and either PML, SC35, or nucleolin in HD patient fibroblasts, quantified in (B) ($n = 150, 141, \text{ and } 148$ respectively from three independent experiments, chi square test, analyzed with unpaired t test, $*** = p < 0.001$). Analysis of PML bodies and Nuclear Speckles in (B) performed by Chelsea Strojny-Okyere. Scale bar, $5\mu\text{m}$. (C) qRT-PCR analysis of endogenous HTT in either IMR-90s or HD patient fibroblasts after siRNA knock-down of PML or a negative control. Values normalized to GAPDH, analyzed with an unpaired t test ($** = p < .05$). qPCR analysis in (C) performed by Alessandra Garcia.

We first verified the RPM technique in normal IMR-90 fibroblasts and saw nucleolar localization pattern of puromycin (PMY)-labeled nascent polypeptides consistent with previous reports in different cell types. This PMY signal was properly diminished with pretreatment of translation inhibitors anisomycin and harringtonine. Omission of the NP40 detergent extraction of the cytoplasm revealed a large cytoplasmic signal that diminished the nucleolar signal (Fig. 3.8A). Western blotting of cells with or without brief incubation in labeling media indicated that peptides were indeed labeled with puromycin. Pre-treatment of cells with harringtonine reduced polypeptide labeling while pre-treatment with the protease inhibitor MG132 increased the labeled polypeptides (Fig. 3.8B). These data verify that the RPM technique effectively visualizes peptide synthesis in IMR-90 cells.

To determine the localization of ribosome-bound nascent polypeptides during proteotoxic stress, we performed RPM on IMR-90s expressing Atxn1 (81). In cells expressing 32Q-Atxn1, PMY localized similarly with nucleoli and PML bodies. However, cells expressing 84Q-Atxn1 had significantly more PMY localized with PML bodies than nucleoli (Fig. 3.9). While the RPM method has proven to accurately depict ribosome-bound polypeptide synthesis, we used the L-homopropargylglycine (HPG) ‘click chemistry’ protein synthesis assay to validate our results. Again, in cells expressing 84Q-Atxn1, the nascent protein synthesis signal overlapped with inclusions at PML bodies (Fig 3.10). These results indicate that active translation relocates from nucleoli to PML bodies during proteotoxic stress.

To corroborate PML bodies as sites for active ribosomes, we utilized the lacO/LacI-GFP system to immobilize acidic ribosomal P proteins (RPLPs), at which we detected significant co-localization with PML bodies, PMY, and 84Q-Atxn1 aggregates. The RPLP proteins form a

pentameric complex on 80S monosomes and polysomes that localize soluble translation factors, notably eEF-2, to the ribosome during translation. Previous studies demonstrated that RPLP0, -1, and -2 co-localize with PML bodies (9). To determine whether foci formed by GFP-LacI-RPLPs can localize with PML bodies, we employed the LacO repeat array system along with LacI fused RPLPs to immobilized RPLPs in the nucleus (24). We performed an immunofluorescence analysis on HeLa-LacO cells expressing the GFP tagged LacI ribosomal fusion proteins and found that all three of the LacI-RPLP fusions localized significantly with endogenous PML bodies over the LacI control. RPLP0 had the strongest association with PML bodies at 60% of foci localizing with a PML body (Fig. 3.11). This results suggests a strong association of PML bodies with Ribosomal proteins.

To determine if the localization of PML with RPLPs is associated with peptide synthesis, we ectopically expressed RPLP0 and performed RPM. We observed mostly nucleolar PMY signal, with a 12.1% overlap between LacI-RPLP0, PML bodies, and PMY. To test if cellular stress affects this localization, we subjected cells expressing LacI-RPLP0 to UV irradiation and performed RPM. We detected a significant increase in the amount of localization between LacI-RPLP0, PML bodies, and PMY (Fig. 3.12A, B). To determine if PML bodies associated with 84Q-Atxn1 can localize a LacI bound ribosomal protein, we co-expressed LacI-RPLP0 and 84Q-Atxn1 and found a significant increase in localization with PML bodies over the LacI control (Fig. 3.12C, D). These data indicate that PML bodies associate with proteins involved in translation as well as puromycylated polypeptides significantly more during cell stress.

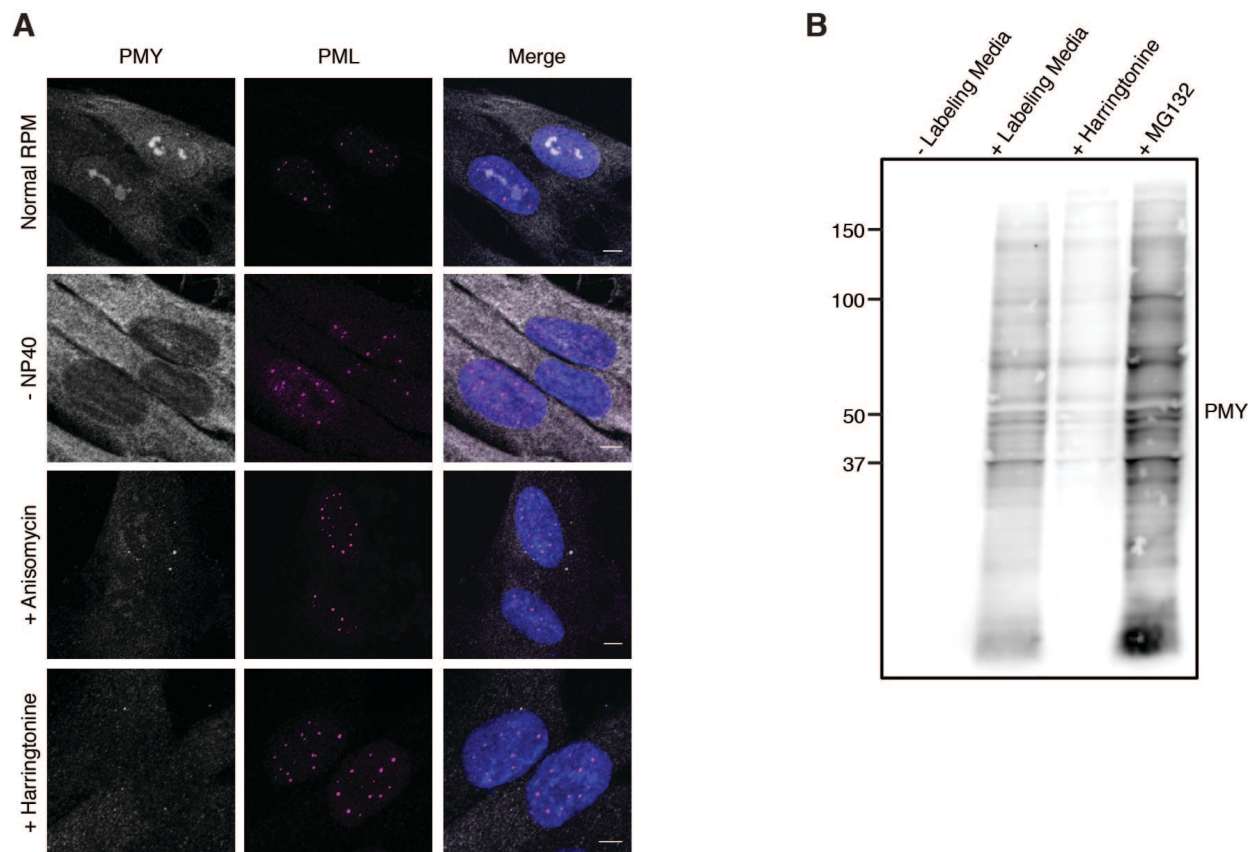


Figure 3.8 RPM technique is verified to detect nuclear translation in IMR-90 fibroblasts. (A) Confocal images normal RPM technique (top row) and RPM controls in IMR-90s stained with PML and PMY. Controls are as follows: omission of NP40 detergent extraction of cytoplasm (second row), anisomycin translation inhibitor treatment before labeling media (third row), and harringtonine translation inhibitor treatment before labeling media. Scale bar, 5 μ m. (B) Western blot of IMR-90s either treated without labeling media, with labeling media, with harringtonine before labeling media, or with MG132 before labeling media. Western blot in (B) performed by Alexis Cogswell.

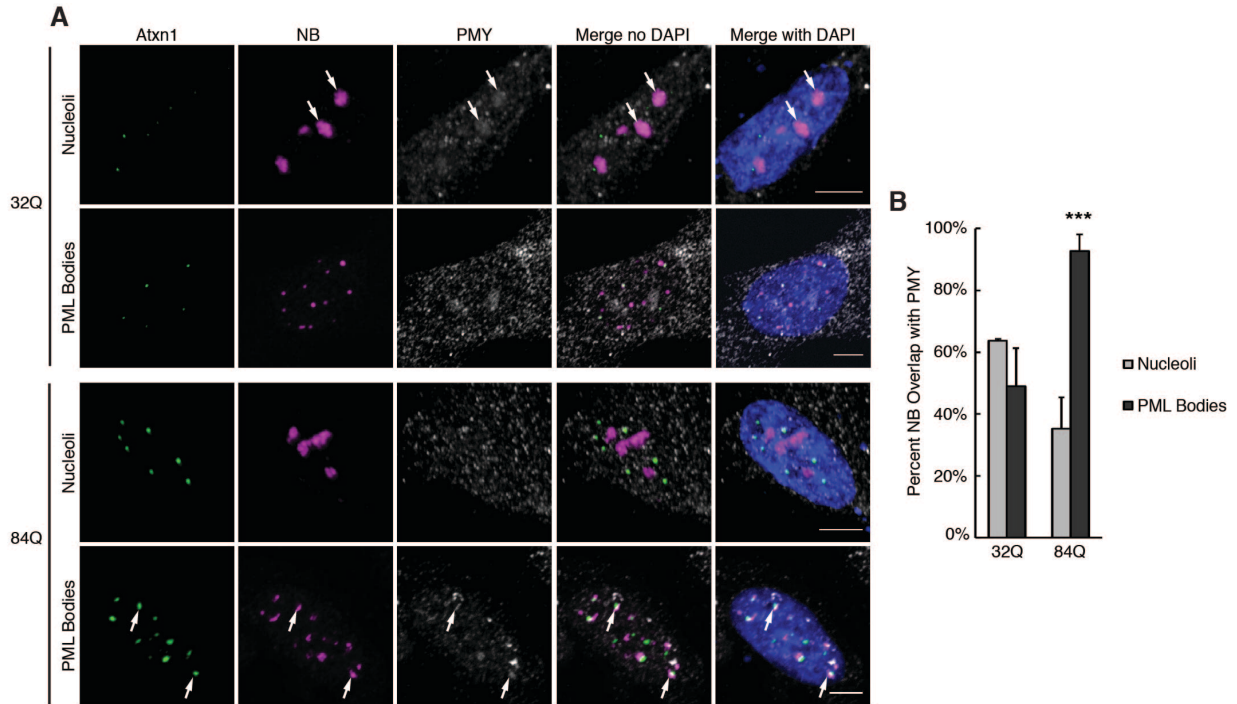


Figure 3.9 Translation signal relocates to PML bodies during 84Q-Atxn1 expression. (A) Confocal microscopy image of RPM in IMR-90s 24 h after expressing either 32Q-Atxn1 or 84Q-Atxn1, stained with nucleolin or PML and PMY, quantified in (B) as percent nucleolin or PML overlap with PMY in each condition. Values represent the average colocalization \pm SD of three biological replicates with $n \approx 100$ per replicate, analyzed with an unpaired t test, *** = $p < .001$). Analysis in (B) performed by Alexis Cogswell.

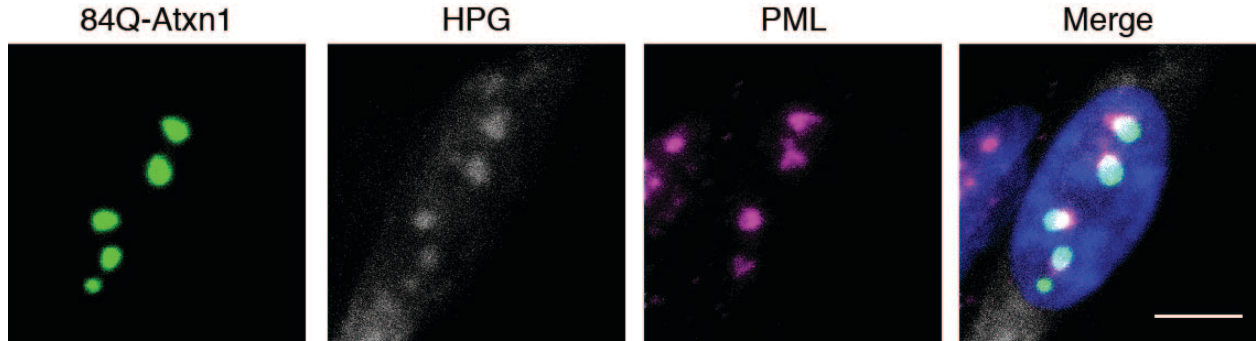


Figure 3.10 Active translation signal via HPG localizes with 84Q-Atxn1 inclusions. Confocal image of IMR-90 cell expressing 84Q-Atxn1 treated with HPG protein synthesis detection reagent and stained with a PML antibody. Scale bar, 5 μ m. Image generated by Steven Kosak.

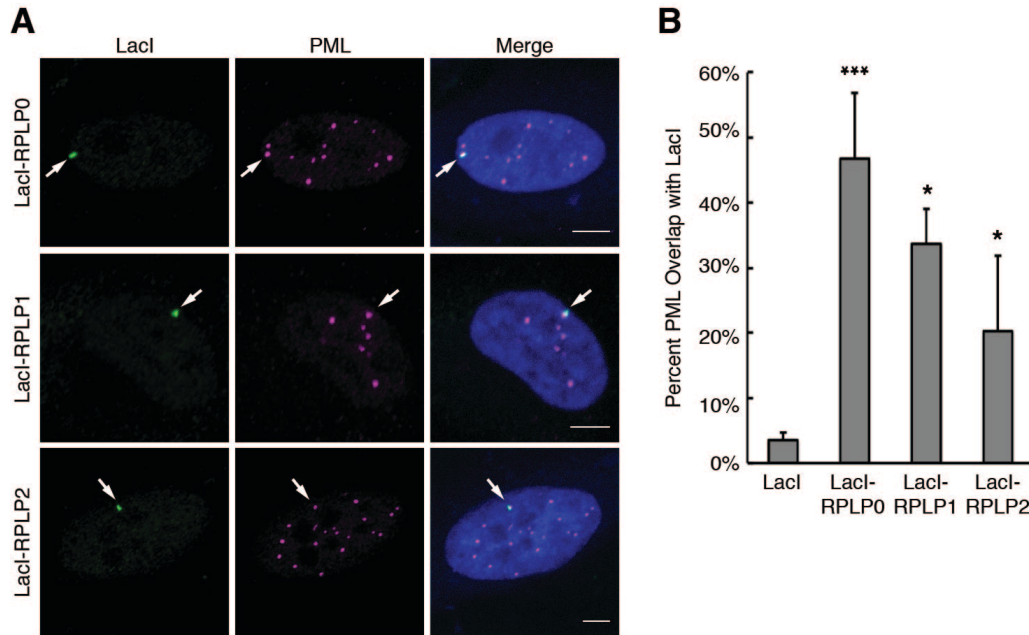


Figure 3.11 Ribosomal Stalk Proteins associate with PML bodies. (A) Confocal images of GFP-LacI fused RPLP0, 1, or 2 expressed in HeLa-LacO cells immunofluorescently stained with PML indicating overlap between PML and LacI foci, quantified in (B) as average percent association \pm SD between LacI foci and PML body from 3 independent experiments ($n \geq 80$ per condition in each experiment, analyzed with unpaired t test, *** = $p < 0.001$, * = $p < 0.05$).

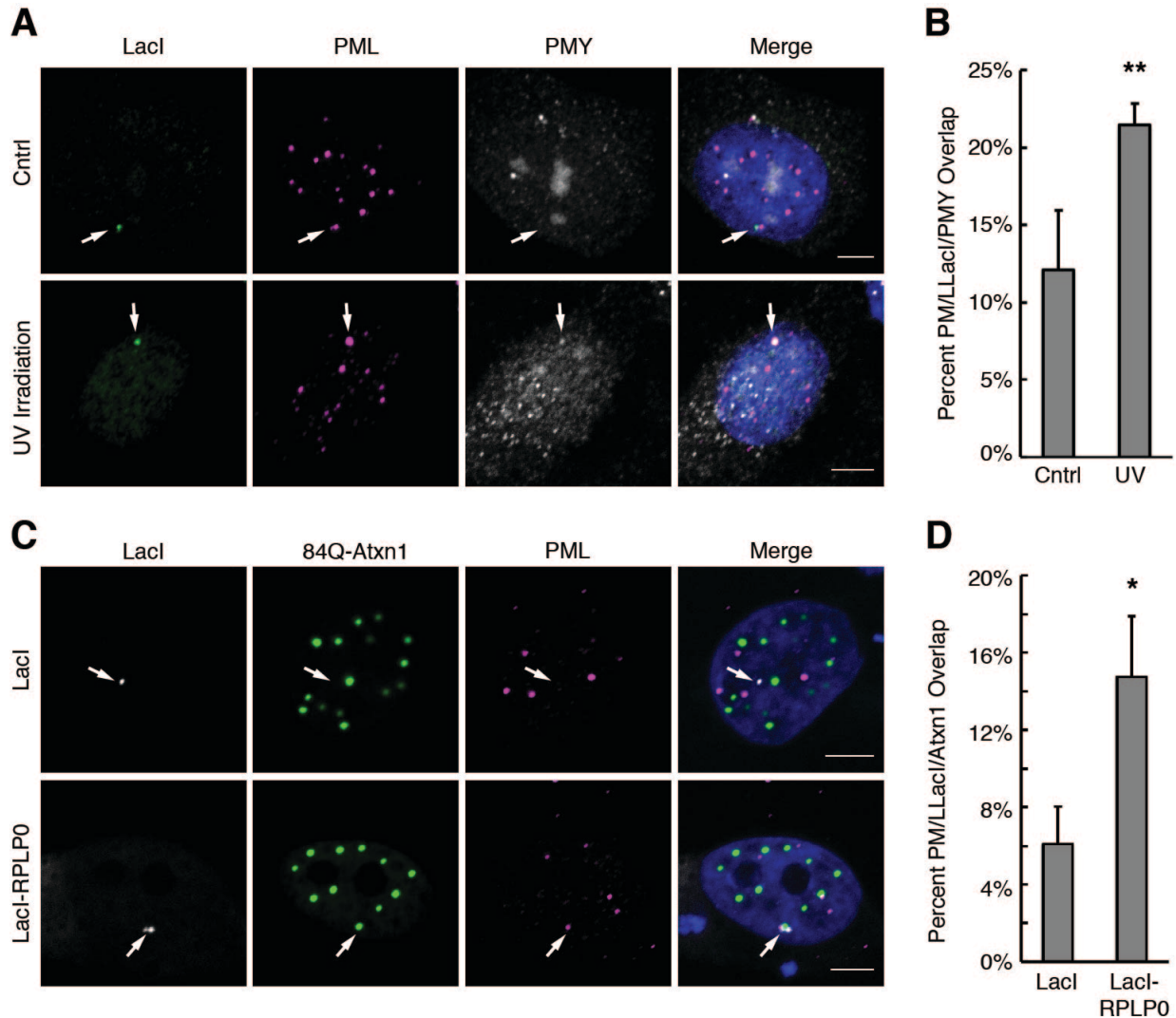


Figure 3.12 RPLP0 associates with PML bodies during cell stress. (A) Confocal images of GFP-LacI-RPLP0 expressed in HeLa-LacO cells with or without UV irradiation stress, immunofluorescently stained with PML indicating overlap between PML and LacI foci, quantified in (B) as average percent association \pm SD between LacI foci, PMY, and PML body from 3 independent experiments ($n \geq 87$ per condition in each experiment, analyzed with an unpaired t test, ** = $p < .01$). (C) Confocal images of mcherry-LacI-RPLP0 or mcherry-LacI alone expressed in HeLa-LacO cells co-expressed with 84Q-Atxn1, immunofluorescently stained with PML indicating overlap between PML and LacI foci, quantified in (D) as average percent association \pm SD between LacI foci, 84Q-Atxn1 inclusion, and PML body from 3 independent experiments ($n \geq 99$ per condition in each experiment, analyzed with an unpaired t test, ** = $p < .05$). Scale bar, $5\mu\text{m}$.

To more accurately visualize the localization pattern of PMY-labeled nascent polypeptides with PML bodies and 84Q-Atxn1 inclusions, we performed structured illumination microscopy (SIM) following RPM. We observed PMY co-localized with the PML body shell ('doughnut') structure surrounding an 84Q-Atxn1 inclusion (Fig. 3.13). To determine if the puromycylated peptides localize with *ATXN1* mRNA foci, we performed RPM and RNA-FISH in tandem on cells expressing 84Q-*ATXN1* and 32Q-*ATXN1*. We found a significant increase in association between 84Q-*ATXN1* mRNA and nuclear PMY compared to 32Q-*ATXN1* (Fig. 3.14). These data demonstrate that proteotoxic stress is linked to polypeptide synthesis at PML bodies.

To determine if the association of PML bodies with translating *ATXN1* mRNA is associated with localization at the *ATXN1* genomic locus, we performed immuno-DNA-FISH on SCA1 cells. We observed that PML bodies associated with the *ATXN1* genomic locus in 30% of SCA1 cells (Data not shown). A follow-up experiment with a non-pathogenic cell line control will be required to test the significance of this observation.

Modulation of PML expression disrupts peptide synthesis and mutant Atxn1 aggregates.

We next altered PML expression to evaluate its role in polypeptide synthesis during proteotoxic stress. When we suppressed endogenous PML expression through RNAi, we observed a significant decrease of nuclear PMY signal intensity, accompanied by an increase in nuclear 84Q-Atxn1 protein expression (Fig. 3.15A-C). This result suggests PML bodies are necessary for nuclear polypeptide synthesis of 84Q-Atxn1 and its synthesis is associated with its degradation. When we ectopically expressed PML isoforms and 84Q-Atxn1 together, we also observed a decrease in PMY signal intensity but now accompanied by a decrease in 84Q-Atxn1 (Fig. 3.15D-F). Moreover, increasing expression of PML through interferon beta ($\text{Ifn}\beta$) treatment also

diminished PMY staining and 84Q-Atxn1 expression (Fig. 3.16A, B). Interestingly, 32Q-Atxn1 expression was also diminished during Ifn β treatment (Fig. 3.16C). These results suggest PML-localized polypeptide synthesis is concurrent with the degradation of mutant Atxn1 protein.

Taken together, these data suggest that PML bodies link protein synthesis and degradation during proteotoxic stress.

Polypeptide synthesis localizes to nucleoli and PML bodies in human IMR90 fibroblasts.

PML bodies play a multifaceted role in the cell stress response, which alters both their structure and protein composition. To expand upon the characterization of puromycylated peptides in the nucleus beyond proteotoxic stress, we tested other stressors, including: heat shock, oxidative stress, serum starvation, and ultraviolet-c (UV-C) irradiation in IMR-90s. After each cellular insult, we observed the PMY signal colocalized with nucleoli markedly decrease, concomitant with a significant increase in PML bodies colocalized with PMY signal (Fig. 3.17). The shifts in PMY-localization are stress-dependent, with UV-C irradiation and serum starvation revealing the greatest changes. These results suggest PML-localized polypeptide synthesis represents an important component of a general stress response in the nucleus.

***ATXN1* mRNA is targeted by no-go decay in the nucleus during proteotoxic stress.** mRNA surveillance represents a major source of post-transcriptional quality control (109). One such pathway, no-go decay (NGD), is induced by stalled ribosomes caused by repetitive or otherwise aberrant mRNAs (68). The highly repetitive CAG tract of *ATXN1* may initiate NGD, although NGD of repeat-expanded mRNAs in mammalian cells has not been established (114). To address the possibility of NGD at PML bodies, we analyzed the localization of Pelota (PELO) and HBS1-like protein (Hbs1L), two proteins necessary for NGD in mammals (74). Interestingly,

after 12 h of 84Q-*ATXN1* expression, we observed Hbs1L and PELO localized with CAG-repeat RNA foci (Fig. 3.18). After 24 h expression of 84Q-Atxn1 compared to controls, Hbs1L was mainly cytoplasmic, with some nuclear localization. Conversely, nuclear PELO localization increased during expression of Atxn1, forming nuclear puncta adjacent to 84Q-Atxn1 inclusions (Fig. 3.19). These results suggest that Hbs1L and PELO can be localized to the nucleus during proteotoxic stress.

To determine the role of Hbs1L and PELO in the regulation of mutant Atxn1, we altered their expression. When we knocked-down Hbs1L and PELO with RNAi, 84Q-Atxn1 protein expression increased, while 32Q-Atxn1 expression was not affected (Fig. 3.20A, B). When we knocked down the two proteins in SCA1 fibroblasts, we observed a significant increase in *ATXN1* mRNA (Fig. 3.20C). Conversely, when we co-expressed 84Q-Atxn1 with Hbs1L and PELO, we observed Hbs1L-PELO puncta in the nucleus correlated with decreased 84Q-Atxn1. (Fig 3.21). Taken together, these results suggest that Hbs1L and Pelota are necessary for the regulation of mutant Atxn1 expression and that NGD can occur in the nuclear fraction of mammalian cells.

The results presented here suggest a model in which PML bodies act as organizational hubs for the interface between RNA and protein quality control in the nucleus, functionally organizing regulatory translation of repetitive transcripts (Fig 4.1). Under normal conditions polypeptide synthesis occurs in the nucleolus, which may function to test the translational capacity of newly synthesized ribosomal proteins prior to their cytoplasmic export. Some researchers postulate that polypeptide synthesis in the nucleus may have additional roles in the response to viral infection and disease (89). We show here that the localization of protein

synthesis in the nucleus is altered by cell stress. In the case of proteotoxicity, *ATXN1* mRNAs are localized to PML bodies with associated NGD proteins. This novel finding correlates with our evidence for nuclear translation at the sites of PML bodies associating with 84Q-Atxn1 inclusions. In this way, mRNA stalling can be quickly detected and the resulting polypeptide can be SUMOylated by PML and ubiquitinated by RNF4 as previously described for mature misfolded proteins. We speculate that aberrant mRNA can be detected before export into the cytoplasm as a way to use special proximity to save energy on cytoplasmic PQC. The regulatory translational mechanism of NGD is postulated here, complementing previous reports of nuclear localized mRNA surveillance and providing evidence for NGD in mammalian cells (87, 88). This study provides novel insight into the functional significance of protein synthesis in the nucleus and a new perspective on the role of PML bodies in orchestrating multiple nuclear processes. Additionally, this study opens new therapeutic targets for diseases caused by repeat-expansion mutations. Namely, increased expression of PML may expedite the nuclear PQC process and clear repeat-expanded mRNAs and protein. Further studies on the link between PML localized translation and mRNA degradation will expand our findings. Given that nuclear protein aggregates as well as mRNA foci are a common feature of polyQ disorders, we suggest that the novel regulatory mechanism we describe will be of broad interest for fields ranging from cellular stress to neurodegeneration.

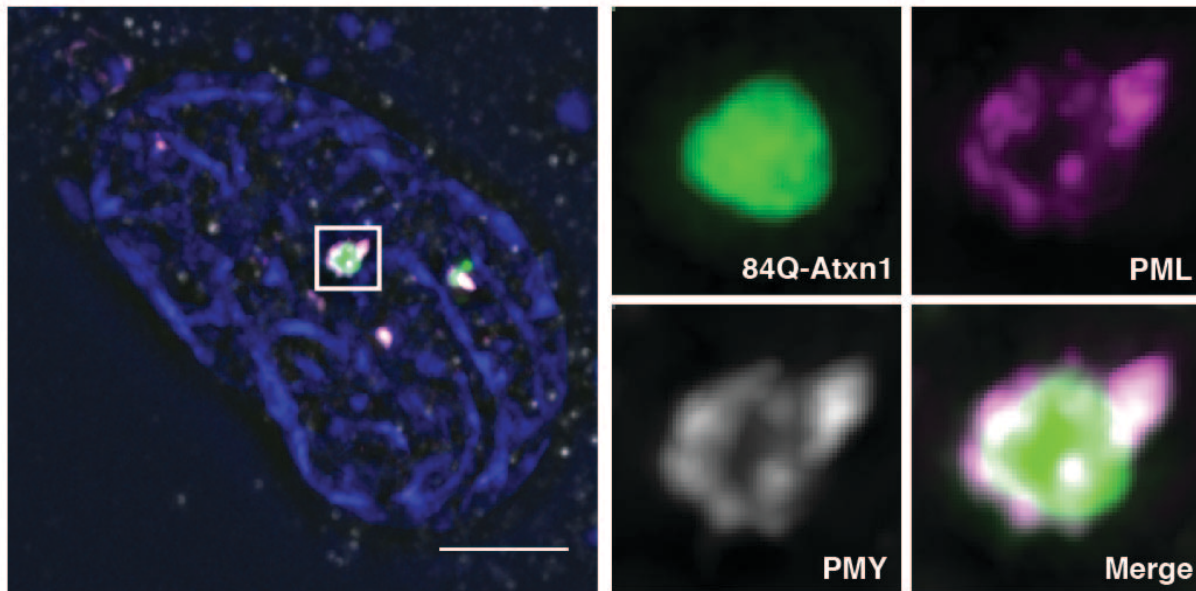


Figure 3.13 Active translation signal associates with PML bodies and 84Q-Atxn1 inclusions. SIM microscopy image illustrating the localization of PMY between the PML ring structure and the 84Q-Atxn1 protein inclusion. Image generated by Arturo Gorza-Gongora.

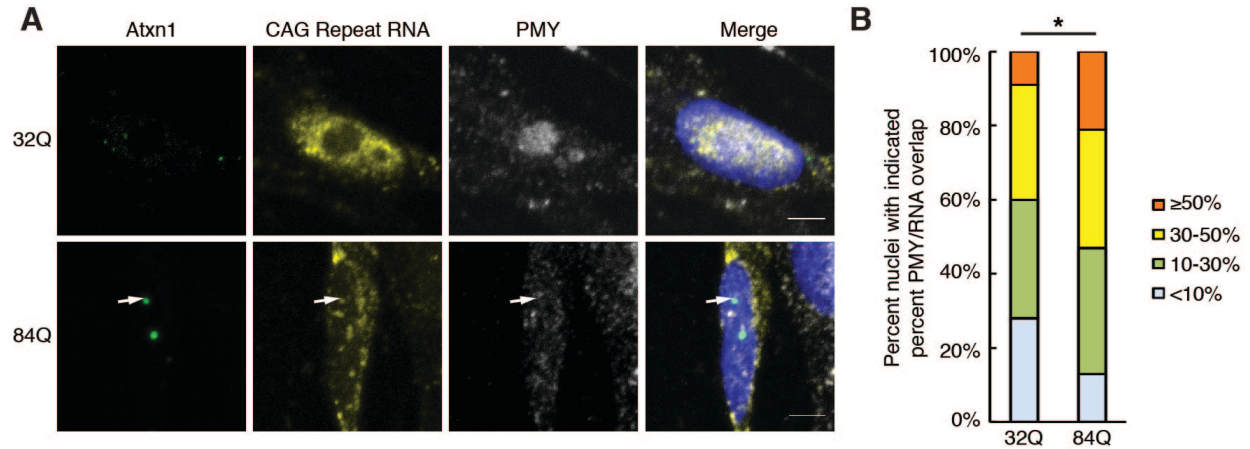


Figure 3.14 Active translation signal significantly increases in association with 84Q-ATXN1 mRNA. (A) RPM-RNA-FISH in IMR-90s 12 h post transfection with 32Q-*ATXN1* or 84Q-*ATXN1*, stained with CAG repeat probe and PMY, quantified in (B) as percent nuclei with indicated percent overlap between CAG repeat RNA and PMY (n = 149 and 150 respectfully, from 3 independent experiments, chi square test analyzed with an unpaired t test, * = $p < .05$). Scale bar, 5 μ m. Arrows highlight typical signal overlap. Image and analysis performed by Chelsea Strojny-Okyere.

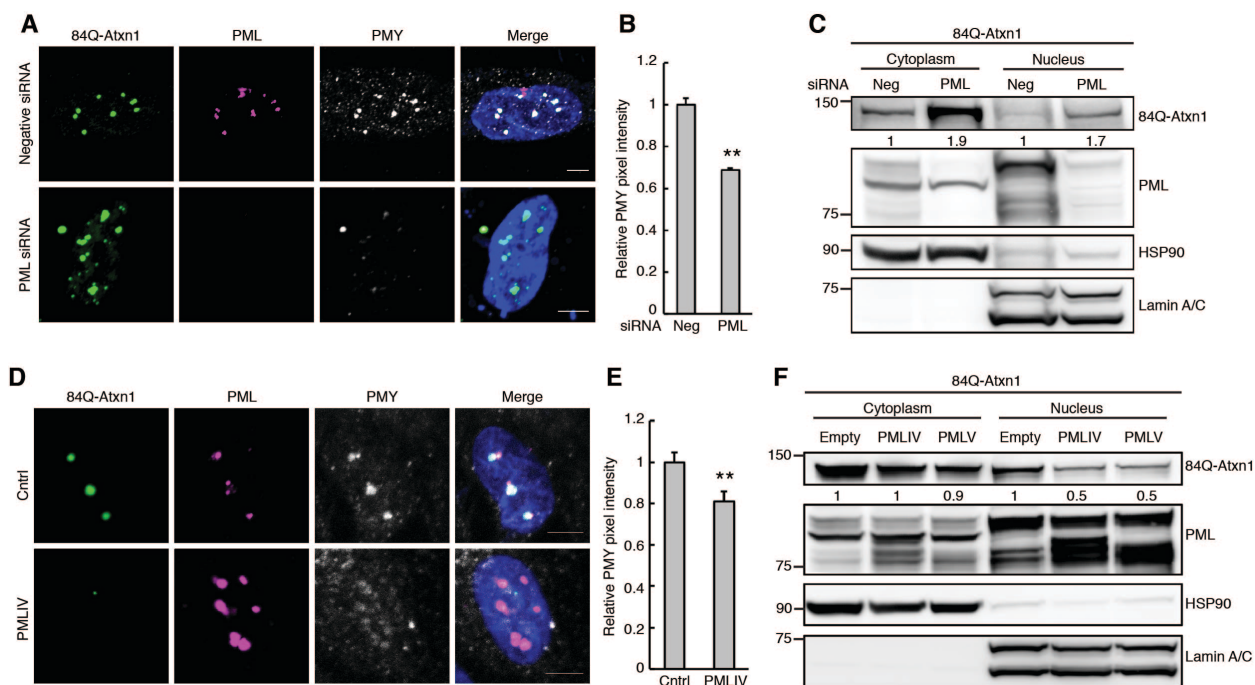


Figure 3.15 Modulation of PML expression disrupts peptide synthesis and mutant Atxn1 aggregates. (A) Confocal microscopy image of RPM in IMR-90s expressing 84Q-Atxn1 after siRNA interference of PML or a negative control, quantified in (D) as relative maximum pixel intensity of PMY particles in each condition. Values represent the average \pm SD of three replicates, analyzed with an unpaired t test, ** = $p < .01$). (C) Western blot of cytoplasmic and nuclear extracts of IMR-90s expressing 84Q-Atxn1 alone or co-expressing with PMLIV or PMLV. 84Q-Atxn1 is stained with an anti-GFP antibody and PML isoforms are stained with an anti-PML antibody. The cytoplasm is demarked by Hsp90 and the nucleus is demarked by lamin A/C. (D) RPM in IMR-90s 24 h after co-expressing 84Q-Atxn1 and either an empty vector control or PMLIV, stained with PML and PMY, indicating PMY staining distribution quantified in (E) as relative maximum pixel intensity of PMY particles in each condition. Values represent the average \pm SD of three replicates, analyzed with an unpaired t test, ** = $p < .01$). Scale bar, 5 μ m. (F) Western blot of cytoplasmic and nuclear extracts from IMR-90s expressing 84Q-Atxn1 after siRNA knock-down of PML compared to a negative control siRNA.

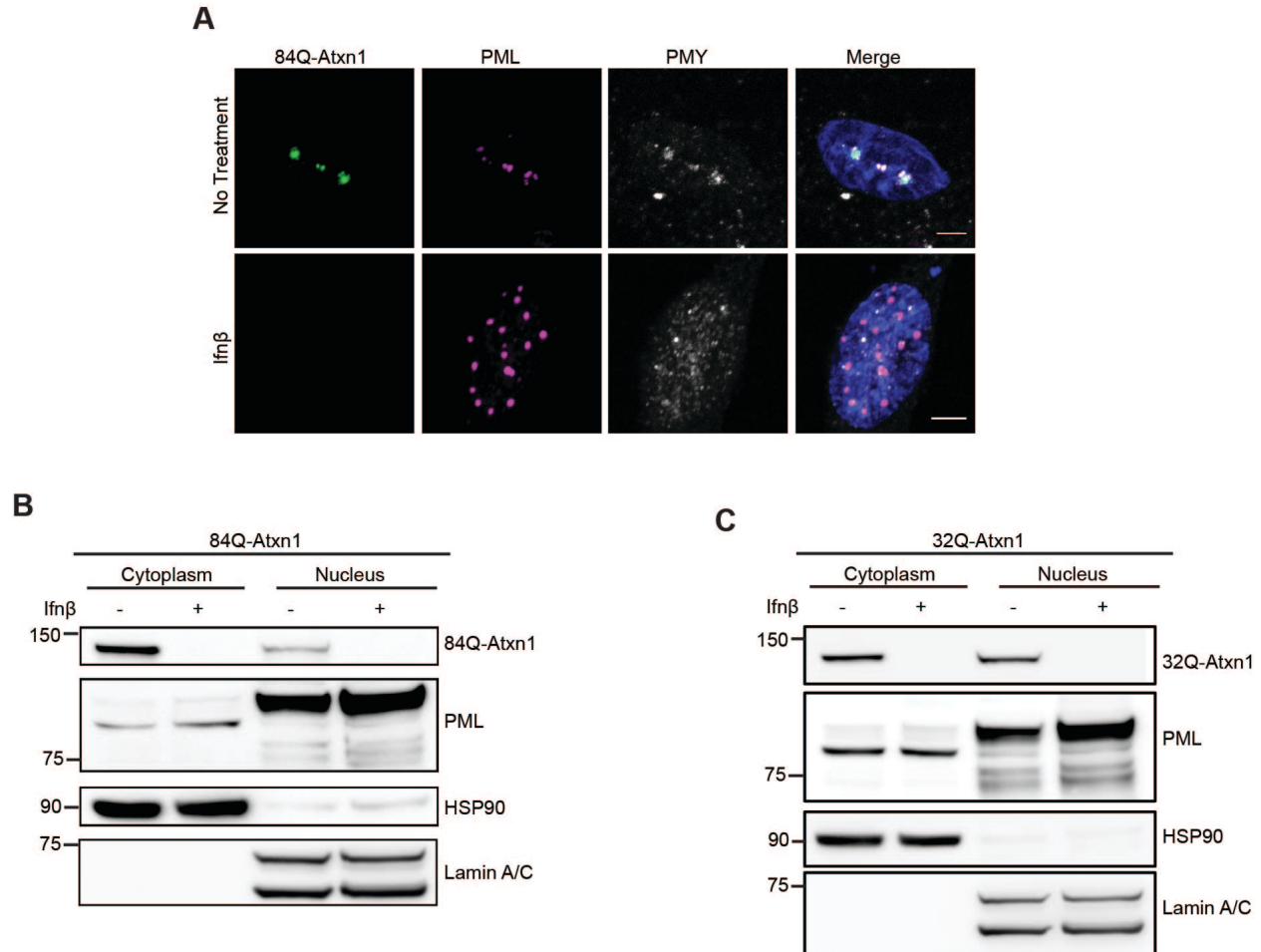


Fig. 3.16 Ifnβ treatment disrupts nuclear translation localization and 84Q-Atnx1 expression. (A) Confocal microscopy image of ribopuromycylation on IMR-90s expressing 84Q-Atnx1 protein with or without 48 h treatment with Ifnβ. Scale bar, 5μm. (B) Western blot of cytoplasmic and nuclear extracts from IMR-90s expressing 84Q-Atnx1 with or without 48 h treatment with Ifnβ.

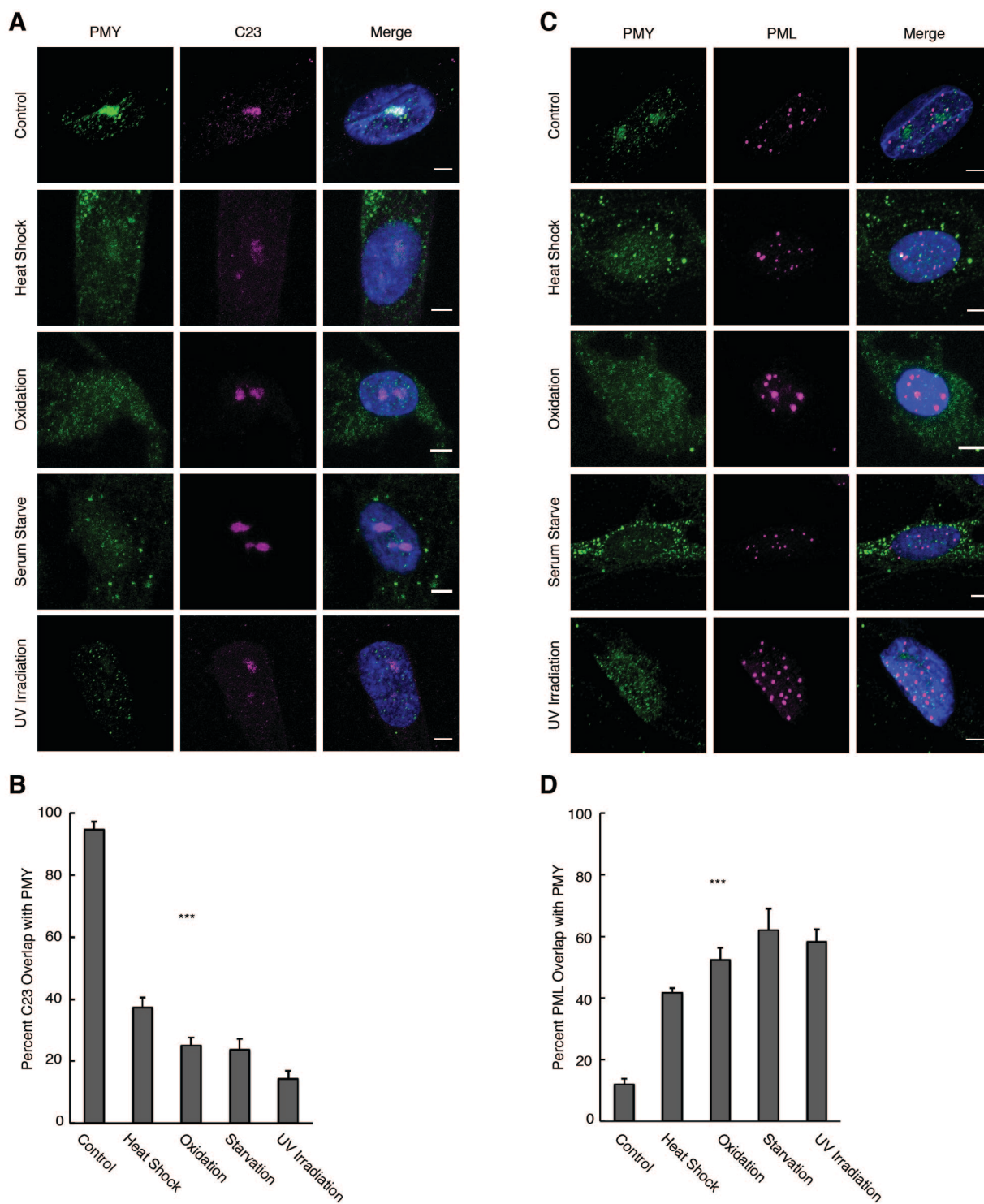


Figure 3.17 Polypeptide synthesis localizes to nucleoli and PML bodies in human IMR90 fibroblasts. (A) Confocal images of ribopuromycylation in IMR-90s under normal conditions, heat shock, oxidative stress, serum starvation, or UV irradiation, indicating localization patterns between PMY and C23 (nucleolar marker), quantified in (B) as average percent colocalization \pm

SD between PMY and C23 from 3 independent experiments ($n > 100$ for all conditions per experiment, one-way analysis of variance and Bonferroni test correction (selected pairs), *** = $p < .001$). (C) Confocal images of ribopuromycylation in IMR-90s under normal conditions, heat shock, oxidative stress, serum starvation, or UV irradiation, indicating localization patterns between PMY and PML, quantified in (D) as average percent colocalization \pm SEM between PMY and PML from 3 independent experiments (analysis same as in B). Scale bar, 5 μ m. Images and analysis performed by Alexis Cogswell.

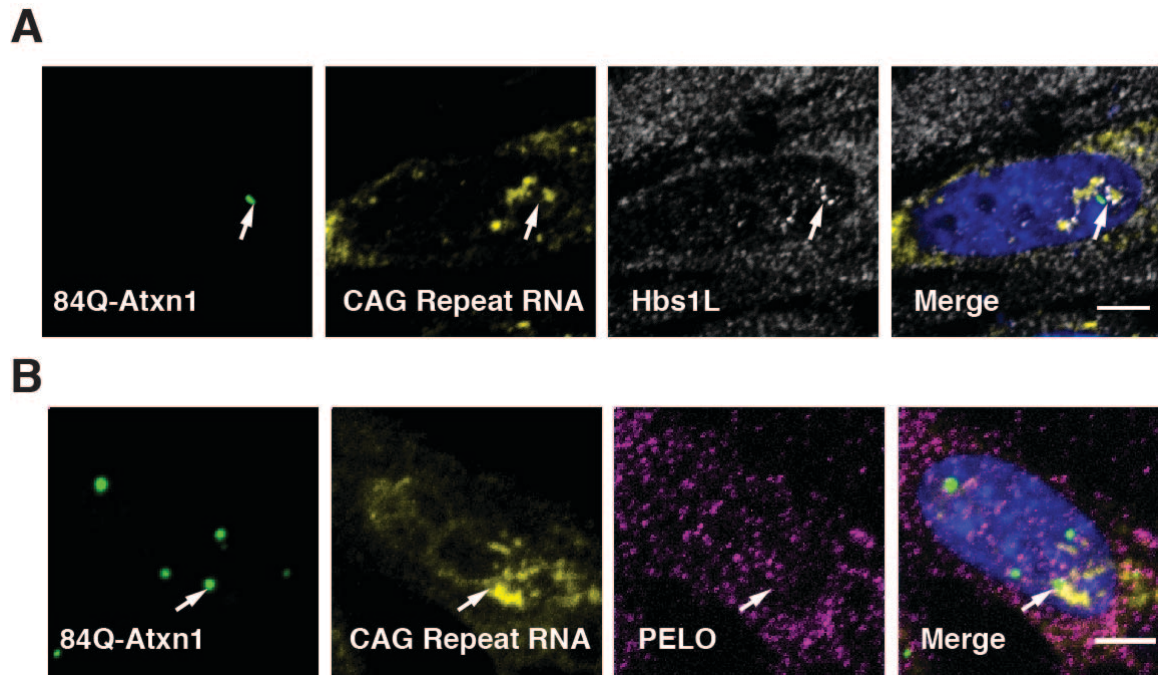


Figure 3.18 Signature No-Go decay proteins associate with 84Q-ATXN1 mRNA foci. (A, B) immuno-RNA-FISH in IMR-90s 12 h after expression of 84Q-*ATXN1* depicting endogenous Hbs1L or PELO localization, respectively. Arrows highlight typical signal overlap.

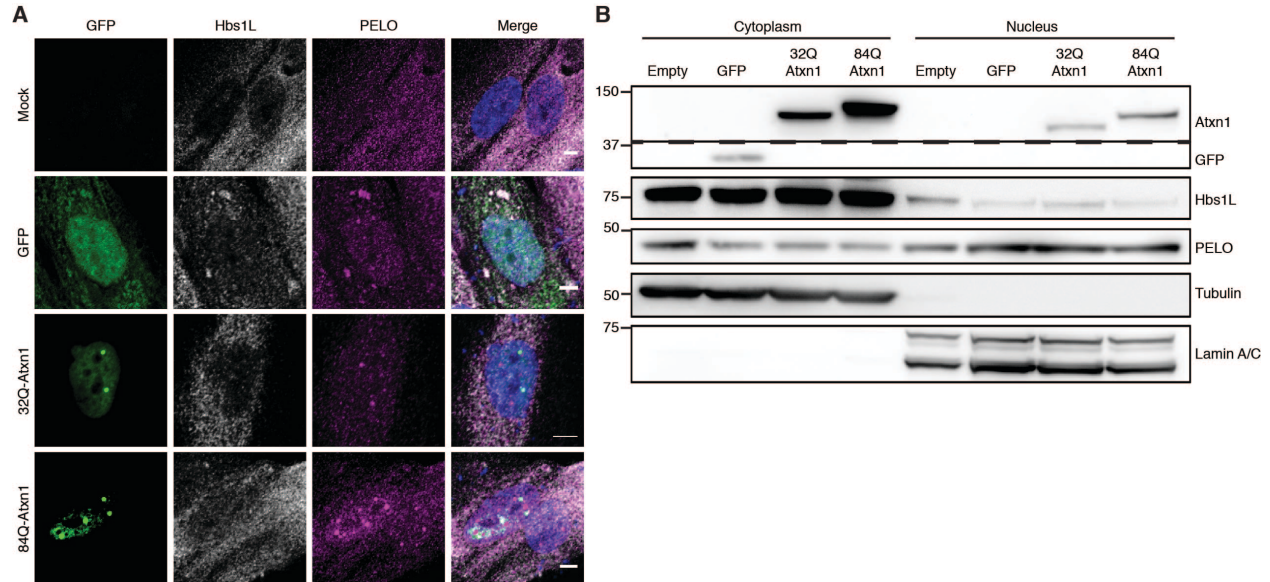


Figure 3.19 Proteotoxic stress alters the nucleo-cytoplasmic distribution of No-Go decay proteins. (A) Confocal microscopy images of IMR-90s 24 h after expression of either a mock control, GFP, 32Q-Atxn1, or 84Q-Atxn1, depicting immunofluorescence staining of endogenous Hbs1L and PELO localization patterns. (B) Western blot of cytoplasmic and nuclear extracts from IMR-90s 24 h after expression of either a mock control, GFP, 32Q-Atxn1, or 84Q-Atxn1, indicating Hbs1L and PELO localization. Tubulin is used to demark the cytoplasm and lamin A/C is used to demark the nucleus.

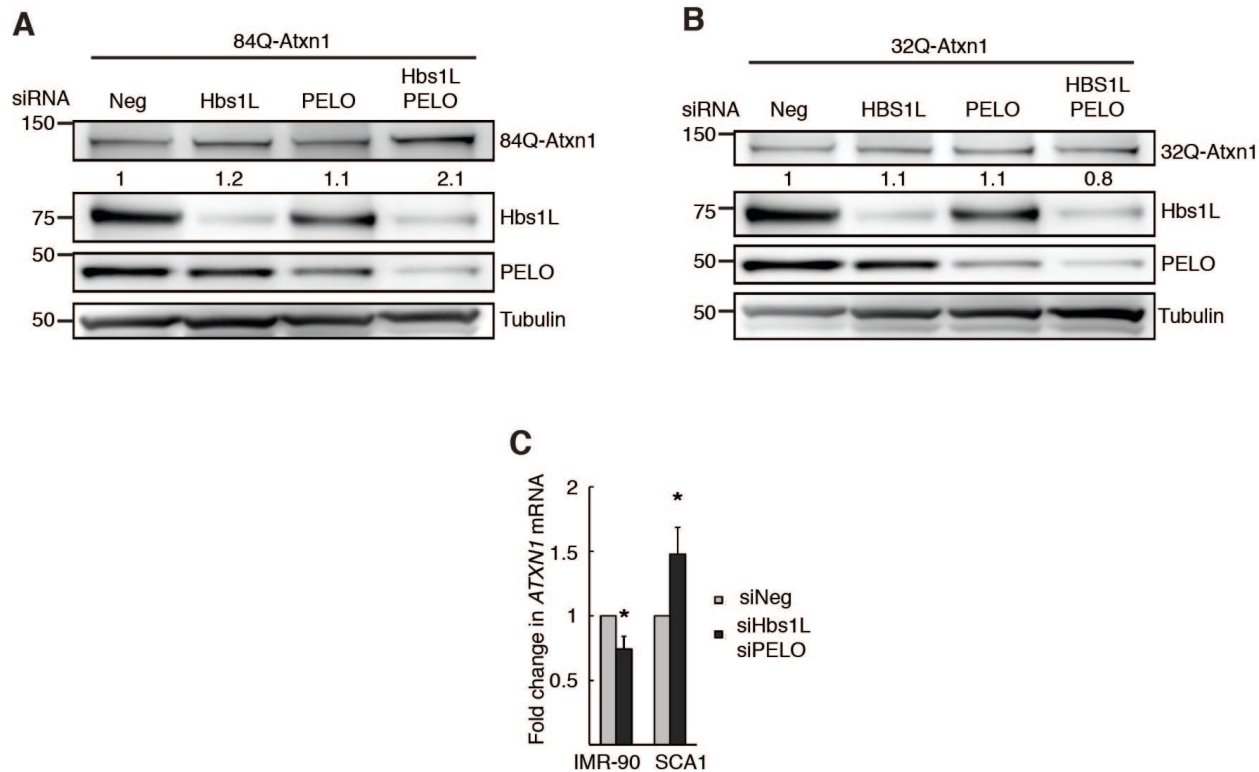


Figure 3.20 Diminished expression of Hbs1L and PELO increases mutant Atxn1 expression. (A) Western blot of whole cells expressing 84Q-Atxn1 protein after siRNA interference of Hbs1L, PELO, or both compared to a negative control siRNA. (B) Western blot of whole cells expressing 32Q-Atxn1 protein expression after siRNA interference of Hbs1L, PELO, or both compared to a negative control siRNA. (C) qRT-PCR analysis of endogenous *ATXN1* in either IMR-90s or SCA1 cells after siRNA knock-down of Hbs1L and PELO, or a negative control. Values normalized to *GAPDH*, analyzed with an unpaired t test (* = $p < .05$).

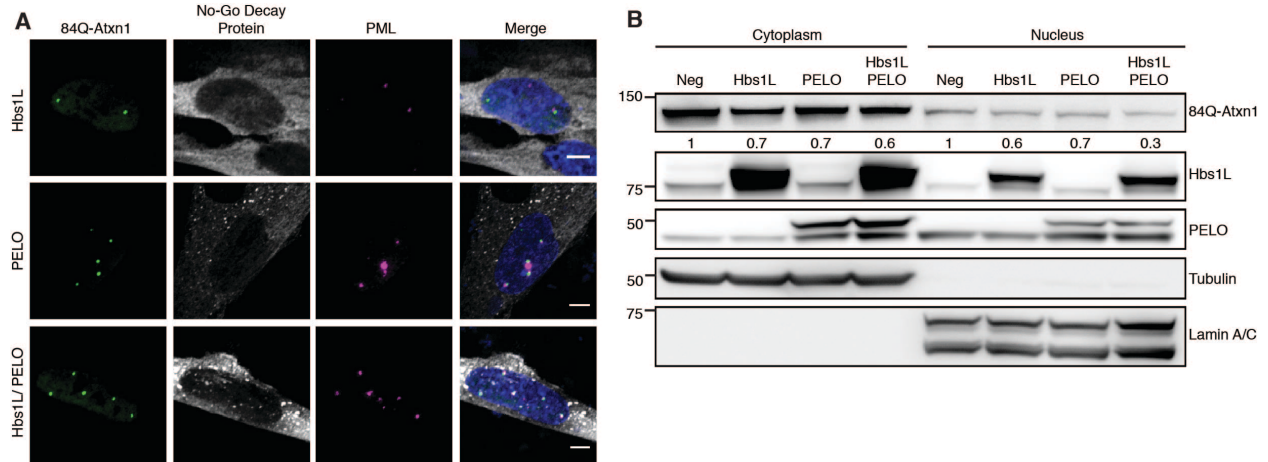


Figure 3.21 Ectopic expression of Hbs1 and PELO decreases expression of 84Q-Atxn1 and alters nuclear morphology. (A) Confocal images of IMR-90s 24 h after co-expression of 84Q-Atxn1 and flag-Hbs1L, flag-PELO, or both. Cells immunofluorescently stained with either flag-Hbs1L, flag-PELO, or both, and PML. Scale bar, 5 μ m. (B) Western blot of cytoplasmic and nuclear extracts from IMR90 cells 24 h after co-expression of 84Q-Atxn1 and flag-Hbs1L, flag-PELO, or both compared to an empty vector control.

3.2 Identification of proteins conditionally associated with PML bodies

3.2.1 Background

The various roles attributed to PML NBs share a common feature in that they are often instigated by cellular stress (115). Moreover, PML bodies specifically are known to be altered both in structure and in protein composition by cellular stress, including UV irradiation and proteotoxic stress (22). These different stressors alter the formation of PML bodies in unique ways. For example, oxidative stress causes an increase in PML body size and a decrease in number of PML bodies per cell. This is due to the redox sensitive TRIM motif that causes multimerization of PML proteins via SUMO binding during oxidative stress (35). Alternatively, under UV irradiation, the number of PML bodies increases. This is linked to both the disruption of PML body formation from UV damage as well as PML's role in DNA damage repair (32, 34). Lastly, PML bodies respond to proteotoxic stress induced by misfolded proteins by colocalizing with and forming ring structures around the misfolded proteins. This change in PML localization is linked to their role in promoting the degradation of misfolded proteins (49). All of these desperate responses to specific cell stressors hypothetically require spatial access to specific protein binding partners that perform vastly different functions. PML protein is known to associate with hundreds of unrelated proteins in sum (27). However, the specific protein compositions of PML bodies during different cellular stress conditions have not been resolved. In the current study, we sought to explore PML body composition during specific cell stress conditions. To identify stress-specific compositions of PML, we employed the unbiased BioID proteomics technique that identifies proximal and dynamic interacting partners of a given protein of interest (116). We examined the composition of PML bodies using an unbiased high-

throughput proteomics technique during both UV irradiation and proteotoxic stress to compare and contrast the composition of PML bodies in these specific conditions compared to normal conditions.

3.2.2 Results

There are several challenges that arise when assessing the composition of a PML body during specific cellular conditions. First, PML protein contained in a PML body is insoluble, thus making it notoriously difficult to immunoprecipitate. Second, many of the interacting proteins of PML bodies are transient or proximal, rather than covalent or long-term (25). PML interacting partners may not interact directly or stably with the PML protein itself, making standard immunoprecipitation studies difficult. Lastly, each PML body in a given nucleus can contain a unique composition of proteins that are unrelated to other PML bodies in the same nucleus (117). These factors make traditional immunoprecipitation methods unsuited for the proteomic study of PML bodies.

My goal for identifying PML binding partners during specific cell stress was to employ a technique that would overcome the challenges of studying the protein composition of PML bodies. I initially tested the *in vivo* crosslinking immunoprecipitation method to generate PML body associated proteins. This method allows for temporary and spatially proximal protein interactions to be covalently linked together in live cells before the immunoprecipitation of the protein of interest. This method would overcome the transient nature of PML body composition, giving me a snapshot of PML body composition in specific conditions. I used the DSP crosslinker that has a 12 Å spacer arm to crosslink proximal proteins. After addition of 25 mM DSP in the growth media of HeLa cells for 30 min, I immunoprecipitated PML and

immunoblotted the precipitated proteins. Unfortunately, the crosslinking method did not yield PML protein or PML associated DAXX protein detectable by immunoblot (Fig 3.22). The *in vivo* crosslinking method did not overcome the challenge of pulling down the insoluble PML bodies.

To overcome the challenge of insolubility of PML bodies as well as the transient nature of PML interactions, I employed the proximity-dependent biotinylation (BioID) method of protein identification. The BioID method employs a genetically modified, promiscuous biotin ligase (BirA*) that is fused to a protein of interest. When the protein is expressed in cells and excess biotin is added to the culture media, the BirA* will biotinylate any protein that is within 10-20nm the fusion protein, depending on the biophysical properties of the fusion protein. Any protein that is biotinylated is isolated by biotin affinity capture and identified by mass spectrometry (108). This technique works best for immobile proteins of interest that transiently or conditionally interact with a low to moderate amount of proteins.

In order to initiate the BioID study I generated N-terminally myc-tagged BirA* and C terminally HA-tagged BirA* fusion constructs for PML isoforms IV and V via standard molecular cloning. I chose these specific isoforms because PMLIV has specific reported protein quality control function and PMLV is deemed a scaffolding isoform of a PML body (24, 117). There are a few considerations that need to be addressed when using BirA*-PML fusion proteins. First, the fusion protein is contained in an overexpression vector. PML bodies from ectopic expression of an overexpression vector are extremely large and irregular in morphology. This would make identification of the interacting proteins of the ectopically expressed BirA*-PML fusion proteins poorly physiologically relevant. Thus, a steady and low expression of the

fusion protein would be necessary to form PML bodies from the fusion protein that resemble normal morphology.

Another important variable in the BioID method for PML bodies is to determine the cell type in which to express the fusion protein. The stably expressed protein would need to be in a cell type that is immortalized or transformed for long-term use. However, transformed or immortalized cell lines may be under oncogenic stress and thus may not have normal protein composition. HeLa cells and HEK293 cells were analyzed for their ability to stably express the protein in physiologically relevant conditions. The last consideration was the timeframe of the excess biotin incubation. Previous studies showed that increased time in the biotin-saturated media corresponded to an increased number of proteins identified by mass spectrometry. I tested different time points of biotin incubation to determine a reasonable timeframe for biotin labeling. These considerations were all done in the following validation experiments.

To validate the localization and biotinylation capacity of the constructs, I ectopically expressed the mycBirA* and mycBirA*-PMLIV constructs in HeLa cells. I found that the constructs had similar expression and localization as non-tagged PML overexpression constructs in both cell types, indicating that the addition of BirA* did not disrupt PML body formation. Additionally, known PML binding partner, Daxx, colocalized to the myc puncta (fig. 3.23). To determine the timeframe for biotin incubation, I transfected mycBirA*-PMLV in HEK293 cells and incubated the cells in 50 μ M excess biotin for 4, 8, 24, 48, and 72 h. I found that 24 h was sufficient for strong detection of labeled proteins without excess labeling of the fusion protein visible at higher time points (Fig. 3.24). After addition of 50 μ M excess biotin to the growth media for 24 h, I found colocalization between biotin and the myc-BirA* fusion proteins. This

indicated that biotinylated proteins were localized within the radius of the fusion protein (fig. 3.23). However, HeLa cells contained a highly excessive amount of a high molecular weight band that was troubling. Additionally, HeLa cells contain PML bodies, while HEK293 cells do not, allowing for the cells to act as PML knock-out cell lines for PML isoform-specific studies. HEK293 cells were validated next to see if they had more physiological banding patterns than HeLa cells. The N-terminally tagged myc-BirA* fusion was chosen for downstream experiments.

Immunoblotting of HEK293 cell lysates treated with biotin showed an abundance of biotinylated proteins distinct from the mycBirA* control. Additionally, biotinylated proteins were enriched over the non-biotinylated control. The fusion proteins were validated for the correct size and single banding pattern (Fig 3.25A). Streptavidin Immunoprecipitation of HEK293 cell lysates expressing the constructs in excess biotin conditions yielded detectable amounts of PML protein. Additionally, the PML binding-partner Daxx was detected in the immunoprecipitation (Fig 3.25B). Streptavidin immunoprecipitation of myc-BirA-PMLV-expressing HEK293 cells subject to UV irradiation showed an ability for proteins to be biotinylated and showed an increase in biotinylated proteins under UV stress (Fig 3.25C). HEK293 cells showed a nice abundance of the fusion protein at the correct size, as well as other protein bands that may be different PML isoforms. Due to these findings, HEK293 cells were used for all further experiments. These collective results demonstrate the validity of the BioID method for detecting PML body associated proteins subject to cell stress.

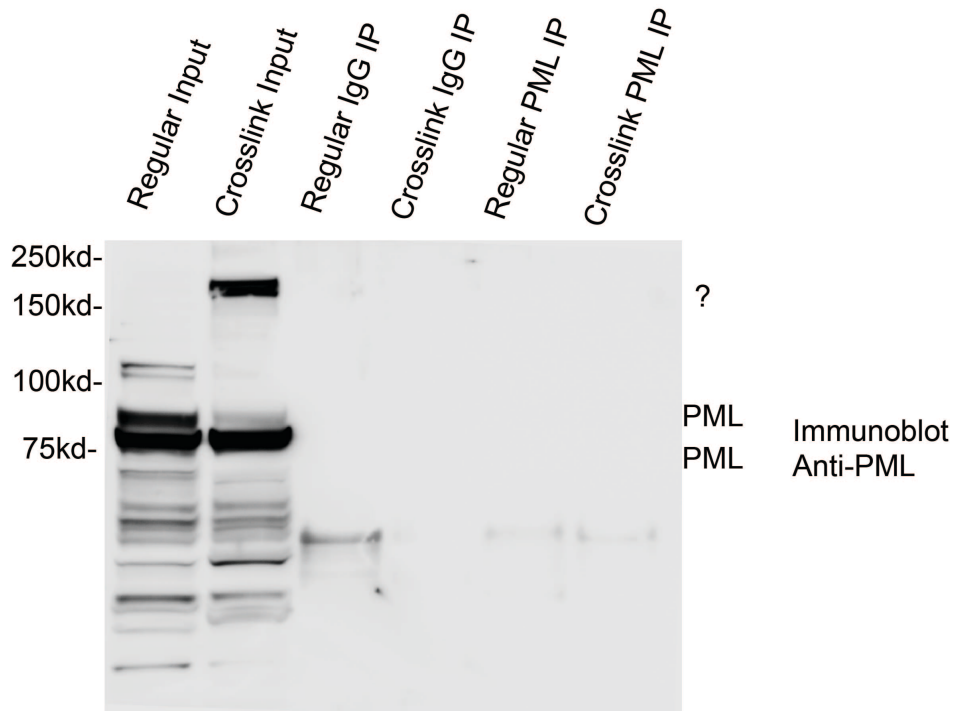


Figure 3.22 In vivo crosslinking of cellular proteins do not yield PML binding partners. Immunoblot showing an immunoprecipitation of crosslinked proteins pulled down by a PML antibody compared to a control IgG antibody. Controls are uncrosslinked cells and input of all conditions.

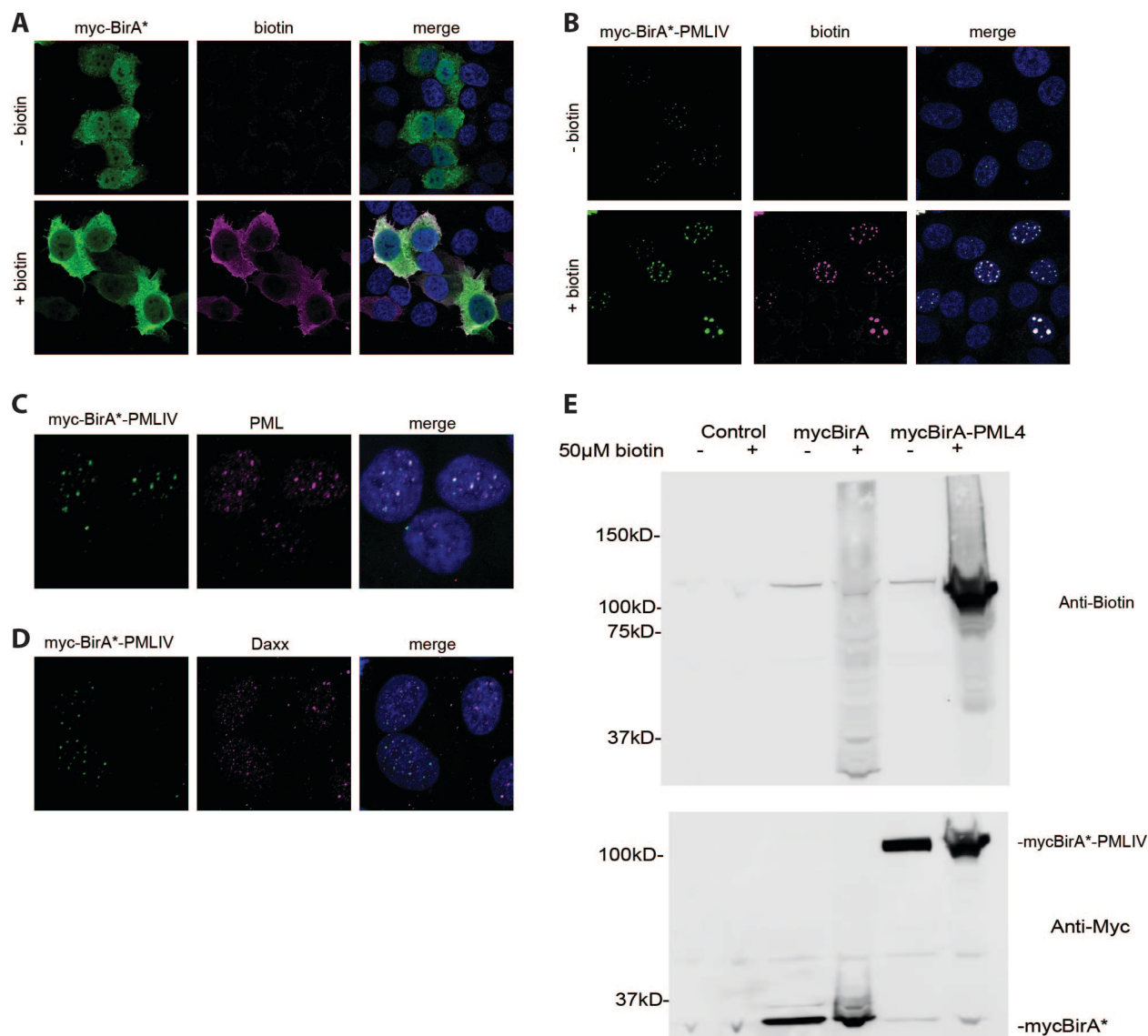


Figure 3.23 Validation of BirA* fusion proteins in HeLa cells. (A) Confocal images of HeLa cells transiently transfected with mycBirA* with or without 24 h incubation with excess biotin. (B) Confocal images of HeLa cells transiently transfected with mycBirA*-PMLIV with or without 24 h incubation with excess biotin. (C, D) HeLa cells transfected with mycBirA*-PMLIV immunostained with myc and either a PML antibody or a Daxx antibody. (E) Western blot of HeLa cells expressing mycBirA*-PMLIV or controls of mycBirA* or no expression after 24 h incubation with excess biotin. Blot stained with an anti biotin antibody and an anti-myc antibody.

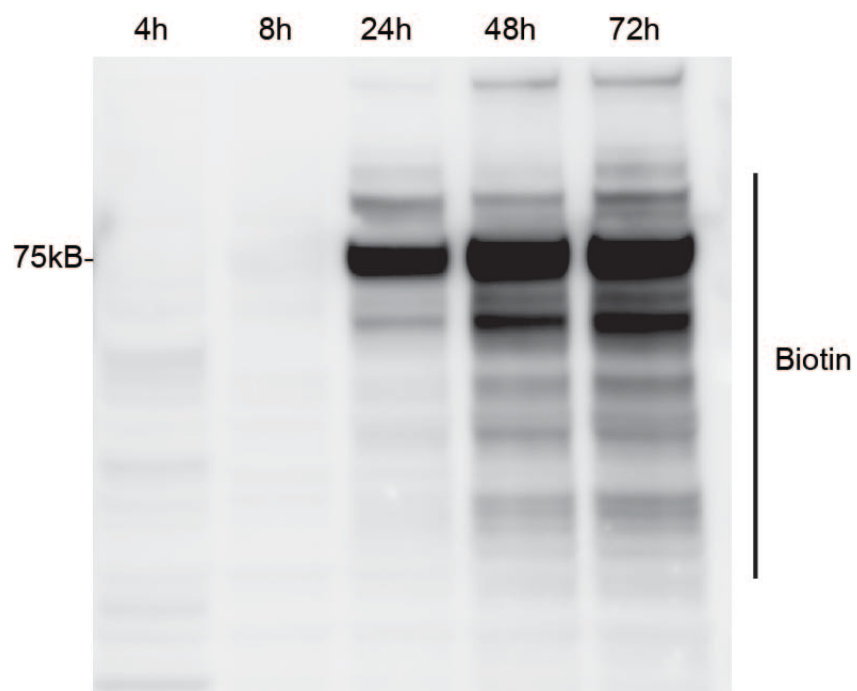


Figure 3.24 Timecourse of biotin incubation reveals proper incubation time for proteomics analysis. Western blot depicting timecourse of biotin incubation of HeLa cells ectopically expressing mycBirA*-PMLIV. Blot stained with an anti-biotin antibody.

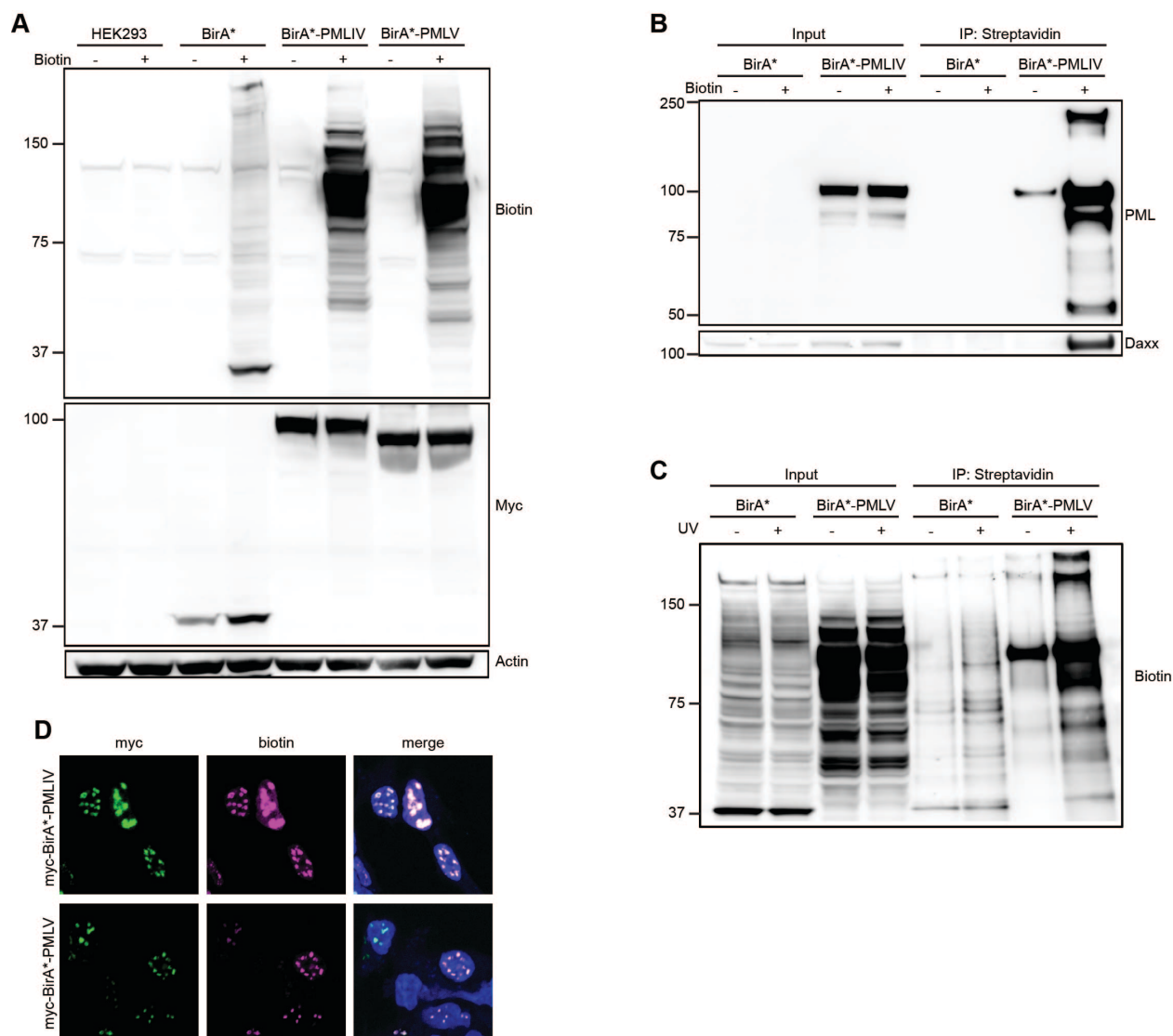


Figure 3.25 Validation of BirA* fusion proteins in HEK293 cells. (A) Western blot depicting the mycBirA* fusion proteins compared to mycBirA* and untransfected control conditions. HEK293 cells in all conditions were incubated with or without excess biotin for 24 h. Blot was stained with biotin and myc, with an actin control. (B) Blot of HEK293 cells expressing mycBirA*-PMLIV or a mycBirA* control, with or without incubation with excess biotin that were immunoprecipitated with streptavidin-tagged magnetic beads. Blot was stained with either PML or Daxx antibodies. (C) Blot of HEK293 cells expressing mycBirA*-PMLV, incubated with excess biotin, with or without exposure to UV irradiation that were immunoprecipitated with streptavidin-tagged magnetic beads. Blot was stained with a biotin antibody. (D) Images of HEK293 cells ectopically expressing mycBirA*-PMLIV or mycBirA*-PMLV, stained with myc and biotin antibodies.

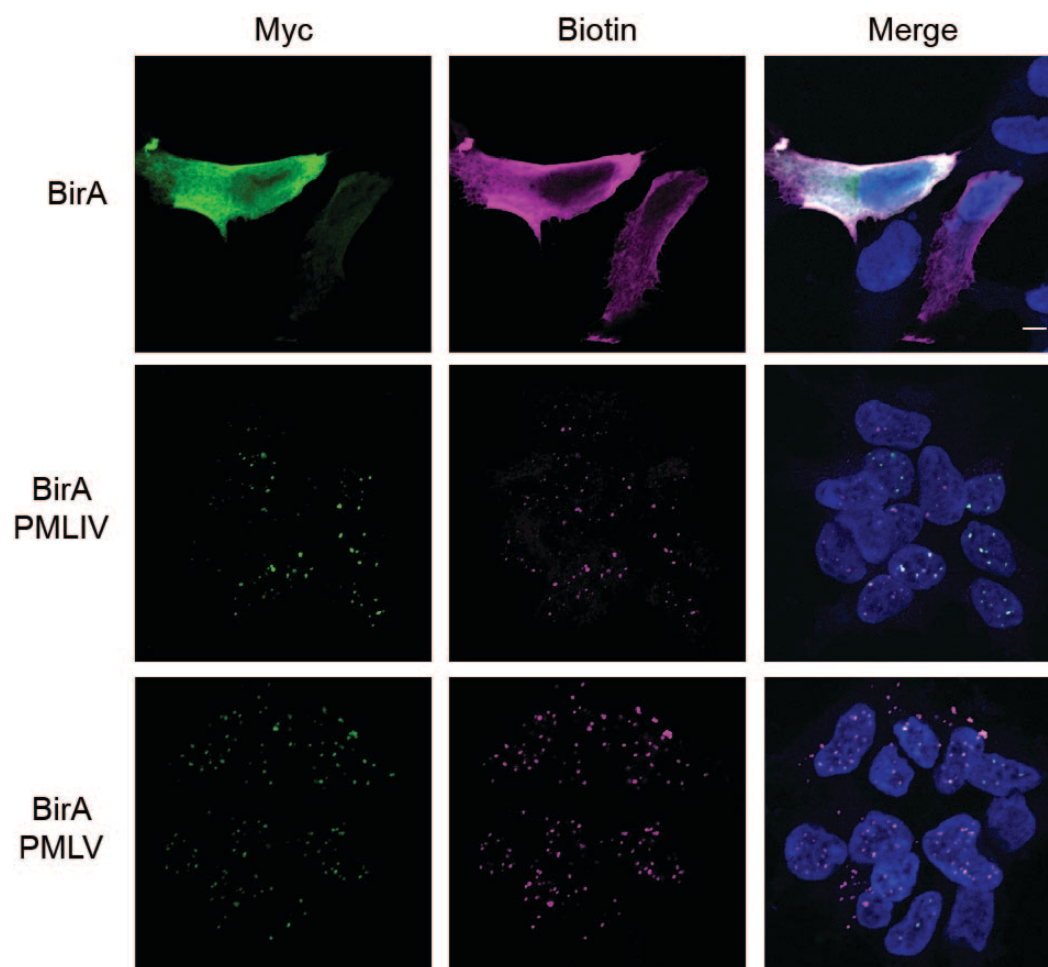


Figure 3.26 Validation of mycBirA* fusion proteins stably expressed in HEK293 cells. Confocal images of HEK293 cells stably expressing mycBirA*, or PML fusion proteins. Cells are stained with myc and biotin antibodies.

Ectopic expression of the myc-BirA* fusion constructs produced large, sometimes irregular PML bodies (Fig 3.25D). To overcome the negative effects of the overexpression protein, I generated HEK293 cell lines stably expressing the BirA*, BirA*-PMLIV, and BirA*-PMLV constructs at low levels. The stable cell line generation was done via Geneticin selection and the expression of the fusion protein was validated by immunofluorescence analysis. mycBirA* had predominant diffuse cytoplasmic localization. BirA*-PMLV had irregular and cytoplasmic PML bodies in all viable clones (Fig 3.26). BirA*-PMLIV showed normal PML body localization pattern of nuclear puncta with overlapping biotinylated proteins after 24 hours incubation in medium supplemented with 50 μ M biotin (Fig 3.26). Thus, PMLIV was chosen over PMLV for further BioID analysis of PML interacting proteins.

I sought to identify PML body composition during UV irradiation and SCA1-induced proteotoxic stress to represent distinct stress phenotypes with documented morphological response from PML bodies. To model proteotoxic stress, I employed a mutant version of 84Q-ATXN1 along with a 32Q-ATXN1 control. I exposed stable HEK293 BirA*-PMLIV cell lines to either 25 minutes of UV irradiation or transient expression of 84Q-ATXN1 stress conditions with non-stressed and 32Q-ATXN1 control conditions. I also included a BirA* control. At the onset of stress, I incubated the cells in in medium supplemented with 50 μ M biotin. 24 h after incubation, I isolated biotinylated proteins by biotin affinity capture and collaborated with the Northwestern Proteomics Core to analyze them via mass spectrometry. The resulting spectra were surveilled for common mass spectrometry contaminants as well as endogenously biotinylated proteins, some histones, and limited ribosomes. These contaminants were excluded from all samples. Initial mass spectrometry analysis of HEK293 BirA*-PMLIV cells in normal

conditions revealed several unique proteins enriched over the mycBirA* control, including known PML binding partners (Fig 3.27).

159 proteins in unstressed conditions, 82 proteins in 32Q-ATXN1 expressing cells, 154 proteins in 84Q-ATXN1 expressing cells, 148 proteins in UV irradiated cells were identified through BioID. (Additionally, 464 proteins were identified in the BirA* control). Only 12 proteins in the unstressed condition and 13 proteins across all conditions were known PML interacting partners as found in the BioGRID database (Fig 3.28). This discrepancy may reflect condition-specific, PML isoform specific, or cell line specific interactions as well as the nature of BioID identification of both proximal and transient interactions and not necessarily direct protein-protein binding. Notably, well-documented binding partners DAXX ATRX, and ZFN451 were detected in all BirA*-PMLIV conditions. The interaction with DAXX was confirmed in HEK293/BirA*-PMLIV cells by immunoprecipitation with streptavidin (Fig. 3.25). Noted proteins absent from the samples were HBS1L and PELO, although EEF1a-1, a homolog of HBS1L, was identified. A PANTHER database gene ontology functional classification by protein class of the unstressed HEK293/BirA*-PMLIV cells revealed a majority of nucleic acid-binding proteins (Fig 3.29).

There was a large amount of overlap between the proteins identified in the unstressed sample and both the proteotoxic stress sample and the UV irradiated sample (Fig 3.30). A Statistical overrepresentation test by molecular function of proteins exclusively found in the 84Q-ATXN1 expressing HEK293/BirA*-PMLIV cells (and not unstressed or 32Q-ATXN1 expressing cells) showed an enrichment of RNA-binding proteins (Fig 3.31). The same analysis of proteins exclusively found in UV irradiated cells (and not unstressed cells) also showed an

enrichment of cytoskeletal proteins and RNA binding proteins (Fig. 3.32). RNA is shown to associate with the periphery of PML bodies but the function of this association is unknown (28). Potential candidates from the GO enrichment analysis from the UV treated samples include DDX42, a RNA helicase important for translation initiation, and spliceosome assembly and HNRNPU, a ribonucleoprotein that binds pre-mRNA. Several ribosomal proteins and translation factors were identified in all samples.

In order to quantitatively analyze the change in protein composition between cellular conditions, I performed a series of three trials of BioID immunoprecipitations. For these series of experiments, I employed a flag-tagged ATXN1 with 85 glutamines (flag-85Q-ATXN1) to address the potential off target effects of a large GFP tag. In each trial, I subjected HEK293 cells to 24 h of 50 μ M biotin incubation plus transient expression of flag-85Q-ATXN1 or sub-pathogenic control of flag-30Q-ATXN1, as well as a pCDNA empty vector control or untransfected control. Then I performed biotin affinity capture and collaborated with the Northwestern Proteomics Core to analyze the resulting peptides via mass spectrometry and a label-free intensity based quantification (Fig 3.33). Unfortunately, the results from this quantitative analysis were too variable between trials of the same condition to reveal statistically significant differences between samples. The samples, submitted on different days, had too much variation in protein quantity, even when normalized to overall sample protein quantity. To overcome this technical challenge, future trials of this experiment must be set-up, performed, and submitted in tandem, rather on separate days.

Overall, the BioID analysis of conditional PMLIV interacting partners revealed potential unique PML body compositions during specific stress conditions and revealed a potential role of

PML in RNA regulation during proteotoxic and UV irradiation stress. Future studies done by the Kosak lab will need to address the function of candidate proteins during the given cell stressors. Additionally, expansion of the above proteomics study to include additional stress conditions as well as additional PML isoforms will lead to a robust analysis of PML body composition and reveal new and important PML interaction partners in an environmental condition-specific manner.

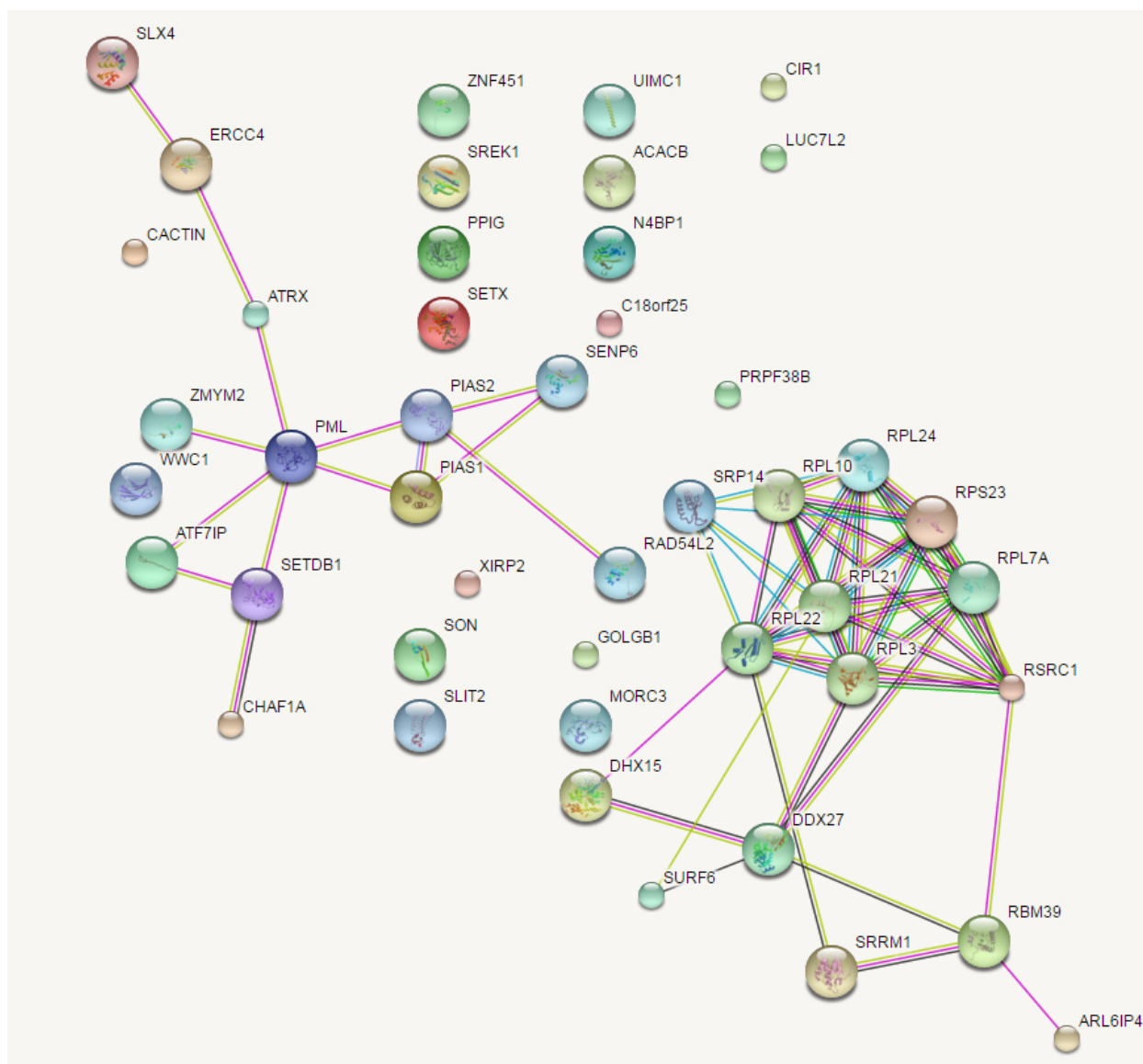


Figure 3.27 PML binding partners are enriched in BioID analysis of PMLIV. STRING analysis of HEK293/mycBirA*PMLIV cells in normal conditions reveals enrichment of unique proteins compared to mycBirA* control. Initial STRING analysis performed by Paul Thomas of the Northwestern Proteomics Core.

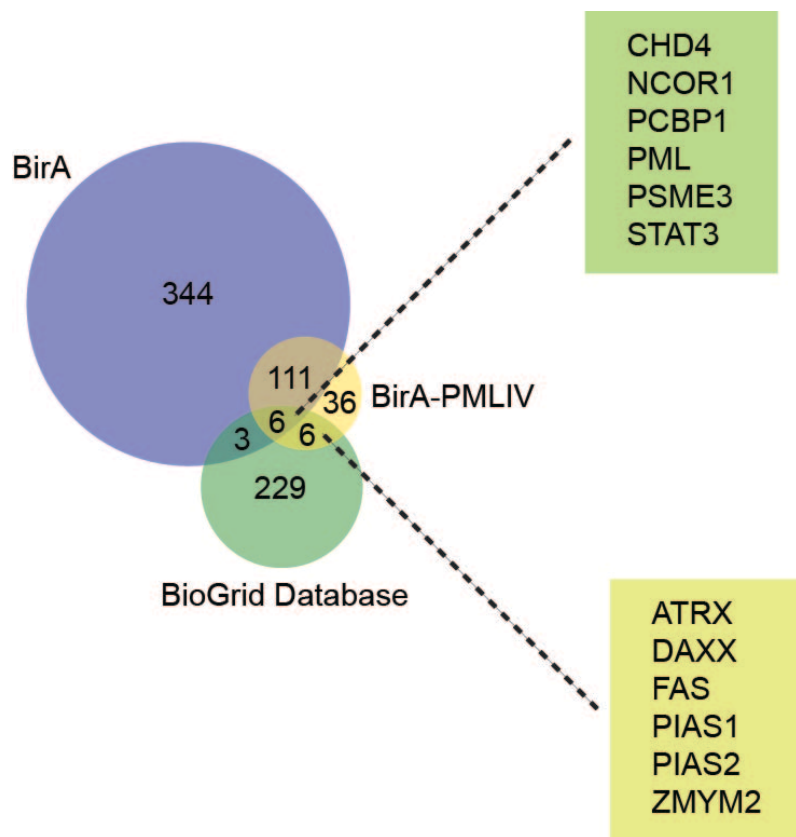


Figure 3.28 Known binding partners of PML identified as a subset of interacting proteins. Venn diagram depicting the overlap between proteins identified by BioID mass spectrometry analysis of HEK293/mycBirA*-PMLIV and mycBirA* cells compared to known PML interacting partners in the BioGrid Database. Data organized for proteomics analysis was aided, in part, by Chelsea Strojny-Okyere.

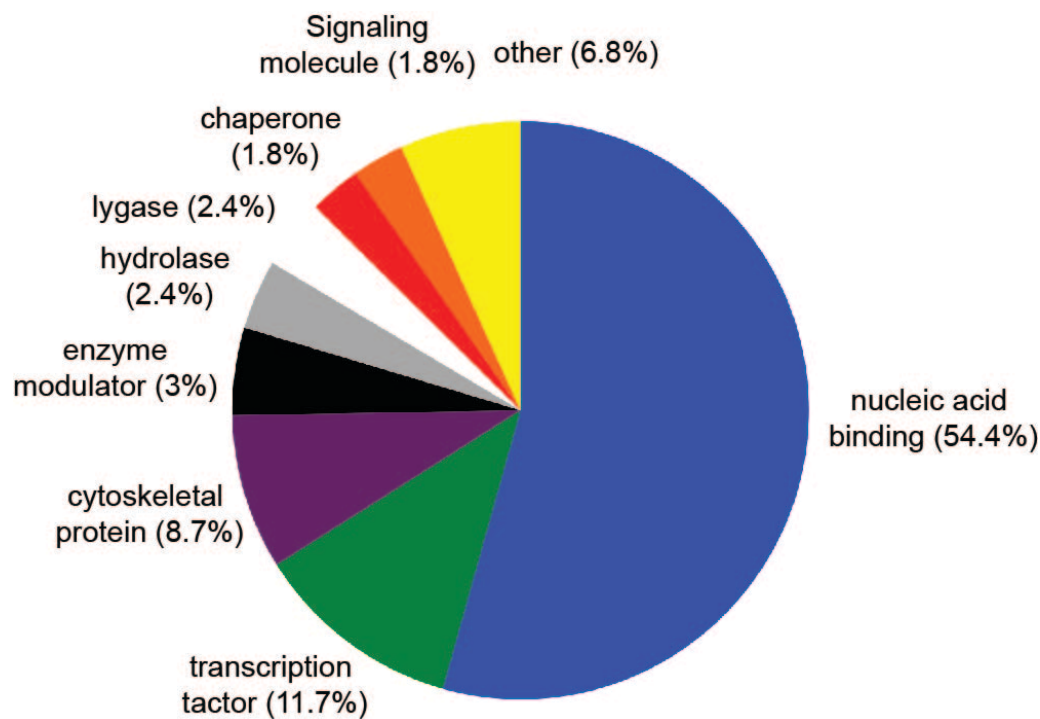


Figure 3.29 PML interacting partners are predominantly nuclei acid binding proteins. Venn diagram of a PANTHER database gene ontology functional classification by protein class of the unstressed HEK293/BirA*-PMLIV cells.

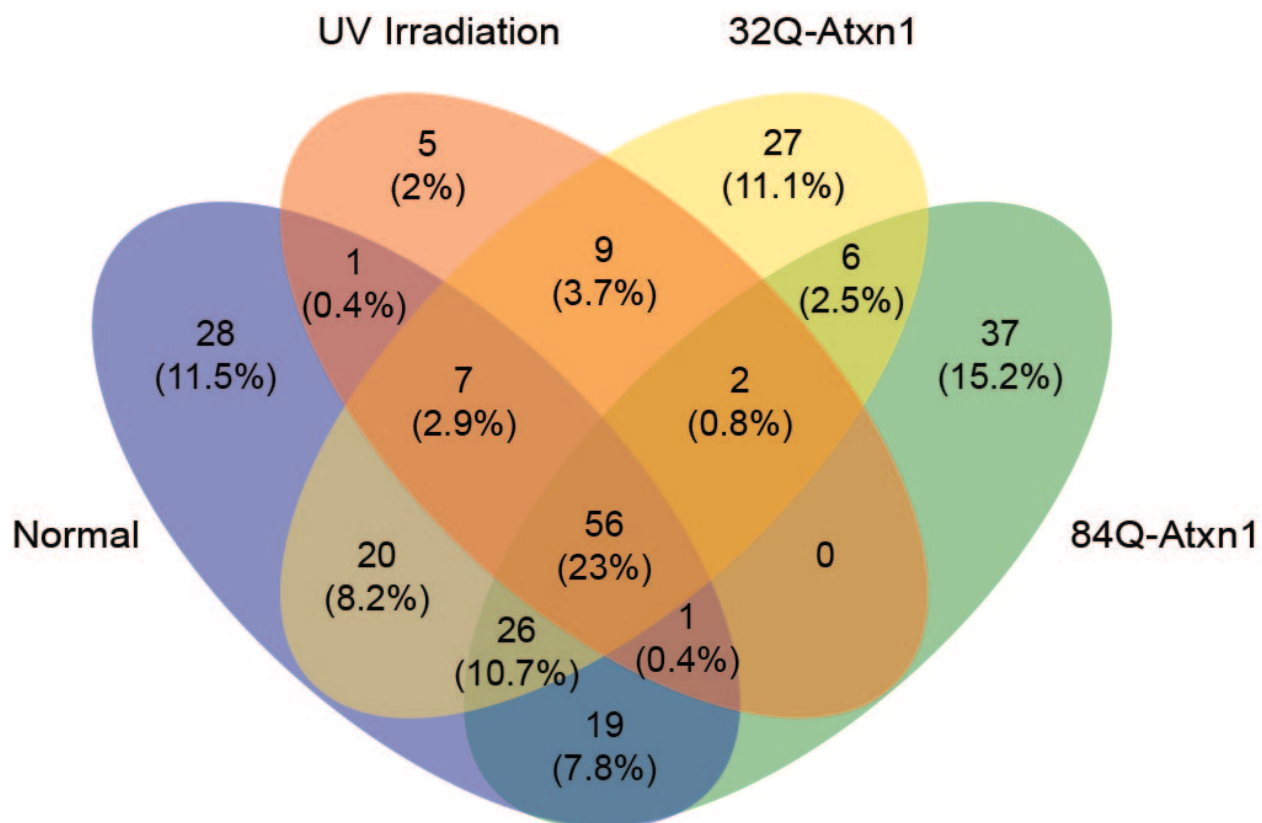


Figure 3.30 Identified proteins largely overlap between cell stress conditions. Venn diagram of proteins identified by BioID mass spectrometry from HEK293/mycBirA*-PMLIV cells in normal and stress conditions.

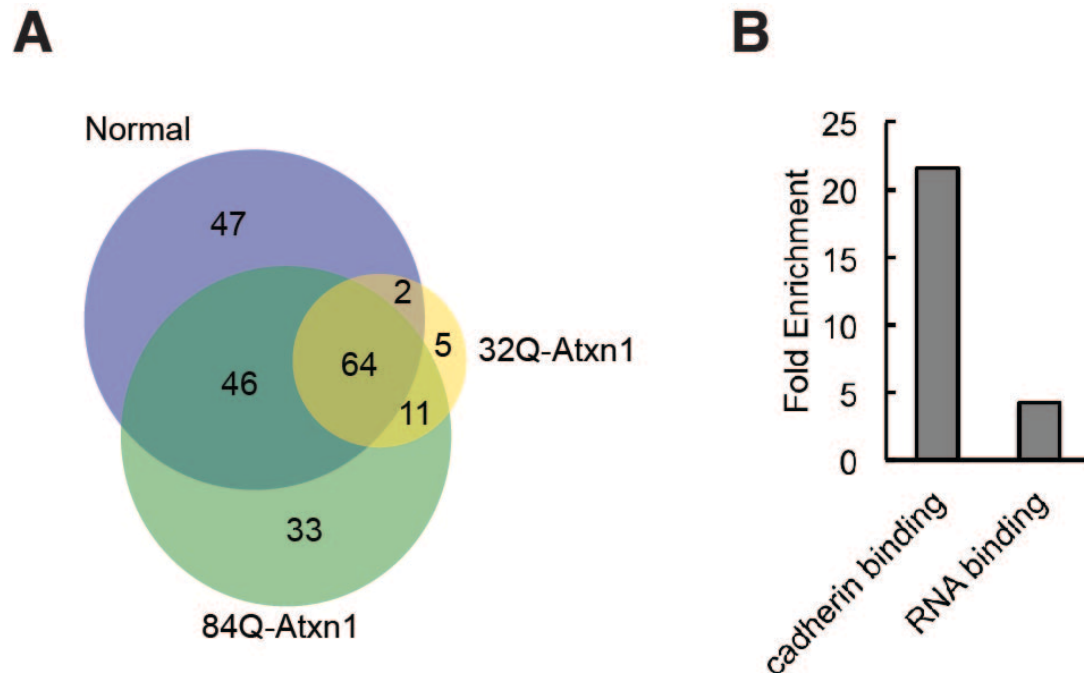


Figure 3.31 RNA binding proteins are enriched at PML bodies during proteotoxic stress. (A) Venn diagram of proteins identified by BioID mass spectrometry from HEK293/mycBirA*-PMLIV cells during ATXN1-mediated proteotoxic stress compared to normal and nonproteotoxic ATXN1 controls. (B) Statistical overrepresentation test by molecular function of proteins found exclusively in the 84Q-ATXN1 expressing HEK293/BirA*-PMLIV cells.

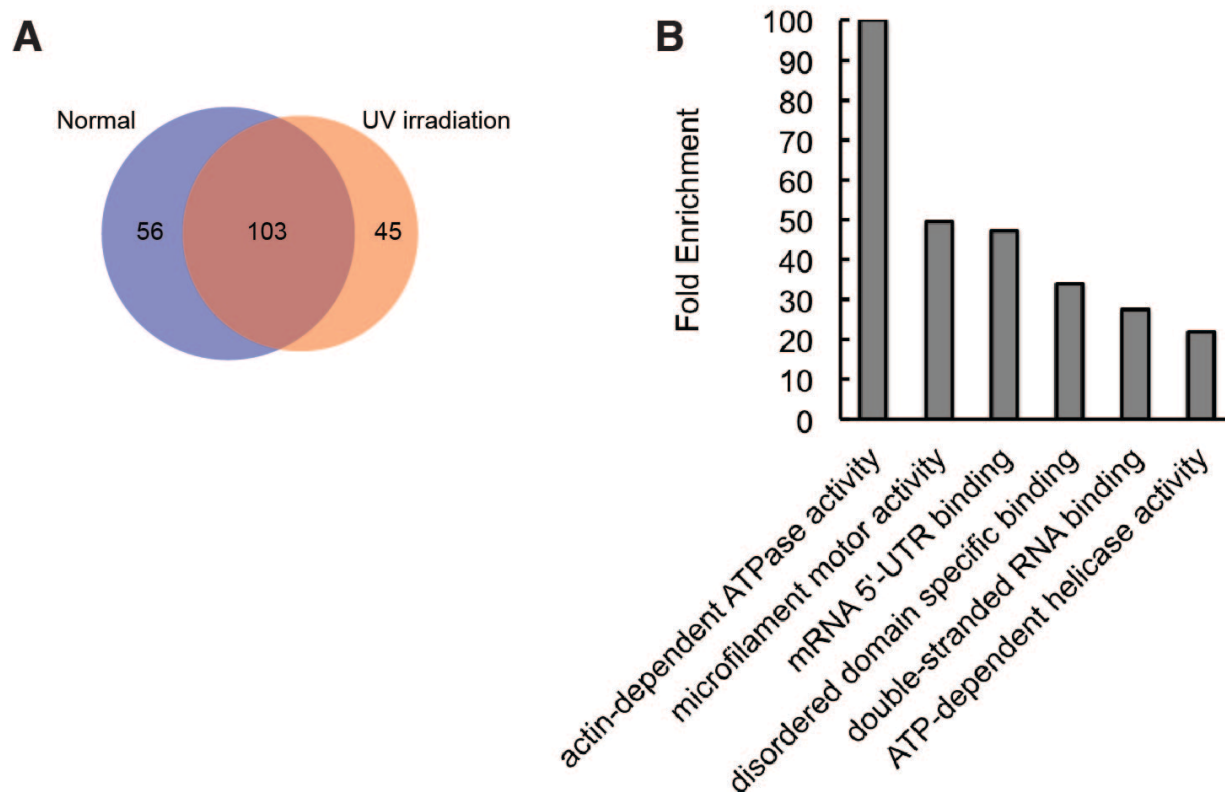


Figure 3.32 Cytoskeletal and RNA-binding proteins are enriched at PML bodies during UV irradiation stress. (A) Venn diagram of proteins identified by BioID mass spectrometry from HEK293/mycBirA*-PMLIV cells during UV irradiation stress compared to normal conditions. (B) Statistical overrepresentation test by molecular function of proteins found in the UV irradiated HEK293/BirA*-PMLIV cells compared to normal control.

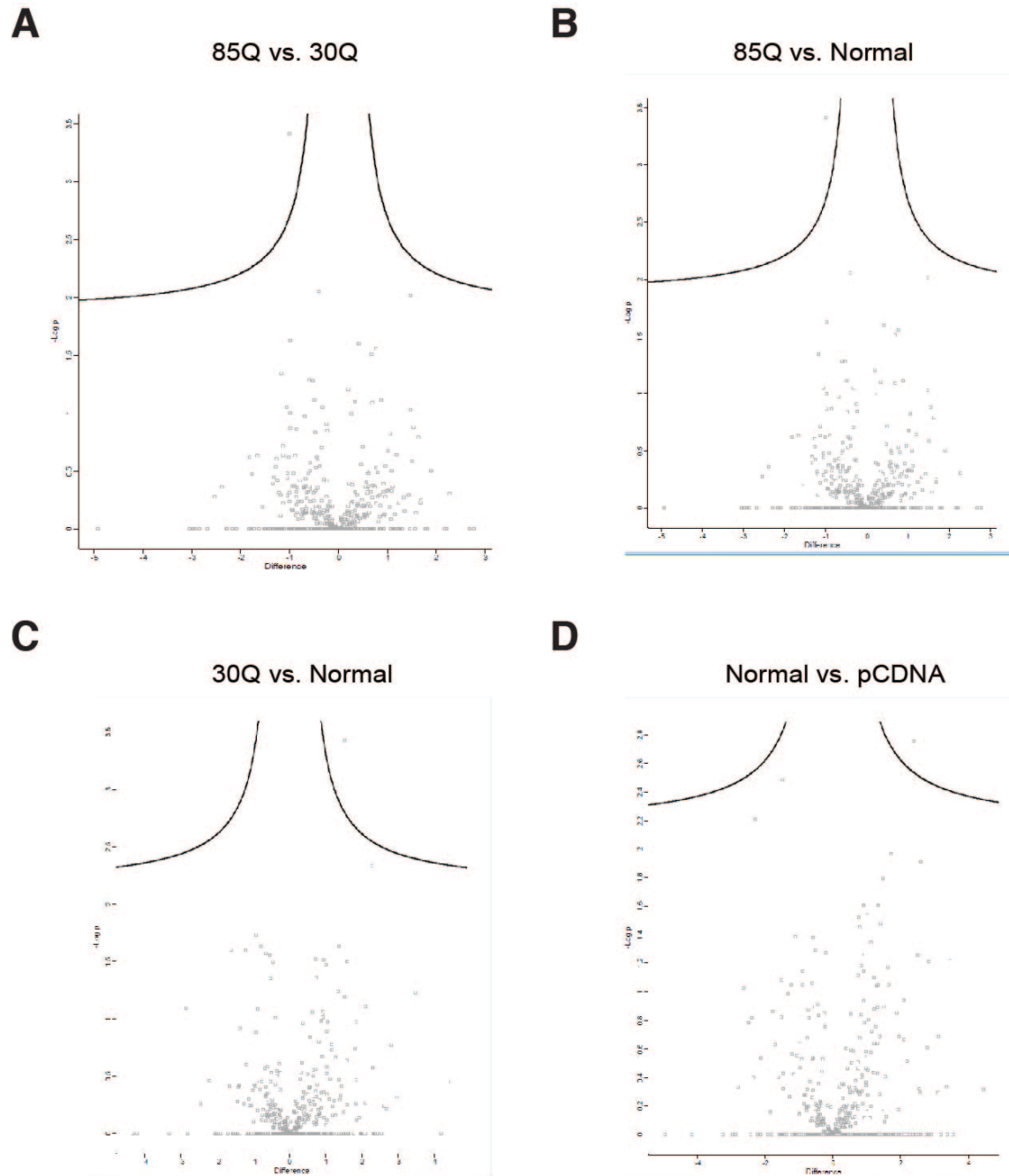


Figure 3.33 Initial quantitative analysis of PML binding proteins during cell stress did not reveal enriched proteins. Volcano plots of quantitative analysis comparing conditions of (A) 85Q-Atxn1 and 30Q-Atxn1 expression, (B) 85Q-Atxn1 expression and normal conditions, (C) 30Q-Atxn1 expressing and normal conditions, and (D) normal conditions and an empty vector control. Quantification analysis performed by Young Ah Goo and the Northwestern Proteomics Core.

Chapter 4: Discussion and Future Studies

4.1 Discussion

PML bodies are exemplified by complexity. From the range of PML protein isoforms condensed in a PML body, to the plethora of protein interactions, to the dynamic nature of their assembly and localization, PML bodies are endlessly complicated. Indeed there may be no single PML body that encompasses a unifying function. Instead, different PML body compositions may arise depending on cellular conditions (22). For these reasons, assigning an overarching function to PML bodies is difficult. My goal was to identify key and novel organizational functions of PML bodies during specific cellular conditions. To achieve the goal of identifying novel PML body functions, I used a top down proteomics approach as well as a targeted mechanistic approach. These two approaches led me to an exploratory model for a novel function of PML bodies, while keeping the possibilities for future directions open.

4.1.1 A model for protein synthesis as a function of PML localized quality control

Before the study illustrated in chapter 3, evidence for PML bodies as hubs for post-translational quality control nuclear proteins was growing (118). This function allows for PML bodies to play a role in several regulatory processes, from protein degradation to apoptosis. However, studies on the larger function of PML bodies in protein quality control were still lacking. In fact, studies on the role of the nucleus in protein quality control lagged far behind studies on the cytoplasm (115, 119, 120). Evidence for PML bodies in active-translational quality control of protein production did not yet exist. The idea our group had that PML bodies may play a role in translation-based quality control came from evidence of PML's interactions with translation factors, ribosomal proteins, and mRNAs (92, 95, 110, 111). At the onset of this

study, nuclear localized mRNA surveillance or mRNA surveillance-like pathways had not yet been addressed in the literature. In fact, evidence for mRNA surveillance in higher eukaryotes was sparse. However, as our study progressed, evidence that translation was a significant form of nuclear quality control modestly grew in the literature. For example, nuclear translation was linked to nonsense-mediated decay and antigen generation for immune surveillance (88, 121). Our work provided additional evidence for the importance of nuclear translation for protein quality control.

The results from chapter 3 lead to a model in which PML bodies act as organizational hubs for a novel pathway that links aberrant mRNA and protein quality control in the nucleus, functionally organizing the factors required for scanning, translating, and degradation of resulting polypeptides. In the case of proteotoxicity induced by polyQ disorders, mutant ATXN1 mRNAs form nuclear foci localize to nuclear bodies including, surprisingly, PML bodies. This PML localization of mutant ATXN1 mRNA is linked to a redistribution of active peptide synthesis from nucleoli to PML bodies and Atxn1 inclusion bodies. We hypothesize that this redistribution of noncanonical translation localization to PML bodies occurs due to stalling of scanning translation machinery that are recognized by and self organized with PML bodies. In turn, these stalled translation machinery can be quickly detected and the resulting polypeptides can be SUMOylated by PML and degraded, as previous studies indicate (49). The detection of the stalled translation machinery, we hypothesize, is conducted by HBS1L and PELO to initiate the no-go decay mRNA surveillance pathway or a related quality control pathway. Finally, we demonstrate that this PML localized translation-based quality control pathway potentially

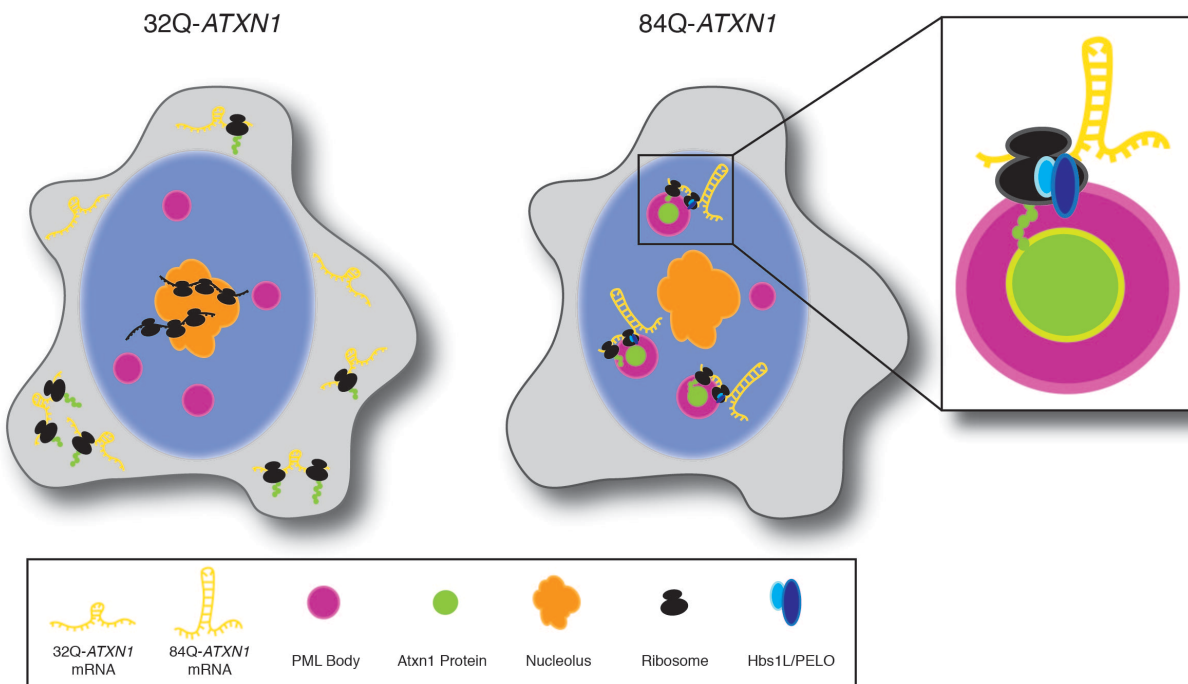


Figure 4.1 Model of regulatory translation at PML bodies in response to proteotoxic stress induced by 84Q-ATXN1. When nonpathogenic 32Q-*ATXN1* is expressed in cells, mRNA transcripts are translated exclusively in the cytoplasm and nuclear translation is localized at nucleoli. However, when mutant 84Q-*ATXN1* is expressed, nuclear translation signal relocates to PML bodies, where *ATXN1* mRNAs are subject to regulation by the no-go decay (NGD) pathway.

functions in response to several types of cell stress, indicating that this function of PML may be broadly important to cell health.

Maintenance of nuclear protein homeostasis is essential under normal and stress conditions. Both RNA and protein quality control mechanisms function in the nucleus (*122-125*). Thus nuclear translation-based quality control can hypothetically be a logical link between these two systems, as it often is in the cytoplasm (*126*). Nuclear localization of an mRNA surveillance-like quality control pathway may be advantageous to the cell because retaining abnormal mRNA in the nucleus for proofreading may prevent the mass export from the nucleus and subsequent mass synthesis of a misfolded protein in the cytoplasm. The cytoplasmic mRNA stress response is a robust field of study and evidence for cytoplasmic mRNA surveillance in higher eukaryotes is growing (*127, 128*). Nuclear mRNA surveillance can potentially be a form of biological redundancy to ensure the fidelity of translation proteins. Alternatively, nuclear mRNA surveillance can be part of a signaling pathway that activates cytoplasmic mRNA surveillance or other stress responses. As such, nuclear mRNA surveillance could be part of a sequential proofreading process that occurs through out protein synthesis. Moreover, misfolded proteins and highly structured RNAs common to neurodegenerative diseases are highly stable and hard to degrade (*56, 129*). Several of these mutated proteins and RNAs have a nuclear localization, making cytoplasmic quality control mechanisms potentially ineffective. Even in normal conditions, nuclear proteins have a tendency to contain more disordered regions and behave more dynamically in structure and localization than cytoplasmic proteins (*130*). Nuclear localized mRNA surveillance-like mechanisms may be critical to regulate nuclear protein homeostasis in mammals. Studies of mRNA surveillance in mammalian cells are just starting to

gain traction (127, 128). There remains a high level of uncertainty about the mechanism of mRNA surveillance in higher eukaryotes. Thus, all of these potential biological explanations for the purpose of my model of PML localized translation warrant further study and speculation.

Robust nuclear localized protein quality control mechanisms are especially important for post-mitotic cells like neurons. As stated in section 1.3.2, post-mitotic cells do not have the capacity to disperse misfolded proteins through cell division (66). This in addition to the fact that at least 15 categories of neurodegenerative disease are characterized by nuclear localized protein and RNA make the nucleus a prime location for quality control (51). PML protein is able to solubilize highly stable misfolded proteins like mutant Atxn1 and promote their degradation (49). Our findings suggest PML may localize a comprehensive system that includes not only protein degradation, but also RNA regulation and scanning. Thus, PML bodies may be a critical defense to both prevent misfolded protein accumulation and degrade existing misfolded proteins in cells that are more susceptible to misfolded protein buildup. PML bodies may play a comprehensive role in protecting against neurodegeneration. However, if a PQC mechanism such as mRNA surveillance occurs at PML bodies, endogenous levels of this regulation are inadequate for the prevention of long-term adverse effects of diseases caused by mRNA and protein aberrations (66). I can speculate that at some point that the endogenous system is saturated by the accumulation of disordered gene products. By understanding the endogenous mechanism for PML localized regulatory translation, we can overcome this saturation through therapeutic intervention.

The potential for therapeutic intervention based on PML localized protein quality control is emerging. For example, our study confirms other studies showing that treatment with the

cytokine $\text{Ifn}\beta$ clears misfolded Ataxin proteins by increasing the expression of PML protein. One preclinical study in SCA7 knock-in mice showed that interferon treatment increased PML expression in mouse tissues. This was correlated with a clearance of Atxn7 inclusions and improvement in motor functions (47, 48). $\text{Ifn}\beta$ -1a is currently used to treat multiple sclerosis but no clinical trials are currently found for the treatment of SCA-type diseases (131). Adverse effects of the cytokine treatment, including liver failure, indicate a need for a targeted therapy for SCAs (132). Additionally, information about the ability of $\text{Ifn}\beta$ -1a to cross the blood-brain barrier is not available to my knowledge. By understanding the mechanism behind PML localized PQC, clinicians can target the protein to harness or amplify its neuro-protective effects. Further pre-clinical studies showing the efficacy of increased PML expression on the clearance of other misfolded proteins should be done, given evidence for PML's protective effects against several cell stressors.

There are possible alternative explanations for our evidence. One intriguing hypothesis that describes PML's association with nuclear mRNA foci is that the PML protein is interacting with, and SUMOylating, RNA-binding proteins that are sequestered in the repeat expanded mRNA (133). PML may identify these RNA-binding proteins as misregulated, tagging them for degradation by the RNF4-dependent ubiquitination pathway. Another alternative explanation for the accumulation of puromycylated peptides at PML bodies is that the short nascent RAN translation polypeptides freely diffuse into the nucleus and accumulate at PML bodies to be SUMOylated. The short timeframe in which nascent polypeptides are labeled in the ribopuromycylation method make this explanation implausible, yet possible (81). Additionally, we cannot yet rule out the possibility for documented extraribosomal functions of RPs associated

with PML bodies (111). We also cannot yet rule out the possibility of tRNA amino-acyl synthetase activity at PML bodies, although our use of translation inhibitor controls makes this unlikely (79). In order to rule out possible alternative explanations for our data, a better understanding of nuclear translation in general must be generated.

4.1.2 Overcoming the enigma of nuclear translation

Nuclear translation remains a controversial subject despite recent experimental innovations. The evidence for such a phenomenon, though building, currently suffers from a lack of resources, evidence, and enthusiasm. Some of the lack of enthusiasm comes from harsh critique, or perhaps a hesitation to update a strongly held view of the compartmentalized eukaryotic cell (80). Indeed introducing the idea of nuclear localized translation can be viewed as an update to the central dogma of eukaryotic molecular biology, where mRNA is synthesized in the nucleus and translated in the cytoplasm. However, our group and other groups that study nuclear translation rationalize that the central dogma is constantly updating with every new study showing the vast complexity of the cell. Every step of protein production is tightly monitored by redundant mechanisms in multiple locations that allow for the quick response to a sudden change in cellular conditions. Nucleus localized protein synthesis pathways may exist to add another layer of complex regulation.

There are two main reasons why the phenomenon remains mysterious. The first is that a technology that definitively and unambiguously detects the localization patterns of nuclear nascent polypeptide synthesis *in vivo* has yet to be invented. There are a few elegant approaches that come close, such as ribopuromycylation, HPG click-chemistry or even Raman scattering microscopy, yet these experiments have drawbacks including low resolution, cytoplasmic

contamination, and ambiguity of the mechanism (81, 85, 86). Detecting the nuclear localization of active polypeptide synthesis is difficult for technical and theoretical reasons. First, if the method of nuclear translation is a noncanonical quality control mechanism such as mRNA surveillance, the resulting polypeptides and mRNA may be promptly degraded. Evidence for rapid proteasomal degradation of nascent polypeptides is growing (see section 1.4) (69). Thus, it would be difficult to detect the translation products or aberrant mRNAs. Second, nuclear translation could happen at such a low rate in normal, steady-state conditions that it is hard to detect with low-resolution techniques. This would be the case if nuclear translation is a pioneer round of translation or part of a stress response that decreases overall protein translation (see below) (84). In our study, we detect robust peptide synthesis signal as seen by microscopy, so the pioneer round mechanism may be unlikely. Third, isolating nuclei for classical translation analyses like ribosomal profiling, or enriching for nuclei in microscopy-based assays is technically challenging. Cytoplasmic polyribosome contamination is a major issue these techniques. Additionally, isolating nuclei may lead to disruption weakly interacting ribosomes with mRNAs. Technical challenges can be overcome through innovation. Below, in section 4.2.3, I've highlighted some experiments based on recent studies that may overcome some of these technical challenges.

The second reason why nuclear translation remains controversial is based on a broad biological question: how does nuclear translation function in a cell? This question encompasses all that the scientific community needs to know about nuclear translation in order for it to become a conventional topic. Without the technical evidence laid out above, we do not yet know how much translation, if any, occurs in the nucleus. Additionally, without a defined mechanism

or mechanisms for nuclear translation in conditions of homeostasis and pathology, we do not yet know the purpose of it. We currently have to resign to the possibility that even if some form of translation occurs in the nucleus, it could be vestigial. The question of how nuclear translation functions in the cell can be broken down into three more tangible questions: what is doing the translating, what is being translated, and what is the purpose of nuclear translation?

What is doing the translating? In order to understand the mechanism of nuclear translation, we must identify the nucleus localized translation machinery. Our study suggests that at least some important ribosomal proteins are present at PML bodies and have the capacity for active translation. Additionally, other studies identified translation machinery that interacts with PML bodies (92, 95, 110, 111). However, we do not know if a fully functional ribosome is present at these sites. It is possible, and backed by a recent study, that a fully functioning 80s ribosome is responsible for nuclear translation (86). However, to expand upon this finding, evidence must be acquired that identifies a mature, fully processed ribosome identical to the classical cytoplasmic ribosome is present and actively translating mRNA in the nucleus. Alternatively, it is possible that an alternative form of translation machinery exists in the nucleus to scan, proof-read, or “test-translate” mRNA transcripts before export into the cytoplasm. Defining nuclear translation machinery through high throughput proteomics methods is a crucial first step in delineating a mechanism for its action.

It is critical to identify nuclear translation machinery in vertebrate, ideally human, models. The majority of the evidence for the nuclear export and cytoplasmic processing of ribosomal subunits comes from studies in yeast (134). Although most of the *trans*-acting factors in cytoplasmic ribosomal processing are homologous between yeast and higher eukaryotes,

evidence for their function in vertebrates is incomplete (*135*). It therefore cannot be ruled out that vertebrates could have evolved to have nuclear localized translation events that are not present in yeast models. In general, identifying every step in ribosome biogenesis, function, and regulation in multicellular organisms such as vertebrates may possibly lead to understanding of noncanonical forms of translation.

The need for a better understanding of the complexity for translation regulation in higher vertebrates may lead to a better understanding of the heterogeneity of ribosomes. Several emerging studies suggest that ribosome protein and rRNA composition can be ‘specialized’ to translate specific types of transcripts or in a specific location of the cell. For example, one recent high throughput study quantified the absolute abundances of ribosomal proteins in translating ribosomes and found that certain ribosomal proteins were enriched for binding to certain mRNA transcripts. Those ribosomal protein variants, such as RPL10A, were required to translate certain transcripts (*136*). Another study found tissue-specific translation of Hox genes that were linked to the presence of PRL38 (*137*). Accessory proteins that dock specific ribosomes to specific organelles or other subcellular locations have been identified. For example, the RACK1 ribosomal scaffolding protein can bind to integrin receptors that allow it to dock to the plasma membrane (*138*). Classically seen as a “molecular machine” with a single defined purpose, a ribosome may be an active and heterogenic tool for gene expression regulation (*139*). In this way, the possibility for a nuclear variant of the ribosome cannot yet be ruled out. Unbiased proteomic experiments like the BioID studies outlined below will be critical to identify specific nuclear translation machinery.

What is being translated? The answer to this question will help us understand the significance of nuclear translation. Our targeted study suggests that aberrant mRNA from repeat expansion disorders is translated in the nucleus in a regulatory manor. We suggest this regulatory translation may be broadened to other cell stressors, as evidenced by our RPM analysis of UV irradiation, oxidative stress, etc. However, without broadening the scope of our study to include other types of mRNA aberrations or features, we cannot know what is being translated in broader stress conditions- although my speculations based on our study and others are suggested below. Additionally, nuclear translation may serve several different functions during normal conditions and cell stress. Assessing what is translated in the nucleus will help us understand the scope of the translation mechanisms.

In addition to our study, recent publications present evidence that sequences with premature stop codons are translated in the nucleus, leading to the possibility of nucleus localized NMD (84, 140). Other direct aberrations like damaged or cross-linked bases, low complexity regions, additional stem-loop structures, and sequences lacking a stop codon should all be assessed for their potential to be translated in the nucleus. Additionally, recent studies indicated the possibility of alternative translation initiation elements besides the AUG start codon, especially in genes associated with cell stress (141). mRNAs with non-AUG dependent translation initiation elements should be assessed for nucleus-localized translation capacity. Additionally, sequences containing introns must be assessed for their capacity to be translated in the nucleus, as a recent study suggested that mRNAs containing introns were translated in the nucleus in order to produce peptide substrates for the MHC (83). All of these recent studies lead

to the question: are there sequence elements required for a transcript to be translated in the nucleus?

Evidence for noncanonical translation elements is growing. For example, internal ribosome entry sites (IRES) allow for cap-independent translation initiation. TP53 contains an IRES, allowing for the activation of cellular senescence during cell stress conditions (38). Perhaps cap-independent translation occurs in the nucleus with modified translation machinery. Additionally, several studies indicate that translation can be location-specific and that *cis*-acting elements in the mRNA transcript can signal for this activity. For example, β -actin mRNA transcripts were found specifically at the axonal growth cone of a neuron. β -actin contains a *cis*-element in the 3'-UTR that drives this localization (142). Based on this evidence, hypothetically there could be an mRNA sequence element that signals for a transcript to be translated in the nucleus. However, we will need to know what kinds of transcripts contain these hypothetical sequence elements and how much of the cell's total transcriptome has the capacity to be translated there. Perhaps there are stress-induced elements on a transcript that signal for its nuclear translation. Identifying these potential elements, as well as how they interact with unique elements on a ribosome, is critical for understanding nucleus-localized translation.

What is the purpose of nuclear translation? Our model, as described above, suggests that nuclear translation is a protective function of the cell, namely mRNA surveillance, to regulate aberrant mRNAs. Thus, it acts as another level of complex control of gene expression. This type of regulation may indeed occur in the nucleus. However, we cannot rule out other explanations for the function of nuclear translation. For example, one study mentioned in this thesis suggests that nucleolar localized translation during normal conditions functions to either aid in the rapid

synthesis of ribosomal proteins or test their translational capacity (81). This hypothesis is based on RPM data showing robust peptide synthesis signal in nucleoli in normal cells. Another study mentioned above suggests that some nuclear translation exists in the nucleoplasm to produce peptide for the MHC complex (83). We cannot treat different types of nuclear translation as mutually exclusive. Indeed several functions of nuclear translation may occur in a single nucleus. In order to determine the significance of nuclear translation, the percentage of total translation that occurs during specific cellular conditions in the nucleus must be calculated. Several recent studies, including one that detected nuclear translation, indicated that a high percentage of nascent polypeptides are degraded promptly after synthesis (69). The purpose of this seemingly metabolically wasteful phenomenon must be determined.

Nuclear translation can be a part of a housekeeping function of the cell. One possible housekeeping function may be the pioneer round of translation. This involves docking and scanning of a ribosome by the cap-binding protein heterodimer (CBC) before loading of eIF4E. Pioneer round, or CBC-dependent translation, has been shown to be preferred over eIF4E-dependent translation during certain cell stress conditions, such as heat shock (143). As such, some hypothesize that the pioneer round of translation is linked to NMD so that newly mature mRNAs do not mass-produce truncated proteins. This is evidenced by studies showing the exclusive interaction of the exon junction complex (EJC) and NMD factor UPF1 with CBC-bound mRNA and not eIF4E-bound mRNA (144). This combined with studies indicating NMD can occur in the nucleus suggests that the pioneer round of translation may function in the nuclear compartment (84, 140). Although, a study using a microscopy-based method of detecting the localization of the pioneer round of translation of single mRNAs in human cells (TRICK

assay) did not detect translation activity in the nuclear compartment for their reporter (145). A similar study that probes other types of mRNAs including those with premature stop codons and other aberrations will be required to determine if NMD and pioneer round translation events occur in human nuclei (146). This study will build evidence for nuclear translation as a protective housekeeping function of the cell.

Alternatively, translation in the nucleus may be a pathological function of proteotoxic stressors. Namely, RAN translation could occur in the nucleus of cells expressing expanded repeat mRNAs. RAN translation, introduced in section 1.3.1, produces repetitive polypeptides that contribute to proteotoxicity (61). RAN translation may occur in the nuclear compartment, where several repeat expanded mRNAs are retained in foci. Indeed we hypothesize that during SCA1, saturation of regulatory nuclear translation may lead to an increase in pathological forms of nuclear translation like RAN translation. Overall, identifying both the nuclear translation machinery and the translated transcripts will aid in the development of potential functions of this phenomenon.

4.2 Future Studies

4.2.1 Identify the PML isoform-specific interactome

Identifying key functional binding partners of PML bodies is nearly impossible without first identifying isoform-specific interactions. The C-terminus of the PML mRNA is alternatively spliced at a high rate, between nine exons, creating several isoforms of the protein that have unique structural and localization domains. Although all isoforms are able to nucleate a PML body due to their TRIM motif, they potentially can have vastly different functions. The isoforms

are present at different abundances in the cell. PMLI is the most abundant isoform in the cell, yet it is one of the most poorly understood. This is in spite the fact that it has both a nuclear import and nuclear export signal, giving it the ability to shuttle between the nucleus and the cytoplasm. PML isoform IV is the most widely studied, due to its ability to interact with diverse and important proteins through exon 8. PMLIV has relatively low abundance in the cell, but its exclusive capacity to mediate viral resistance makes it fascinating to microbiologists and immunologists. PML isoform V is quite unique as it may mediate the stability of a PML body and act as a scaffolding isoform (117).

As the above isoforms represent, the characterization of the function of each isoform as well as the evolutionary significance of the high number of PML isoforms is critical to understand. Yet, little is known about how each isoform interacts within a given PML body during a given condition. In order to begin to answer these questions, a proteomics study of the individual PML isoforms is desperately needed. However, proteomics studies of PML bodies have been problematic due to the insolubility of the body's doughnut structure and the dynamic nature of their protein-protein interactions. BioID or some updated variation thereof can be the tool most qualified for these much needed studies, as it can turn the problems of insolubility and weak interactions into advantages. Fusing BirA* to all of the major PML isoforms of PML, and expressing each fusion protein in PML knockdown cells for their specific BioID analyses will generate a comprehensive proteomics analysis for isoform-specific PML interactions.

4.2.2 Quantitative proteomics analysis of PMLIV during cell stress conditions

There are many obvious questions about nuclear translation to be addressed, most importantly: what is the basic biological significance of this process in normal and pathologic

states? A first step in addressing this question is to identify and characterize the components that participate in nuclear translation during different stress conditions. Namely, we must identify the translation machinery and the transcripts present at PML bodies during different conditions.

A comprehensive, quantitative proteomics analysis of PML bodies during several specific cell stress conditions may lead to the identification of translation machinery specific to the nuclear compartment during cell stress. Repetition of the quantitative analysis attempted in section 3.2.2, accounting for the variability of the results by submitting equivalent total protein concentrations in all samples, will sufficiently generate the quantitative data necessary for proteomics analysis. The potential stress conditions we would benefit from analyzing are heat shock, UV irradiation, serum starvation, oxidative stress, viral infection, cellular transformation and 84Q-ATXN1 proteotoxicity. Additionally, we would benefit from analyzing additional repeat expansion disorders such as other SCAs, HD and ALS. The cell type used in all of these analyses must be carefully chosen, as the cell type used may contribute to or change the stress conditions outlined above. For example, transformed cell types such as HeLas may not represent canonical PML body interactions and may represent instead a cell stress type.

Once compiled, our group will identify the classes of proteins through GO analysis using the PANTHER database. Additionally, we will determine the change in expression levels using a label-free intensity analysis. The top 50 differentially expressed proteins will be ranked by positive and negative expression changes. If possible, the SUMOylation status of the identified proteins will be determined, as most proteins that interact with PML are SUMOylated (147). However, identifying SUMOylated proteins will present technical challenges such as identifying the SUMO sequence tag via mass spectrometry.

Using the data generated by this proteomics analysis, we will be able to identify key proteins that are upregulated during specific cell stressors. We will be especially interested in differential expression of ribosomal proteins and translation factors during different cell stress conditions. Ribosomes and translation factors are often omitted from BioID screens due to the ability of the BirA* fusion protein to biotinylate proteins shortly after translation, while the protein is still near the ribosome. However, since we are analyzing PML's role in translation, we will be interested in identifying PML body-interacting ribosomes and translation factors. A quantitative analysis will decrease the background level of ribosomal protein detection and potentially detect a significant change in interaction between PML bodies and translation machinery during cell stress.

The key candidate proteins will be subject to further characterization as outlined below. Once a list of candidates is generated, we should determine the necessity of each candidate protein for PML localized translation through siRNA interference. We will also need to determine the effect of the ablated proteins on stress-induced, PML-localized translation through RPM analysis and PML immunofluorescence. Conversely, we will need to assess the effects of silencing PML to ablate stress induced PML localized translation on the expression and activity of the candidate proteins. To study the functionality of the candidate proteins, we will need to determine the effect of increased expression of the candidates on the accumulation of 84Q-Atxn1 aggregates. Conversely, we will need to determine the necessity of the candidate proteins for the clearance of ATXN1 mRNA and 84Q-Atxn1 protein through siRNA interference analysis of the candidates. These analyses will characterize the sufficiency and necessity of each protein to carry out PML localized nuclear translation. Ideally, these results will allow us to determine the

translation machinery necessary to formulate a defined mechanism for PML localized translation.

4.2.3 Characterization of transcripts translated at PML bodies during cell stress

In section 3.2.2, I show that PML bodies significantly associate with expanded mutant ATXN1 mRNA. I hypothesize that this interaction is linked to a regulatory translation pathway. An important and necessary step in elucidating the mechanism of PML localized translation is to identify the transcripts actively translated in the nucleus during stressed and unstressed conditions.

To begin to characterize the repeat expansion transcripts that are actively translated by PML bodies, we need to determine whether the secondary structure formed by repeat-containing transcripts is required for co-localization with PML and sites active translation, through targeted mutation in the stem-loop to disrupt formation of secondary structures, as previously described (114, 148, 149). We will next need to define the role of RNA structure. Namely, we will need to test the minimum number of repeats required to observe protein synthesis at PML bodies. Additionally, we would need to test the necessity of a start codon, correct reading frame, and presence of a stop codon for synthesis at PML bodies. To determine if there is a direct binding between PML and the transcripts, we can perform RNA immunoprecipitations (RIPs) on nuclear isolates from fibroblasts subject to expanded ATXN1 ectopic expression.

In order to expand the scope of PML localized translation beyond the proteotoxic stress model and into other stress conditions, we must employ high-throughput analysis to identify actively translated transcripts in the nucleus during different stress conditions. To specifically identify and quantify the nascent polypeptides, puromycin-associated nascent chain proteomics

(PUNCH-P), or other updated methods of this protocol can be used (150). This method is currently advantageous to use over other conventional methods of identifying nascent peptides (such as SILAC) because it can readily be used during different cell conditions. Isolating the nuclei will be necessary for nucleus-specific nascent polypeptide identification. Mass spectrometry analysis of the nuclear nascent polypeptides during different cell stress conditions will determine the fluctuation of newly synthesized peptides in the nucleus during stressed and unstressed conditions. These peptides can be analyzed for aberrations such as low complexity motifs or expanded repeats. In tandem, these peptides can be assessed in a GO classification to determine if proteins translated in the nucleus during stress conditions are important for the stress response. Identified peptides can be followed up with RPM and immunofluorescence assays for proximity to PML bodies.

An important and related approach to identifying the translated transcripts is to identify the mRNAs bound to nuclear ribosomes. This complimentary approach to nascent polypeptide identification is necessary to confirm that nascent peptides come from transcripts translated in the nucleus and not in the cytoplasm. To define which transcripts are being translated in the nucleus under normal and stressed conditions, an adapted form of ribosome profiling of isolated nuclei from different stress conditions will be the quintessential experiment. Technical considerations such as the quantity of starting material and accession of the purity of nuclear extracts will make this a challenging experiment. This analysis can generate a list of the relative abundances of mRNAs that are actively translated in the nucleus during stress compared to normal conditions. Ideally, transcripts associated with nuclear ribosomes under conditions of stress will be related to the specific type of cellular stress and the stress response. Transcripts

identified by ribosome profiling must be verified using RPM followed by RNA-FISH to determine the localization of these transcripts within the nucleus, interrogate whether these transcripts are found at PML bodies or other sub-nuclear structures, and address if these transcripts have altered localization following cell stress. In total, these studies will allow us to gain insight into the functional significance of nuclear protein synthesis, investigate the role of the PML body in this process, and uncover novel regulatory mechanism governing gene expression.

References

1. S. T. Kosak, M. Groudine, Gene order and dynamic domains. *Science* **306**, 644-647 (2004).
2. M. Dunder, Nuclear bodies: multifunctional companions of the genome. *Current opinion in cell biology* **24**, 415-422 (2012).
3. M. Dunder, T. Misteli, Biogenesis of nuclear bodies. *Cold Spring Harb Perspect Biol* **2**, a000711 (2010).
4. T. Misteli, The concept of self-organization in cellular architecture. *J Cell Biol* **155**, 181-185 (2001).
5. M. Carmo-Fonseca, J. Rino, RNA seeds nuclear bodies. *Nat Cell Biol* **13**, 110-112 (2011).
6. A. M. Wood, A. G. Garza-Gongora, S. T. Kosak, A Crowdsourced nucleus: understanding nuclear organization in terms of dynamically networked protein function. *Biochimica et biophysica acta* **1839**, 178-190 (2014).
7. C. Brangwynne, T. Mitchison, A. Hyman, Active liquid-like behavior of nucleoli determines their size and shape in *Xenopus laevis* oocytes. *Proceedings of the National Academy of Sciences of the United States of America* **108**, 4334-4339 (2011).
8. K. McCann, S. Baserga, Driving nucleolar assembly. *Genes & development* **28**, 211-213 (2014).
9. T. Moss, F. Langlois, T. Gagnon-Kugler, V. Stefanovsky, A housekeeper with power of attorney: the rRNA genes in ribosome biogenesis. *Cellular and molecular life sciences : CMLS* **64**, 29-49 (2006).

10. C. Rubbi, J. Milner, Disruption of the nucleolus mediates stabilization of p53 in response to DNA damage and other stresses. *The EMBO journal* **22**, 6068-6077 (2003).
11. S. Bursac, M. Brdovcak, G. Donati, S. Volarevic, Activation of the tumor suppressor p53 upon impairment of ribosome biogenesis. *Biochimica et biophysica acta* **1842**, 817-830 (2014).
12. Z. Nizami, S. Deryusheva, J. Gall, The Cajal body and histone locus body. *Cold Spring Harbor perspectives in biology* **2**, (2010).
13. B. Jady, P. Richard, E. Bertrand, T. Kiss, Cell cycle-dependent recruitment of telomerase RNA and Cajal bodies to human telomeres. *Molecular biology of the cell* **17**, 944-954 (2006).
14. M. Hebert, Signals controlling Cajal body assembly and function. *The international journal of biochemistry & cell biology* **45**, 1314-1317 (2013).
15. J. Stern, K. Zyner, H. Pickett, S. Cohen, T. Bryan, Telomerase recruitment requires both TCAB1 and Cajal bodies independently. *Molecular and cellular biology* **32**, 2384-2395 (2012).
16. D. Spector, A. Lamond, Nuclear speckles. *Cold Spring Harbor perspectives in biology* **3**, (2011).
17. J. Brown *et al.*, Association between active genes occurs at nuclear speckles and is modulated by chromatin environment. *The Journal of cell biology* **182**, 1083-1097 (2008).

18. L. Shopland, C. Johnson, M. Byron, J. McNeil, J. Lawrence, Clustering of multiple specific genes and gene-rich R-bands around SC-35 domains: evidence for local euchromatic neighborhoods. *The Journal of cell biology* **162**, 981-990 (2003).
19. D. Carter, C. Eskiw, P. Cook, Transcription factories. *Biochemical Society transactions* **36**, 585-589 (2008).
20. Q. Hu *et al.*, Enhancing nuclear receptor-induced transcription requires nuclear motor and LSD1-dependent gene networking in interchromatin granules. *Proceedings of the National Academy of Sciences of the United States of America* **105**, 19199-19204 (2008).
21. A. Wood, A. Garza-Gongora, S. Kosak, A Crowdsourced nucleus: understanding nuclear organization in terms of dynamically networked protein function. *Biochimica et biophysica acta* **1839**, 178-190 (2014).
22. R. Bernardi, P. P. Pandolfi, Structure, dynamics and functions of promyelocytic leukaemia nuclear bodies. *Nature reviews. Molecular cell biology* **8**, 1006-1016 (2007).
23. S. Nisole, M. A. Maroui, X. H. Mascle, M. Aubry, M. K. Chelbi-Alix, Differential Roles of PML Isoforms. *Front Oncol* **3**, 125 (2013).
24. Y. Chu, X. Yang, SUMO E3 ligase activity of TRIM proteins. *Oncogene*, (2011).
25. V. Lallemand-Breitenbach, H. de Thé, PML nuclear bodies. *Cold Spring Harbor perspectives in biology* **2**, (2010).
26. E. Van, K. Laukens, T. H. Dang, X. Van, A manually curated network of the PML nuclear body interactome reveals an important role for PML-NBs in SUMOylation dynamics. *Int J Biol Sci*, (2010).

27. E. Van Damme, K. Laukens, T. H. Dang, X. Van Ostade, A manually curated network of the PML nuclear body interactome reveals an important role for PML-NBs in SUMOylation dynamics. *International Journal of Biological Sciences* **6**, 51-67 (2010).
28. V. LaMorte, J. Dyck, R. Ochs, R. Evans, Localization of nascent RNA and CREB binding protein with the PML-containing nuclear body. *Proceedings of the National Academy of Sciences of the United States of America* **95**, 4991-4996 (1998).
29. M. Bras, V. Lallemand-Breitenbach, Acute promyelocytic leukemia, arsenic, and PML bodies. *The Journal of cell biology* **198**, 11-21 (2012).
30. U. Sahin, V. Lallemand-Breitenbach, H. de Thé, PML nuclear bodies: regulation, function and therapeutic perspectives. *J Pathol* **234**, 289-291 (2014).
31. O. Bischof *et al.*, Regulation and localization of the Bloom syndrome protein in response to DNA damage. *The Journal of cell biology* **153**, 367-380 (2001).
32. R. Carbone, M. Pearson, S. Minucci, P. Pelicci, PML NBs associate with the hMre11 complex and p53 at sites of irradiation induced DNA damage. *Oncogene* **21**, 1633-1640 (2002).
33. E. Soutoglou, T. Misteli, Activation of the cellular DNA damage response in the absence of DNA lesions. *Science (New York, N.Y.)* **320**, 1507-1510 (2008).
34. P. Yeung *et al.*, Promyelocytic leukemia nuclear bodies support a late step in DNA double-strand break repair by homologous recombination. *Journal of cellular biochemistry* **113**, 1787-1799 (2012).
35. U. Sahin *et al.*, Oxidative stress-induced assembly of PML nuclear bodies controls sumoylation of partner proteins. *The Journal of Cell Biology* **204**, 931-945 (2014).

36. C. Shiels *et al.*, PML bodies associate specifically with the MHC gene cluster in interphase nuclei. *Journal of cell science* **114**, 3705-3716 (2001).
37. T. Ulbricht *et al.*, PML promotes MHC class II gene expression by stabilizing the class II transactivator. *The Journal of cell biology* **199**, 49-63 (2012).
38. R. Ching, K. Ahmed, P. Boutros, L. Penn, D. Bazett-Jones, Identifying gene locus associations with promyelocytic leukemia nuclear bodies using immuno-TRAP. *The Journal of cell biology* **201**, 325-335 (2013).
39. Y. A. Rivera-Molina, B. R. Rojas, Q. Tang, Nuclear domain 10-associated proteins recognize and segregate intranuclear DNA/protein complexes to negate gene expression. *Virology* **9**, 222 (2012).
40. T. S. Rai *et al.*, Histone chaperone HIRA deposits histone H3.3 onto foreign viral DNA and contributes to anti-viral intrinsic immunity. *Nucleic Acids Res* **45**, 11673-11683 (2017).
41. P. Xu, B. Roizman, The SP100 component of ND10 enhances accumulation of PML and suppresses replication and the assembly of HSV replication compartments. *Proc Natl Acad Sci U S A* **114**, E3823-E3829 (2017).
42. V. Lallemand-Breitenbach *et al.*, Arsenic degrades PML or PML-RARalpha through a SUMO-triggered RNF4/ubiquitin-mediated pathway. *Nat Cell Biol* **10**, 547-555 (2008).
43. A. Gärtner, S. Muller, PML, SUMO, and RNF4: Guardians of Nuclear Protein Quality. *Molecular cell*, (2014).
44. E. de Stanchina, E. Querido, M. Narita, R. V. Davuluri, PML is a direct p53 target that modulates p53 effector functions. *Molecular cell*, (2004).

45. S. Yujie, K. D. Linda, G. K. Theodore, Specific interaction of PML bodies with the TP53 locus in Jurkat interphase nuclei. *Genomics* **82**, (2003).
46. P. Skinner *et al.*, Ataxin-1 with an expanded glutamine tract alters nuclear matrix-associated structures. *Nature* **389**, 971-974 (1997).
47. A. Janer *et al.*, PML clastosomes prevent nuclear accumulation of mutant ataxin-7 and other polyglutamine proteins. *The Journal of cell biology* **174**, 65-76 (2006).
48. A. Chort *et al.*, Interferon β induces clearance of mutant ataxin 7 and improves locomotion in SCA7 knock-in mice. *Brain : a journal of neurology* **136**, 1732-1745 (2013).
49. L. Guo *et al.*, A Cellular System that Degrades Misfolded Proteins and Protects against Neurodegeneration. *Molecular Cell* **55**, 15-30 (2014).
50. J. M. Pérez Ortiz, H. T. Orr, Spinocerebellar Ataxia Type 1: Molecular Mechanisms of Neurodegeneration and Preclinical Studies. *Adv Exp Med Biol* **1049**, 135-145 (2018).
51. H. Y. Zoghbi, H. T. Orr, Glutamine repeats and neurodegeneration. *Annual review of neuroscience*, (2000).
52. H. Paulson, Repeat expansion diseases. *Handb Clin Neurol* **147**, 105-123 (2018).
53. W. J. Krzyzosiak *et al.*, Triplet repeat RNA structure and its role as pathogenic agent and therapeutic target. *Nucleic Acids Res* **40**, 11-26 (2012).
54. R. Nalavade, N. Griesche, D. P. Ryan, S. Hildebrand, S. Krauß, Mechanisms of RNA-induced toxicity in CAG repeat disorders. *Cell Death & Disease* **4**, e752 (2013).

55. M. Jazurek, A. Ciesiolka, J. Starega-Roslan, K. Bilinska, W. J. Krzyzosiak, Identifying proteins that bind to specific RNAs - focus on simple repeat expansion diseases. *Nucleic Acids Research*, gkw803 (2016).
56. A. Jain, R. D. Vale, RNA phase transitions in repeat expansion disorders. *Nature* **546**, 243-247 (2017).
57. M. Fernández-Nogales, M. Santos-Galindo, I. H. Hernández, J. R. Cabrera, J. J. Lucas, Faulty splicing and cytoskeleton abnormalities in Huntington's disease. *Brain Pathol* **26**, 772-778 (2016).
58. M. G. Kearse, J. E. Wilusz, Non-AUG translation: a new start for protein synthesis in eukaryotes. *Genes Dev* **31**, 1717-1731 (2017).
59. T. Zu *et al.*, Non-ATG-initiated translation directed by microsatellite expansions. *Proceedings of the National Academy of Sciences* **108**, 260-265 (2011).
60. K. M. Green, A. E. Linsalata, P. K. Todd, RAN translation—What makes it run? *Brain Research* **1647**, 30-42 (2016).
61. M. Bañez-Coronel *et al.*, RAN Translation in Huntington Disease. *Neuron* **88**, 667-677 (2015).
62. M. Wojciechowska, M. Olejniczak, P. Galka-Marciniak, M. Jazurek, W. J. Krzyzosiak, RAN translation and frameshifting as translational challenges at simple repeats of human neurodegenerative disorders. *Nucleic Acids Research* **42**, 11849-11864 (2014).
63. X. Tong *et al.*, Ataxin-1 and Brother of ataxin-1 are components of the Notch signalling pathway. *EMBO Rep* **12**, 428-435 (2011).

64. A. Matilla *et al.*, Mice lacking ataxin-1 display learning deficits and decreased hippocampal paired-pulse facilitation. *J Neurosci* **18**, 5508-5516 (1998).
65. M. W. C. Rousseaux *et al.*, ATXN1-CIC Complex Is the Primary Driver of Cerebellar Pathology in Spinocerebellar Ataxia Type 1 through a Gain-of-Function Mechanism. *Neuron* **97**, 1235-1243.e1235 (2018).
66. J. Lim, Z. Yue, Neuronal aggregates: formation, clearance, and spreading. *Developmental cell* **32**, 491-501 (2015).
67. C. A. Ross, M. A. Poirier, Opinion: What is the role of protein aggregation in neurodegeneration? *Nat Rev Mol Cell Biol* **6**, 891-898 (2005).
68. H. Yuriko, P. Roy, No-go decay: a quality control mechanism for RNA in translation. *Wiley interdisciplinary reviews. RNA*, (2010).
69. G. Kramer, D. Boehringer, N. Ban, B. Bukau, The ribosome as a platform for co-translational processing, folding and targeting of newly synthesized proteins. *Nature structural & ...*, (2009).
70. C. L. Simms, E. N. Thomas, H. S. Zaher, Ribosome-based quality control of mRNA and nascent peptides. *Wiley Interdisciplinary Reviews: RNA*, (2016).
71. C. J. Shoemaker, R. Green, Translation drives mRNA quality control. *Nature Structural & Molecular Biology* **19**, 594-601 (2012).
72. S. Lykke-Andersen, T. H. Jensen, Nonsense-mediated mRNA decay: an intricate machinery that shapes transcriptomes. *Nature Reviews Molecular Cell Biology* **16**, 665-677 (2015).

73. K. Ikeuchi, E. Yazaki, K. Kudo, T. Inada, Conserved functions of human Pelota in mRNA quality control of nonstop mRNA. *FEBS Lett* **590**, 3254-3263 (2016).
74. L. Chen *et al.*, Structure of the Dom34-Hbs1 complex and implications for no-go decay. *Nat Struct Mol Biol* **17**, 1233-1240 (2010).
75. V. G. Allfrey, AMINO ACID INCORPORATION BY ISOLATED THYMUS NUCLEI. I. THE ROLE OF DESOXYRIBONUCLEIC ACID IN PROTEIN SYNTHESIS. *Proc Natl Acad Sci U S A* **40**, 881-885 (1954).
76. J. A. Goidl, D. Canaani, M. Boublik, H. Weissbach, H. Dickerman, Polyanion-induced release of polyribosomes from HeLa cell nuclei. *J Biol Chem* **250**, 9198-9205 (1975).
77. F. J. Iborra, D. A. Jackson, P. R. Cook, Coupled transcription and translation within nuclei of mammalian cells. *Science* **293**, 1139-1142 (2001).
78. T. Pederson, The persistent plausibility of protein synthesis in the nucleus: process, palimpsest or pitfall? *Curr Opin Cell Biol* **25**, 520-521 (2013).
79. J. Dahlberg, E. Lund, Nuclear translation or nuclear peptidyl transferase? *Nucleus* **3**, 320-321 (2012).
80. J. E. Dahlberg, E. Lund, E. B. Goodwin, Nuclear translation: what is the evidence? *RNA* **9**, 1-8 (2003).
81. A. David *et al.*, Nuclear translation visualized by ribosome-bound nascent chain puromycylation. *The Journal of cell biology* **197**, 45-57 (2012).
82. A. David, J. R. Bennink, J. W. Yewdell, Emetine optimally facilitates nascent chain puromycylation and potentiates the ribopuromycylation method (RPM) applied to inert cells. *Histochem Cell Biol* **139**, 501-504 (2013).

83. S. Apcher *et al.*, Translation of pre-spliced RNAs in the nuclear compartment generates peptides for the MHC class I pathway. *Proceedings of the National Academy of Sciences of the United States of America* **110**, 17951-17956 (2013).
84. S. Baboo *et al.*, Most human proteins made in both nucleus and cytoplasm turn over within minutes. *PloS one* **9**, (2013).
85. L. Wei, Y. Yu, Y. Shen, M. Wang, W. Min, Vibrational imaging of newly synthesized proteins in live cells by stimulated Raman scattering microscopy. *Proceedings of the National Academy of Sciences of the United States of America* **110**, 11226-11231 (2013).
86. K. Al-Jubran *et al.*, Visualization of the joining of ribosomal subunits reveals the presence of 80S ribosomes in the nucleus. *RNA* **19**, 1669-1683 (2013).
87. S. Baboo *et al.*, Most Human Proteins Made in Both Nucleus and Cytoplasm Turn Over within Minutes. *PLoS ONE* **9**, e99346 (2014).
88. M. Shi *et al.*, Premature termination codons are recognized in the nucleus in a reading-frame-dependent manner. *Cell Discovery* **1**, (2015).
89. J. Yewdell, A. David, Nuclear translation for immunosurveillance. *Proceedings of the National Academy of Sciences of the United States of America* **110**, 17612-17613 (2013).
90. T. Misteli, Beyond the sequence: cellular organization of genome function. *Cell* **128**, 787-800 (2007).
91. A. Wood, A. Garza-Gongora, S. Kosak, A Crowdsourced nucleus: Understanding nuclear organization in terms of dynamically networked protein function. *Biochimica et biophysica acta*, (2014).

92. N. Cohen *et al.*, PML RING suppresses oncogenic transformation by reducing the affinity of eIF4E for mRNA. *The EMBO journal* **20**, 4547-4559 (2001).
93. H. Lai, K. Borden, The promyelocytic leukemia (PML) protein suppresses cyclin D1 protein production by altering the nuclear cytoplasmic distribution of cyclin D1 mRNA. *Oncogene* **19**, 1623-1634 (2000).
94. S. Strudwick, K. Borden, The emerging roles of translation factor eIF4E in the nucleus. *Differentiation; research in biological diversity* **70**, 10-22 (2002).
95. J. Salsman, J. Pinder, B. Tse, D. Corkery, G. Dellaire, The translation initiation factor 3 subunit eIF3K interacts with PML and associates with PML nuclear bodies. *Experimental cell research* **319**, 2554-2565 (2013).
96. M. Vernier *et al.*, Regulation of E2Fs and senescence by PML nuclear bodies. *Genes & development* **25**, 41-50 (2011).
97. H. de Thé, M. Le Bras, V. Lallemand-Breitenbach, The cell biology of disease: Acute promyelocytic leukemia, arsenic, and PML bodies. *The Journal of cell biology* **198**, 11-21 (2012).
98. S. Strudwick, K. Borden, Finding a role for PML in APL pathogenesis: a critical assessment of potential PML activities. *Leukemia* **16**, 1906-1917 (2002).
99. K. Borden, Pondering the promyelocytic leukemia protein (PML) puzzle: possible functions for PML nuclear bodies. *Molecular and cellular biology* **22**, 5259-5269 (2002).
100. J. Takahashi *et al.*, PML nuclear bodies and neuronal intranuclear inclusion in polyglutamine diseases. *Neurobiology of disease* **13**, 230-237 (2003).

101. C. Fu *et al.*, Stabilization of PML nuclear localization by conjugation and oligomerization of SUMO-3. *Oncogene* **24**, 5401-5413 (2005).
102. L. Ivanschitz, H. De Thé, M. Le Bras, PML, SUMOylation, and Senescence. *Frontiers in oncology* **3**, 171 (2013).
103. C. Pearson, Repeat associated non-ATG translation initiation: one DNA, two transcripts, seven reading frames, potentially nine toxic entities! *PLoS genetics* **7**, (2011).
104. T. Zu *et al.*, Non-ATG-initiated translation directed by microsatellite expansions. *Proceedings of the National Academy of Sciences of the United States of America* **108**, 260-265 (2011).
105. A. Klauer, A. van Hoof, Degradation of mRNAs that lack a stop codon: a decade of nonstop progress. *Wiley interdisciplinary reviews. RNA* **3**, 649-660 (2012).
106. A. David, J. W. Yewdell, Applying the ribopuromycylation method to detect nuclear translation. *Methods Mol Biol* **1228**, 133-142 (2015).
107. M. O. Urbanek, W. J. Krzyzosiak, RNA FISH for detecting expanded repeats in human diseases. *Methods* **98**, 115-123 (2016).
108. K. J. Roux, D. I. Kim, B. Burke, D. G. May, BioID: A Screen for Protein-Protein Interactions. *Curr Protoc Protein Sci* **91**, 19.23.11-19.23.15 (2018).
109. C. L. Simms, E. N. Thomas, H. S. Zaher, Ribosome-based quality control of mRNA and nascent peptides. *Wiley Interdiscip Rev RNA* **8**, (2017).
110. H. K. Lai, K. L. Borden, The promyelocytic leukemia (PML) protein suppresses cyclin D1 protein production by altering the nuclear cytoplasmic distribution of cyclin D1 mRNA. *Oncogene* **19**, 1623-1634 (2000).

111. K. L. Borden, E. J. Campbelldwyer, G. W. Carlile, M. Djavani, M. S. Salvato, Two RING finger proteins, the oncoprotein PML and the arenavirus Z protein, colocalize with the nuclear fraction of the ribosomal P proteins. *Journal of virology* **72**, 3819-3826 (1998).
112. F. Wang, L. A. Durfee, J. M. Huibregtse, A cotranslational ubiquitination pathway for quality control of misfolded proteins. *Molecular cell* **50**, 368-378 (2013).
113. L. Wei, Y. Yu, Y. Shen, M. C. Wang, W. Min, Vibrational imaging of newly synthesized proteins in live cells by stimulated Raman scattering microscopy. *Proc Natl Acad Sci U S A* **110**, 11226-11231 (2013).
114. W. J. Krzyzosiak *et al.*, Triplet repeat RNA structure and its role as pathogenic agent and therapeutic target. *Nucleic Acids Research* **40**, 11-26 (2012).
115. Y. Shibata, R. I. Morimoto, How the Nucleus Copes with Proteotoxic Stress. *Current Biology* **24**, R463-R474 (2014).
116. K. J. Roux, D. I. Kim, M. Raida, B. Burke, A promiscuous biotin ligase fusion protein identifies proximal and interacting proteins in mammalian cells. *The Journal of cell biology* **196**, 801-810 (2012).
117. S. Nisole, M. A. Maroui, X. H. Mascle, M. Aubry, Differential roles of PML isoforms. *Frontiers in ...*, (2013).
118. D. Guan, H. Y. Kao, The function, regulation and therapeutic implications of the tumor suppressor protein, PML. *Cell & bioscience*, (2015).
119. R. G. Gardner, Z. W. Nelson, D. E. Gottschling, Degradation-mediated protein quality control in the nucleus. *Cell* **120**, 803-815 (2005).

120. R. D. Jones, R. G. Gardner, Protein quality control in the nucleus. *Current Opinion in Cell Biology* **40**, 81-89 (2016).
121. S. Apcher *et al.*, Translation of pre-spliced RNAs in the nuclear compartment generates peptides for the MHC class I pathway. *Proceedings of the National Academy of Sciences* **110**, 17951-17956 (2013).
122. M. Boban, R. Foisner, Degradation-mediated protein quality control at the inner nuclear membrane. *Nucleus (Austin, Tex.)* **7**, 41-49 (2016).
123. A. Iwata *et al.*, Intranuclear Degradation of Polyglutamine Aggregates by the Ubiquitin-Proteasome System. *Journal of Biological Chemistry* **284**, 9796-9803 (2009).
124. H. Jonathan, L. John, T. David, RNA-quality control by the exosome. *Nature Reviews Molecular Cell Biology*, (2006).
125. M. Wegener, M. Müller-McNicoll, Nuclear retention of mRNAs - quality control, gene regulation and human disease. *Semin Cell Dev Biol* **79**, 131-142 (2018).
126. A. Aizer *et al.*, Quantifying mRNA targeting to P-bodies in living human cells reveals their dual role in mRNA decay and storage. *J Cell Sci* **127**, 4443-4456 (2014).
127. K. Ikeuchi, E. Yazaki, K. Kudo, T. Inada, Conserved functions of human Pelota in mRNA quality control of nonstop mRNA. *FEBS Letters* **590**, 3254-3263 (2016).
128. S. Saito, N. Hosoda, S. Hoshino, The Hbs1-Dom34 protein complex functions in non-stop mRNA decay in mammalian cells. *J Biol Chem* **288**, 17832-17843 (2013).
129. P. S. Gallagher, M. L. Oeser, A.-c. Abraham, D. Kaganovich, R. G. Gardner, Cellular maintenance of nuclear protein homeostasis. *Cellular and Molecular Life Sciences* **71**, 1865-1879 (2014).

130. F. Meng, I. Na, L. Kurgan, V. N. Uversky, Compartmentalization and Functionality of Nuclear Disorder: Intrinsic Disorder and Protein-Protein Interactions in Intra-Nuclear Compartments. *Int J Mol Sci* **17**, (2015).
131. B. C. Kieseier, The mechanism of action of interferon- β in relapsing multiple sclerosis. *CNS Drugs* **25**, 491-502 (2011).
132. E. U. Walther, R. Hohlfeld, Multiple sclerosis: side effects of interferon beta therapy and their management. *Neurology* **53**, 1622-1627 (1999).
133. V. V. Belzil, T. F. Gendron, L. Petrucelli, RNA-mediated toxicity in neurodegenerative disease. *Molecular and Cellular Neuroscience* **56**, 406-419 (2013).
134. R. Tomecki, P. J. Sikorski, M. Zakrzewska-Placzek, Comparison of preribosomal RNA processing pathways in yeast, plant and human cells - focus on coordinated action of endo- and exoribonucleases. *FEBS Lett* **591**, 1801-1850 (2017).
135. C. R. Trotta, E. Lund, L. Kahan, A. W. Johnson, J. E. Dahlberg, Coordinated nuclear export of 60S ribosomal subunits and NMD3 in vertebrates. *EMBO J* **22**, 2841-2851 (2003).
136. Z. Shi *et al.*, Heterogeneous Ribosomes Preferentially Translate Distinct Subpools of mRNAs Genome-wide. *Mol Cell* **67**, 71-83.e77 (2017).
137. N. Kondrashov *et al.*, Ribosome-mediated specificity in Hox mRNA translation and vertebrate tissue patterning. *Cell* **145**, 383-397 (2011).
138. A. S. Wolf, E. J. Grayhack, Asc1, homolog of human RACK1, prevents frameshifting in yeast by ribosomes stalled at CGA codon repeats. *RNA* **21**, 935-945 (2015).

139. S. Xue, M. Barna, Specialized ribosomes: a new frontier in gene regulation and organismal biology. *Nature reviews. Molecular cell biology* **13**, 355-369 (2012).
140. M. Shi *et al.*, Premature termination codons are recognized in the nucleus in a reading-frame-dependent manner. *Cell Discovery* **1**, 15001 (2015).
141. I. P. Ivanov *et al.*, Translation Initiation from Conserved Non-AUG Codons Provides Additional Layers of Regulation and Coding Capacity. *MBio* **8**, (2017).
142. D. Simsek *et al.*, The Mammalian Ribo-interactome Reveals Ribosome Functional Diversity and Heterogeneity. *Cell* **169**, 1051-1065.e1018 (2017).
143. F. Lejeune, Y. Ishigaki, X. Li, L. E. Maquat, The exon junction complex is detected on CBP80-bound but not eIF4E-bound mRNA in mammalian cells: dynamics of mRNP remodeling. *EMBO J* **21**, 3536-3545 (2002).
144. H. L. Hir, J. Saulière, Z. Wang, The exon junction complex as a node of post-transcriptional networks. *Nature Reviews Molecular Cell Biology* **17**, 41-54 (2016).
145. J. M. Halstead *et al.*, Translation. An RNA biosensor for imaging the first round of translation from single cells to living animals. *Science* **347**, 1367-1671 (2015).
146. J. M. Halstead *et al.*, TRICK: A Single-Molecule Method for Imaging the First Round of Translation in Living Cells and Animals. *Methods Enzymol* **572**, 123-157 (2016).
147. F. P. McManus *et al.*, Quantitative SUMO proteomics reveals the modulation of several PML nuclear body associated proteins and an anti-senescence function of UBC9. *Sci Rep* **8**, 7754 (2018).

148. K. Sobczak, M. de Mezer, G. Michlewski, J. Krol, W. J. Krzyzosiak, RNA structure of trinucleotide repeats associated with human neurological diseases. *Nucleic Acids Res* **31**, 5469-5482 (2003).
149. V. Bernat, M. D. Disney, RNA Structures as Mediators of Neurological Diseases and as Drug Targets. *Neuron* **87**, 28-46 (2015).
150. R. Aviner, T. Geiger, O. Elroy-Stein, Novel proteomic approach (PUNCH-P) reveals cell cycle-specific fluctuations in mRNA translation. *Genes & development*, (2013).